Initial State QED Radiation Aspects for Future e^+e^- Colliders

S. Frixione et al.

Herausgeber und Vertrieb:

Verlag Deutsches Elektronen-Synchrotron DESY

DESY Bibliothek
Notkestr. 85
22607 Hamburg
Germany

Initial state QED radiation aspects for future e^+e^- colliders

Conveners: **S. Frixione,**[1] **E. Laenen**[2,3]

C.M. Carloni Calame,[4] **A. Denner,**[5] **S. Dittmaier,**[6] **T. Engel,**[7,8] **L. Flower,**[9] **L. Gellersen,**[10] **S. Hoeche,**[11] **S. Jadach,**[12] **M.R. Masouminia,**[13] **G. Montagna,**[4,14] **O. Nicrosini,**[4] **F. Piccinini,**[4] **S. Plätzer,**[15,16] **A. Price,**[17] **J. Reuter,**[18] **M. Rocco,**[7] **M. Schönherr,**[9] **A. Signer,**[7,8] **T. Sjöstrand,**[10] **G. Stagnitto,**[8] **Y. Ulrich,**[9] **R. Verheyen,**[20] **L. Vernazza,**[21,2] **A. Vicini,**[22] **B.F.L. Ward,**[23] **M. Zaro**[24]

[1]*INFN, Sezione di Genova, Via Dodecaneso 33, I-16146, Genoa, Italy*

[2]*Nikhef, Science Park 105, 1098 XG Amsterdam, Netherlands*

[3]*Institute of Physics, University of Amsterdam, Science Park 904, 1098 XH Amsterdam, Netherlands*

[4]*INFN, Sezione di Pavia,*
via A. Bassi 6, 27100 Pavia, Italy

[5]*Universität Würzburg, Institut für Theoretische Physik und Astrophysik, Emil-Hilb-Weg 22, 97074 Würzburg, Germany*

[6]*Albert-Ludwigs-Universität Freiburg, Physikalisches Institut, Hermann-Herder-Str. 3, 79104 Freiburg, Germany*

[7]*Paul Scherrer Institut, CH-5232 Villigen PSI, Switzerland*

[8]*Physik-Institut, Universität Zürich, Winterthurerstrasse 190, CH-8057 Zürich, Switzerland*

[9]*Institute for Particle Physics Phenomenology, Durham University, Durham DH1 3LE, United Kingdom*

[10]*Dept. of Astronomy and Theoretical Physics, Lund University, Sölvegatan 14A, SE-223 62 Lund, Sweden*

[11]*Fermi National Accelerator Laboratory, Batavia, IL, 60510, USA*

[12]*Institute of Nuclear Physics Polish Academy of Sciences, Cracow, Poland*

[14]*Dipartimento di Fisica, Università di Pavia,*
via A. Bassi 6, 27100 Pavia, Italy

[15]*Institute of Physics, NAWI Graz, University of Graz, Universitätsplatz 5, A-8010 Graz, Austria*

[16]*Particle Physics, Faculty of Physics, University of Vienna, Boltzmanngasse 5, A-1090 Wien, Austria*

[17]*Theoretische Physik 1, Naturwissenschaftlich-Technische Fakultät, Universität Siegen, Walter-Flex-Strasse 3, D-57068 Siegen, Germany*

[18]*Deutsches Elektronen-Synchrotron DESY, Notkestr. 85, 22607 Hamburg, Germany*

[20]*Dept. of Physics and Astronomy, UCL, Gower St, Bloomsbury, London WC1E 6BT, United Kingdom*

[21]*INFN, Sezione di Torino, Via P. Giuria 1, I-10125 Torino, Italy*

[22]*Dipartimento di Fisica "Aldo Pontremoli", University of Milano and INFN, Sezione di Milano, I-20133 Milano, Italy*

[23]*Baylor University, Waco, TX, USA*

[24]*TIFLab, Dipartimento di Fisica, Università degli Studi di Milano and INFN, Sezione di Milano, Via Celoria 16, 20133 Milano, Italy*

ABSTRACT: This white paper concerns theoretical and phenomenological aspects relevant to the physics of future e^+e^- colliders, in particular regarding initial-state QED radiation. The contributions each contain key technical aspects, and are formulated in a pedagogical manner so as to render them accessible also to those who are not directly working on these and immediately-related topics. This should help both experts and non-experts understand the theoretical challenges that we shall face at future e^+e^- colliders. Specifically, this paper contains descriptions of the treatment of initial state radiation from several Monte Carlo collaborations, as well as contributions that explain a number of more theoretical developments with promise of future phenomenological impact.

Contents

1 Introduction

While the recent, current, and near-future activity of the high-energy particle physics community has been and will be focused on the experimental and theoretical studies of hadronic collisions, owing to the operation of the LHC at CERN, in the longer term there is some consensus towards building an e^+e^- machine. In view of the fact that its basic parameters (such as whether it will be linear or circular, and its running energy/energies) are far from being agreed upon, it is important at this stage to start reviewing the theoretical tools available for e^+e^--collision simulations. More often than not, these have been developed during the LEP era, and have not undergone those major upgrades which will almost certainly be necessary at a future collider. On the other hand, enormous technical progress has been made in the past twenty years, thanks to the challenges posed by the LHC; we expect that a non-negligible part of that can be ported, with a relatively minor effort, to an e^+e^- environment.

    This white paper, which is part of the Snowmass 2021 proceedings, presents a review of the computer programs that have been used in the past at LEP, and/or are being used presently at the LHC, as well as some more theoretical contributions which may inform future phenomenological developments. The status of the codes discussed below is heterogeneous, in that their readiness to

tackle immediately complex e^+e^- simulations varies greatly. We thus encourage the reader to see this paper as giving the descriptions of the various starting points towards the possible achievement of the tools necessary for future sophisticated analyses. At the same times, the reader is urged to not take the successes of the LEP era for granted: it will be essential to thoroughly vet the capabilities, physics scope, and accuracy of each code in an unbiased manner, regardless of whether it has been used frequently, sparingly, or not at all at LEP (or at even smaller energies).

This paper is organised as follows. Sects. 2–4 review the status of general-purpose parton shower Monte Carlos (PSMCs), with an emphasis on their features relevant to e^+e^- simulations. Sects. 5–10 present a variety of tools whose scope is either generally narrower than that of the PSMCs discussed before, or that specialise on matrix-element computations (that can possibly be interfaced to PSMCs). Finally, sects. 11 and 12 discuss, from a more theoretical viewpoint, various issues that are ubiquitous at e^+e^- colliders, and are related to the treatment of collinear/soft radiation, which is in turn essential for a phenomenological-sensible description of the production process.

We finally point out that, in the context of the Snowmass 2021 proceedings, simulation codes relevant to all possible types of high-energy interactions are reviewed in ref. [1].

2   The PYTHIA QED showers

Leif Gellersen, Torbjörn Sjöstrand, Rob Verheyen

2.1   Introduction

PYTHIA [2, 3] has three parton-shower options, the older simple one that still remains default, and the newer Vincia and DIRE ones. Each of these include QCD and QED evolution, and also a varying selection of further branching kinds. Here we only summarize the key QED aspects.

The three parton shower options in PYTHIA span a wide variety of ideas and models, from a purely positive rate dipole model ("simple shower"), an indefinite-sign dipole model (DIRE), to a multipole radiation approach (Vincia). The models further employ different evolution variables, splitting functions, and phase space parametrizations. As an example, α_{EM} can be chosen either fixed at vanishing momentum transfer or running at the shower evolution scale in the simple and Vincia showers, with the latter default, while DIRE only admits the former option. These different choices make PYTHIA a valuable tool to assess QED modelling uncertainties.

None of the three showers has an internal implementation of beamstrahlung, and currently there is no way to input beamstrahlung consistently separated from bremsstrahlung.

2.2   The simple shower QED handling

In e^+e^- annihilation events the simple shower handling of QED initial-state radiation (ISR) and final-state radiation (FSR) is decoupled, i.e. interference effects are neglected. For on-shell Z^0, $W^\pm$ and H^0 production this is a good approximation for photon energies above the respective resonance width. Emissions are ordered in terms of a decreasing $p^2_{\perp\text{evol}}$ scale, i.e. by backwards evolution for ISR [4]. Here

$$p^2_{\perp\text{evol}} = \begin{cases} z(1-z)Q^2 & \text{for FSR}, \\ (1-z)Q^2 & \text{for ISR} \end{cases} \tag{2.1}$$

[5], where Q^2 is the time- or spacelike virtuality associated with a branching, and z describes the energy sharing in it, by standard DGLAP splitting kernels, like

$$\mathrm{d}\mathscr{P}_{f \to f\gamma} = e_f^2 \frac{\alpha_{\mathrm{EM}}}{2\pi} \frac{\mathrm{d}p_{\perp \mathrm{evol}}^2}{p_{\perp \mathrm{evol}}^2} \frac{1+z^2}{1-z} \mathrm{d}z \,, \tag{2.2}$$

where e_f is the electrical charge of the fermion f.

FSR is handled in a dipole picture. In it, the radiation of a $f\overline{f}'$ pair is split as a sum of radiation from the two ends. Specifically, consider the branching $a \to bc$ with a recoiler r at the other end of the (a, r) dipole, and c here representing the radiated photon. The $p_{\perp \mathrm{evol}}^2$ and z values of the branching defines the virtuality $m_a^2 = Q^2 = p_{\perp \mathrm{evol}}^2/z(1-z)$, which leads to a redistribution of E_a and E_r. Thereafter $E_b = zE_a$ and $E_c = (1-z)E_a$. This procedure reproduces the singularity structure of relevant matrix elements. The sum of radiation from the two dipole ends gives a numerator that exceeds the matrix-elements one, so the veto algorithm [2] can be used to correct the emission rate to agree with matrix elements for the first emission [6], modulo Sudakov factors. Fermion mass effects are included in the shower to still match singularities and matrix elements for Z^0 and H^0 decays, whereas the $W^\pm \to f\overline{f}'\gamma$ matrix element is only coded in the massless limit.

A dipole picture is also used to allow $\gamma \to f\overline{f}$ branchings, where the mother parton (b in $a \to bc$) acts as a recoiler. This opens up for the creation of several charge pairs in a resonance decay. There is no multipole handling, but instead each new fermion pair is handled as a dipole fully separated from other dipoles in the event.

For the backwards evolution of ISR, ratios of an already existing PDF need to be used. The starting point is an expression resummed to LL and matched to an exact $O(\alpha^2)$ result [7, 8], too lengthy to be reproduced here, whose leading $x \to 1$ behaviour reads

$$f_e^e(x, Q^2) \approx \frac{\beta}{2}(1-x)^{\beta/2-1} \,; \quad \beta \approx \frac{2\alpha_{\mathrm{EM}}}{\pi}\left(\ln\frac{Q^2}{m_e^2} - 1\right) \,. \tag{2.3}$$

The form is divergent but integrable for $x \to 1$, which gives numerical problems in this limit. To this end the PDF is set to zero for $x > 1 - 10^{-10}$, and is rescaled upwards in the range $1 - 10^{-7} < x < 1 - 10^{-10}$, in such a way that the total area under the parton distribution is preserved:

$$f_{e,\mathrm{mod}}^e(x, Q^2) = \begin{cases} f_e^e(x, Q^2) & 0 \leq x \leq 1 - 10^{-7} \\ \dfrac{1000^{\beta/2}}{1000^{\beta/2} - 1} f_e^e(x, Q^2) & 1 - 10^{-7} < x < 1 - 10^{-10} \\ 0 & x > 1 - 10^{-10} \,. \end{cases} \tag{2.4}$$

The fact that the backwards evolution does not end up with an electron at $x \equiv 1$ is compensated by inserting an extra photon along the beam axis with the remaining energy.

The z variable of the splitting kernel in ISR is given by the mass-square ratio of the radiator+recoiler system before to after the backwards step. This again guarantees the same soft- and collinear-photon singularities as in matrix elements. For the $e^+e^- \to \gamma^*/Z^0$ process this can be used to perform a matrix-element correction for the first/hardest emission [9].

2.3 Vincia's QED shower

Vincia is a $p_\perp$-ordered parton shower based on the antenna formalism. The fundamental branching step is $2 \to 3$, where the two pre-branching momenta are treated on equal footing. The soft

eikonal contribution to the radiation pattern remains unpartitioned, and is fully contained in Vincia's branching kernels, which are referred to as antenna functions. By contrast, the more common dipole showers partition the antenna into two separate dipole functions, in which one of the pre-branching momenta is assigned to be the splitter and acquires all transverse recoil.

For a generic branching $IK \rightarrow ijk$, where j is the radiated momentum, the ordering scale is given by

$$p_\perp^2 = \frac{\bar{q}_{ij}^2 \bar{q}_{jk}^2}{s_{\max}}, \text{ with } \bar{q}_{ij} = \begin{cases} s_{ij} + m_i^2 + m_j^2 - m_I^2 & i \text{ is final-state} \\ s_{ij} - m_i^2 - m_j^2 + m_I^2 & i \text{ is initial-state} \end{cases}, \tag{2.5}$$

where $s_{ij} = 2p_i \cdot p_j$ and $s_{\max}$ is the largest antenna invariant mass, which depends on which momenta are initial-state or final-state. The other major components of the shower algorithm are the phase space factorization, as well as the associated kinematic mapping, and the exact form of the antenna functions. These, and many other details may be found in [10].

Vincia's QED shower has been developed in [11, 12], and is described there in detail. An important component is given by the photon emission antenna function, which, for final-state radiators, is given by

$$A_{\gamma/IK}(s_{ij}, s_{jk}, m_i^2, m_j^2, s_{IK}) = g^2 Q_I Q_K \bar{A}_{\gamma/IK}(s_{ij}, s_{jk}, m_i^2, m_j^2, s_{IK}), \tag{2.6}$$

where

$$\bar{A}_{\gamma/IK}(s_{ij}, s_{jk}, m_i^2, m_j^2, s_{IK}) = -2g^2 Q_I Q_K$$
$$\left[2\frac{s_{ik}}{s_{ij}s_{jk}} - 2\frac{m_i^2}{s_{ij}^2} - 2\frac{m_k^2}{s_{jk}^2} + \frac{1}{s_{IK}}\left(\delta_{If}\frac{s_{ij}}{s_{jk}} + \delta_{Kf}\frac{s_{jk}}{s_{ij}}\right) + \right.$$
$$\left. \delta_{IW}\frac{4}{3}\frac{s_{ij}}{s_{IK}^2}\left(\frac{s_{jk}}{s_{IK} - s_{jk}} + \frac{s_{jk}(s_{IK} - s_{jk})}{s_{IK}^2}\right) + \delta_{KW}\frac{4}{3}\frac{s_{jk}}{s_{IK}^2}\left(\frac{s_{ij}}{s_{IK} - s_{ij}} + \frac{s_{ij}(s_{IK} - s_{ij})}{s_{IK}^2}\right) \right]. \tag{2.7}$$

Here, Q_I and Q_K are the electromagnetic charges of I and K, and the Kronecker deltas ensure the correct collinear terms are incorporated in the case where I and K are either fermions or W-bosons. The corresponding initial-state antenna may be found by employing crossing symmetry.

A straightforward shower implementation in the same spirit of the QCD shower using eq. (2.6) directly suffers from the issue that the product $-Q_I Q_K$ is negative for same-sign antennae, making a probabilistic implementation troublesome. Rather than resorting to negatively weighted events, Vincia's most sophisticated photon radiation algorithm solves this issue by defining a single branching kernel

$$A_{\gamma/\mathrm{coh}} = \sum_{\{IK\}} \sigma_I Q_I \sigma_K Q_K \bar{A}_{\gamma/IK}(s_{ij}, s_{jk}, m_i^2, m_j^2, s_{IK}), \tag{2.8}$$

where $\{IK\}$ runs over all pairs of charged particles, and σ_I and σ_K are $1\,(-1)$ for final-state (initial-state) momenta. This branching kernel is positive, and contains the complete set of soft multipole eikonal factors, as well as all collinear limits [11]. Its singular structure is however not straightforwardly regularized by the ordering scale of eq. (2.5). The QED shower implements eq. (2.8) by

sectorizing the phase space according to

$$A_{\gamma/\text{coh}} \to \sum_{\{ik\}} \Theta_{ik}^{\text{sct}} \bar{A}_{\gamma/\text{coh}}, \quad \text{where } \Theta_{ik}^{\text{sct}} = \theta\left(\min_{\{xy\}} p_{\perp,xy}^2 - p_{\perp,ik}^2\right). \tag{2.9}$$

That is, the radiative phase space is divided into regions such that the photon is always radiated by the two charged particles that have the smallest $p_\perp$ with respect to the photon. This procedure is equivalent to ordering the shower evolution in terms of $\min_{\{ik\}} p_{\perp,ik}^2$, which does indeed regulate all singularities of eq. (2.8). This implementation thus accomplishes a modelling of fully coherent photon radiation without resorting to negative weights, and it is thus the default choice.

However, the above algorithm requires sampling emissions in all sectors, the number of which scales like $O(n_{\text{chg}}^2)$. An alternative, faster and unsectorized approach is also available which instead approximates the radiation pattern as

$$A_{\gamma/\text{pair}} = \sum_{[IK]} Q_{[IK]}^2 A_{\gamma/IK}(s_{ij}, s_{jk}, m_i^2, m_j^2, s_{IK}), \tag{2.10}$$

where $[IK]$ runs over all pairings of charged particles with opposite charges, including the sign factors σ_I and σ_K. All contributions in eq. (2.10) are positive and can thus be sampled individually, similar to leading-N_C QCD. Charges are paired up by minimizing the sum of antenna invariant masses following the principle of maximum screening [12], which is technically accomplished through the Hungarian algorithm [13–15]. While this algorithm is generally faster, it only approximates the soft multipole photon emission structure.

The QED shower also includes photon splittings to charged fermions, both in the initial state and the final state. Photon radiation off quarks and photon splitting to quarks is cut off at a scale close to Λ_{QCD}, but radiation off and splitting to leptons is continued to a much lower scale. Radiation in resonance systems is also included following the procedures set out in [16]. However, QED radiation off charged hadrons and in hadron decays is not currently implemented.

2.4 The DIRE QED shower

The DIRE parton shower for PYTHIA was introduced in [17] and combines the soft-emission treatment of $2 \to 3$ dipole/antenna showers with the identification of collinear emissions familiar from traditional $1 \to 2$ showers. The shower evolution variable t corresponds to a scaled soft transverse momentum and is chosen to be symmetric between the identified radiating parton i and the parton taking the recoil k in a branching $(i1), k \to i, 1, k$,

$$t \propto \frac{(p_i p_1)(p_1 p_k)}{Q^2}. \tag{2.11}$$

Here, Q^2 denotes a dipole-type-dependent maximum scale, and p_i, p_1 and p_k represent the momenta of the involved partons after the branching.

The radiating dipoles in DIRE allow for radiation from any combination of initial and final state partons, i.e. final state radiators with final state recoilers (FF), final state radiators with initial state recoilers (FI), initial state radiators with final state recoilers (IF) and initial state radiators with initial state recoilers (II). The branching rates are constructed from a partial fractioning of the soft

radiation pattern augmented with collinear terms in both the massless and massive case following the ideas presented in [18] and [19, 20].

Details about the ordering, kinematic mappings for the respective dipole types and the branching rates may be found in [17]. DIRE allows for the use of negative splitting functions as described in [17, 21], and is thus not restricted to the formulation of branchings in terms of probabilities bounded by zero and one.

The treatment of QED radiation in DIRE is described in [22, 23] and is in parts inspired by [19, 24]. The QED branchings are similar to the QCD treatment, with the coupling factor replaced by the weak coupling, and colour charge factors replaced by QED charge correlators

$$
q^2 = \begin{cases} -\frac{\eta_{i1}\eta_k q_{i1} q_k}{q_{i1}^2} & \text{for } f \to f\gamma \\ \frac{1}{\#\text{recoilers}} & \text{for } \gamma \to f\bar{f} \end{cases} ,
\tag{2.12}
$$

where q_{i1} and q_k denote the electric charges of the corresponding partons and η is $+1$ for final state and -1 for initial state partons. As opposed to the leading color QCD case, any combination of charges might radiate, leading to a larger number of allowed dipoles. Depending on the sign of the correlator, these might enter with a negative sign, mandating the utilization of the weighted shower algorithm to deal with negative contributions. Following the arguments of [25], the QED coupling is kept fixed at its value in the Thompson limit. This should be appropriate for on-shell final-state photons, but might lead to a suboptimal description of off-shell intermediate photons produced by $\gamma \to f\bar{f}$ branchings.

In DIRE, the description of one or more QED emissions is fully integrated into the shower's merging machinery. In particular, this also means that QED radiation patterns can be improved by employing iterative matrix element corrections. Writing the shower splitting kernels as $P \equiv P(\Phi_{n+1}/\Phi_n)$, where Φ denotes the phase space point for n or $n+1$ partons before and after a branching, the shower generates a Φ_{n+1} configuration with the rate

$$
\sum_{\Phi_n, P} \frac{8\pi\alpha P(\Phi_{n+1}/\Phi_n)}{Q^2(\Phi_n)} \left|\mathcal{M}(\Phi_n)\right|^2 .
\tag{2.13}
$$

This expression may contain both QCD- and QED-like emissions encoded in the splitting kernels, and the coupling α may represent the strong or electroweak coupling depending on the corresponding kernel. For a given state, the reconstruction of all possible shower emission histories leading to this state allows for calculation of a corrective factor

$$
\mathcal{R}(\Phi_{n+1}) = \frac{\left|\mathcal{M}(\Phi_{n+1})\right|^2}{\sum_{\Phi_n'} \frac{8\pi\alpha P(\Phi_{n+1}/\Phi_n')}{Q^2(\Phi_n')} \left|\mathcal{M}(\Phi_n')\right|^2} ,
\tag{2.14}
$$

which is applied again using the weighted shower algorithm. For iterated branchings, the corresponding denominator is constructed by taking multiple branchings and their respective corrections into account. In this way, multiple emissions can be matrix-element corrected. This approach even allows for mixed QCD and QED shower histories, and by employing suitable matrix elements, also interference effects between QCD and QED. For further details, see [23]. This approach in principle also allows for the incorporation of QED interference effects between initial and final state radiation, which we have not yet studied in detail.

The treatment of initial-state lepton PDFs is similar to the simple shower model above, i.e. the lepton PDF is split into the same three regions, to avoid evaluating splittings close to integrable singularities. However, in the case of a leptonic initial state recoiler, even a final state emission might change the "parton" flux of the collision event. Due to the steep rise of the lepton PDF $f_e^e(x, Q^2)$ for $x \to 1$, the corresponding PDF ratios might become (much) larger than unity. This effect is not of immediate concern for weighted shower algorithm, which would still yield correct emission rates without the need to limit the value of the PDF ratio. However, if the overestimate does not attempt to take this enhancement into account, the resulting sample might contain a few events with very high weights. Thus, the shower overestimates for splittings with initial-state lepton recoilers have been judiciously extended with additional terms that, for small $1 - x$, allow to improve the statistical stability of the simulation by employing multi-channel sampling.

Finally, it is worth noting that QED emissions can be enhanced with a method that combines the "boost" of [26] with the weighted shower of [21]. Given that negative contributions to the emission rate – which lead to event weights – are not coupling-suppressed relative to positive contributions, very large "boosts" C with $C\alpha_{\text{EM}} \gg \alpha_s$ can however lead to a poor statistical convergence.

Acknowledgments

3 QED radiation in Herwig

Mohammad Masouminia, Simon Plätzer, Peter Richardson

QED radiation in Herwig is available in the angular ordered shower, and we are also developing it for the dipole shower. In order to understand why QED is not a simple 'downscaling' of the QCD evolution, and how coherent branching algorithms ease the inclusion in existing algorithms, we will briefly review generic features of QCD coherence to introduce how QED radiation is actually handled.

QCD coherence has been a design criterion behind parton branching algorithms since their early application to resummation of event shape variables [27] and the first accurate parton shower algorithms [28]. In particular, soft gluon emission from collinear bundles of partons effectively appear as emissions from the net colour charges carried by the collinear bundle. Observables which globally measure the deviation from a certain jet system, without any particular hierarchy in between the structure of the jets, can thus be reliably described by ordering emissions in decreasing opening angle. The modern version of this evolution, improving on mass effects and a covariant description of the angular ordering variable is at heart of the Herwig angular ordered shower [29, 30].

The non-abelian nature of QCD implies a change of the colour charge distribution, which means that each emission restricts the opening angle available to subsequent emissions. Angular

ordering in this case is also inherent in each dipole of colour charges, which, subject to azimuthal averaging will then give rise to the respective destructive interference outside of the opening cones of each dipole. Dipole-type parton showers, which locally account for this change in the radiation pattern, are usually formulated in the limit of infinitely many colour charges, in which a probabilistic sequence of emissions from a dipole emerges in terms of a transition of one dipole into two colour charge dipoles. Coherent showers, based on angular ordering, do not require the large-N limit and are able to predict full-colour accurate contributions to event shapes deviating from the two-jet limit.

The conservation of colour charge in emission of spin one particles,

$$\sum_{i=1}^{n} \mathbf{T}_i |\mathcal{M}(p_1,...,p_n)\rangle = 0 \ , \tag{3.1}$$

where $\mathbf{T}_i$ are colour-charge operators and $\mathcal{M}$ is a gauge-invariant hard process amplitude, is crucial to simplify colour correlations inherent to large-angle soft radiation and to translate their contribution into the soft enhanced contributions of the (colour-diagonal) QCD splitting functions. This employs the fact that collinear radiation only refers to one leg and as such we can simplify colour correlations using

$$- \sum_{j \neq i} \mathbf{T}_i \cdot \mathbf{T}_j |\mathcal{M}\rangle = \mathbf{T}_i^2 |\mathcal{M}\rangle \tag{3.2}$$

where the Casimir operator of leg i is colour-diagonal. This relation enables one to define dipole shower algorithms including hard-collinear contributions [31], and is at the heart of using coherence to properly describe the large-angle soft radiation pattern which then subsequently is completed by collinear radiation in an angular ordered shower. Spin correlations can also be accounted for in such a framework [32].

QED radiation is, due the spin one nature of the photon, and the conservation of electric charge, in many facettes very similar to QCD. Several simplifications and complications are present at the same time: Due to the abelian nature of the underlying gauge group, the charges Q_i are simple numbers, not operators. To this extent, no complicated tracking of flow of charge is needed. At the same point, however, nothing like a large-N limit exists in QED and while a dipole-type shower (with no branching dipoles, but the same dipole emitting multiple times) is possible, the corresponding charge correlators $-Q_i \cdot Q_j$ can become negative for same-sign charges (in QCD, $-\mathbf{T}_i \cdot \mathbf{T}_j$ is always positive semi-definite in the large-N limit). While we can account for these negative contributions through newly developing weighted shower algorithms [33], with an implementation of QED radiation in the Herwig dipole shower being in progress, coherence can also assist in the QED case: A separation into several collinearly enhanced directions i allows to encode the electric charge correlations to be translated into positive-definite contributions according to the charge squared Q_i^2, and large-angle photon radiation, which is resolved independently as deviating from a jetty system with only small-angle QED radiation, can as well be encoded through an initial condition which identifies angular ordered cones from the electric charge partners in the hard process.

Generally speaking, finding of physically-allowed QED partners only depends on the initial evolution scale of the shower progenitor and the kinematical relationship between the pair, without dependence on the dynamics. The additional complication consists in the need for a separate evolution variable describing angular ordering with respect tot QED dipoles, which needs to be

interleaved with the QCD angular ordering variable. Extensions of this paradigm are currently explored in the Herwig angular ordered shower for other interactions, while we are also making progress in formulating an according dipole-type picture.

Specifically for e^+e^- collisions we still handle initial state radiation with an approach that employs a Weizsäcker-Williams function [34–36]: we randomly sample it twice (once per incoming leg), in order to obtain the fraction of the incoming-beam energy lost to initial-state radiation, and thus the energy available to the hard scattering. However, given the structure of the angular ordered shower, backward evolution will be readily available once a full QED PDF is available through the LHAPDF library. The value of the QED coupling constant is set equal to the Thomson value, unless the production or the branching mechanism(s) involve heavy weakly-interacting bosons, in which case $\alpha(m_Z)$ is used instead. The effects of beam dynamics, and in particular of beamstrahlung, are ignored.

4 Lepton collisions and QED FSR in SHERPA

L. Flower, S. Hoeche, A. Price, M. Schönherr

4.1 Introduction

The SHERPA event generator currently offers two different approaches to treating QED ISR. The first approach uses the so called electron structure function[1], which is a solution of the DGLAP evolution equations [39–42] using leading order (LO) initial conditions [43]. This analytic approach can be combined with a traditional parton shower, extended to QED [44], to generate exclusive kinematic distributions for the collinear photons. In the second approach, the emission of soft photons is resummed to all orders using the Yennie-Frautschi-Suura [45](YFS) formalism. In this method, the photon emissions are considered in a fully differential form where the photons are explicitly created and the treatment of their phasespace is exact.

4.2 Collinear Resummation

The structure function approach [46] resums the leading logarithmic (LL) corrections, using the DGLAP evolution equations, into universal factors. It allows to write the total cross section for the process $e^+e^- \to X$ in the factorized form

$$\mathrm{d}\sigma(s) = \int \mathrm{d}x_1 \mathrm{d}x_2 \, f_{e^+}(x_1, Q^2) f_{e^-}(x_2, Q^2) \, \mathrm{d}\hat{\sigma}(x_1 x_2 s) \,, \tag{4.1}$$

where $\mathrm{d}\hat{\sigma}$ is the partonic cross section. The structure functions $f_{e^\pm}(x, Q^2)$ that are commonly used today are obtained from solutions of the evolution equations using LO initial conditions [43]. For the electron this initial condition is a Dirac delta function in x, $\delta(1-x)$. At LL accuracy, $f_{e^+}(x) = f_{e^-}(x)$ is given by

$$f_{e^\pm}(x, Q^2) = \beta \frac{\exp\left(-\gamma_E \beta + \frac{3}{4}\beta_S\right)}{\Gamma(1+\beta)} (1-x)^{\beta-1} + \beta_H \sum_{n=0}^{\infty} \beta_H^n \, \mathcal{H}_n(x) \,, \tag{4.2}$$

---

[1]In SHERPA this is not a true PDF, as it contains no information on the photon content of the electron, and it is defined in the LL limit. The current state of the art is NLL accurate as described in [37, 38]

–9–

Scheme	β_S	β_H	Refs
Beta	β	β	[47]
Eta	η	η	[48]
Mixed	β	η	[49]

Table 1. The different scheme choices available in SHERPA for the electron structure function, where $\beta = \frac{\alpha}{\pi}\left(\ln(s/m_e^2) - 1\right)$ and $\eta = \frac{\alpha}{\pi}\ln(s/m_e^2)$.

with $\beta = \frac{\alpha}{\pi}\left(\ln(s/m_e^2) - 1\right)$ and the hard coefficients $\mathcal{H}_n(x)$ given in [47–50]. The QED coupling constant α is taken at scale Q^2. By default, SHERPA includes the hard coefficients up to second order ($n = 2$). However, there is some freedom in how non-leading terms are taken into account. The choice reflects how the soft photon residue is treated, i.e. whether it is proportional to $\ln(s/m_e^2)$ or $\ln(s/m_e^2) - 1$. The corresponding options for the corresponding parameters β_S and β_H are listed in Tab. 1. [2]

4.3 Parton Shower

The structure function can be combined with a QED parton shower [44] to generate exclusive multi-photon final states. SHERPA includes two parton showers, CSSHOWER [51] and DIRE [17], but only the CSSHOWER currently supports QED radiation [44]. [3] It is based on Catani–Seymour dipole factorisation [18, 20], with its extension to resummation first proposed in [52], and implemented simultaenously in [51] and [53]. The algorithm builds on a set of generic operators for particle emission off (color) charged dipoles in unintegrated and spin-averaged form. Soft eikonals are matched to collinear splitting functions in order to eliminate double counting of soft singularities. The splittings are ordered by their associated transverse momenta. In the case of QCD, the large-N_c limit is used to restrict the numbers of spectators to the leading ones with positive definite color-correlators. Contributions from neglected spectators can be shown to be suppressed by powers of $1/N_c^2$, contributing little to a standard observables.

SHERPA extends this algorithm to photon emissions off charged fermions, making use of the fact that QCD and QED splittings only differ in their color- or charge-correlators. In the case of QED, to retain positive definiteness, only opposite charges are considered to form valid dipoles, discarding like-signed ones. However, due to the lack of a $1/N_c^2$-like suppression this degrades the quality of the QED parton shower approximation. Efforts are currently underway to extend this algorithm to include also like-sign charged dipoles, restoring the exact soft-photon limit, making use of the weighted Sudakov veto algorithm [21, 26, 44, 54]. In a concurrent development photon split-tings into fermion-antifermion pairs will be included in the near future. While photon emissions

---

[2] There is no such freedom of choice within the YFS resummation. The term $\beta = \frac{\alpha}{\pi}(\ln(s/m_e^2) - 1)$ is a direct result from the analytical integration over the entire soft-photon phasespace and is needed to achieve the cancellation of IR singularities.

[3] An extension of the DIRE shower to include QED radiation is straightforward and will be pursued in the future.

off charged quarks and leptons use the QED coupling constant in the Thomson limit, $\alpha(0)$, photon splittings instead evaluate the coupling constant at the invariant mass of the produced fermion pair.

Within SHERPA, radiation off final state leptons will normally be handled by the YFS simulation module PHOTONS. If the QED shower is to be used, it must therefore be enabled explicitly by the user, and the YFS based resummation needs to be disabled to avoid double counting.

4.4 Beam spectra

In addition to providing the electron structure function, SHERPA allows for a two-step definition of particles entering a hard interaction. The simulated beam particles can differ from the collider bunch particles, and their energy spectra can therefore be modified. For e^+e^- colliders we anticipate that an interface to the CIRCE [55] package, which parametrizes the $e^\pm$, and γ beam-spectra based on the collider geometry. Two prominent examples for beam spectra that change the incident particle species are

- Laser backscattering, where the initial lepton beam sources highly energetic photons through Compton scattering [56–58],

- The equivalent photon approxmination (Weizsäcker–Williams approximation), where the beam particles act as quasi-classical sources of collinear quasi-real photons [35, 59, 60].

The thus generated photons can then either enter the hard interaction directly or be further resolved using, e.g., their respective structure functions [61, 62], upon which they enter parton evolution through a parton shower.

4.5 Soft Resummation

The YFS formalism provides a robust method for resumming the emission of real and virtual photons in the soft limit to all orders. This resummation can be further improved by including exact fixed-order expression in a systematic way. In this chapter, we will first introduce the general YFS framework and then will concentrate on its applications to e^+e^- collisions.

The total cross section for the production of a configuration of particles in the final state, $d\Phi_Q$, including all higher-order corrections, is given by summing over all real and virtual photons, n_γ and n_γ^V, wrt. its leading order configuration,

$$d\sigma = \sum_{n_\gamma=0}^{\infty} \frac{1}{n_\gamma!} d\Phi_Q \left[\prod_{i=1}^{n_\gamma} d\Phi_i^\gamma \right] (2\pi)^4 \delta^4 \left(\sum_{\text{in}} q_{\text{in}} - \sum_{\text{out}} q_{\text{out}} - \sum_{i=1}^{n_\gamma} k_i \right) \left| \sum_{n_\gamma^V=0}^{\infty} \mathcal{M}_{n_\gamma}^{n_\gamma^V + \frac{1}{2} n_\gamma} \right|^2 . \qquad (4.3)$$

$d\Phi_i^\gamma$ is the phase space element of photon i with momentum k_i. In the notation introduced here for the matrix element $\mathcal{M}$, the Born level contribution will be defined as $\mathcal{M}_0^0$, while the matrix element $\mathcal{M}_{n_\gamma}^p$ will refer to the Born process plus n_γ real photons evaluated at an overall power p in the electromagnetic coupling α. While this expression includes photon emissions to all orders in principle, only the first few terms in the perturbative series can be computed in practice. Following the YFS approach the total cross section can be reformulated in such a way that the infrared divergences are

resumed to infinite order yielding,

$$d\sigma = \sum_{n_\gamma=0}^{\infty} \frac{e^{Y(\Omega)}}{n_\gamma!} d\Phi_Q \left[\prod_{i=1}^{n_\gamma} d\Phi_i^\gamma \tilde{S}(k_i) \right] \left(\tilde{\beta}_0 + \sum_{j=1}^{n_\gamma} \frac{\tilde{\beta}_1(k_j)}{\tilde{S}(k_j)} + \sum_{\substack{j,k=1 \\ j<k}}^{n_\gamma} \frac{\tilde{\beta}_2(k_j,k_k)}{\tilde{S}(k_j)\tilde{S}(k_k)} + \cdots \right). \qquad (4.4)$$

Therein,

- $Y(\Omega)$ is the YFS form factor which contains contributions from real and virtual photons, inside the soft domain Ω, summed to infinite order. It can be computed using a dipole decomposition .

- $\tilde{S}(k)$ is the soft YFS eikonal associated with the emission of real photons and can also be decomposed in dipoles, $\tilde{S}(k) = \sum_{i,j} \frac{\alpha}{4\pi^2} Z_i Z_j \theta_i \theta_j \left(\frac{p_i}{p_i \cdot k} - \frac{p_j}{p_j \cdot k} \right)^2$, where i and j label all charged particles of the process, Z_i and Z_j are their charges, and $\theta_{i/j} = +1(-1)$ if particle i/j is in the final (initial) state.

- The remaining terms inside the brackets are the infrared finite residuals $\tilde{\beta}_{n_\gamma}$, comprising infrared subtracted squared matrix elements with n_γ real photons. They can be systematically calculated order-by-order in perturbation theory, $\tilde{\beta}_{n_\gamma} = \sum_{n_\gamma^V} \tilde{\beta}_{n_\gamma}^{n_\gamma^V + n_\gamma}$. For example, up to NLO, we need to include the Born amplitude $\tilde{\beta}_0^0$ as well as the infrared finite renormalised one-loop corrections $\tilde{\beta}_0^1$ and the infrared finite hard remainder of the tree-level expression including one additional photon $\tilde{\beta}_1^1$. In SHERPA, the ISR corrections for e^+e^- initial states have been implemented [63] using explicit differential distributions [64] and for FSR corrections to $Z \to \ell^+\ell^-$ decays explicit matrix elements including up to NLO EW and NNLO QED [65] corrections are used.

- The QED coupling constants associated with the resummation of soft-photon emissions is taken in the Thomson limit, $\alpha(0)$. All other QED couplings present in the Born-level expression $\mathcal{M}_0^0$ may be evaluated at a different suitable scale, typically defined at short-distances, like α_{G_μ}, $\alpha(m_Z)$, etc.

In the SHERPA-2 series this resummation was implemented for the leptonic final states in the PHOTONS module [66]. This was further extended to include NLO_{EW} and $NNLO_{QED}$ [65] effects in the decay of electroweak bosons. More recently, in the SHERPA-3 series the YFS resummation has been extended to include initial state radiation for lepton-lepton collisions [67, 68]. One of the advantages of the YFS method is that perturbative corrections can be included in a systematic way order-by-order. In its current implementation these perturbative corrections are included up to $O(\alpha^3 L^3)$ by using analytical expression derived in [64]. This level of accuracy, while sufficient for LEP, still falls short of the predicted accuracy needed for future lepton colliders [69], such that future refinements are needed. The second advantage of the YFS algorithm is the explicit treatment of the photon phasespace. The photon momenta are distributed according to the eikonal factors [70], which allows for explicit photons in the event record.

In addition to the initial and final state soft photon resummation, a special treatment for QED corrections in processes with W bosons has also been implemented. The infrared factorization of

soft-photons can be easily extended to include the emission from W bosons. This can be seen by considering the amplitude for emission of soft photons from a spin-1 boson with charge Q_W and mass M_W. Due to the spin independence of the soft current, this amplitude has the same form as in the spin-$\frac{1}{2}$ case [71], and the known expressions can be used by substituting $m_f \to m_W$ and $Q_f \to Q_W$ in the respective constituent dipoles. Another important correction to W^+W^- production is that of the electromagnetic Coulomb interaction at the threshold. This exchange leads to large loop-corrections in the threshold region due to the low relative velocity which enhances the cross-section by a factor $\approx \alpha\pi/v$, where v is the relative velocity. The inclusion of this loop-correction was calculated to first-order in [72–75] and it was shown to, in the threshold region, produce a positive correction.

Currently, the dedicated higher-order corrections implemented in SHERPA do not include any coherence effects from interfering initial and final state emissions. These will enter in the infrared-finite $\tilde{\beta}$ and will be included in future improvements. In particular, it is a goal of the SHERPA collaboration to automatically calculate the matrix elements corrections using the ME generators AMEGIC [76] and COMIX [77]. As well as automating the real corrections internally, we plan to include one loop EW corrections in an automated fashion using tools such as OPENLOOPS [78, 79] or RECOLA[80]. These corrections corrections are particular importance in the light of the to-be-achieved the experimental precision of future Higgs factories.

Finally, the YFS soft photon resummation only captures collinear effects through its infrared finite residuals. Thus, an extension to incorporate photon splittings to charged particle pairs in the final-state is currently under development. These splittings are at least of relative $O\left(\alpha^2\right)$ compared to the Born configuration, but the possibility for a photon to split into a pair of charged particles may have important consequences for the dressing dressing of, e.g., the primary leptons who emitted the photons in the first place. Therefore we allow photons to split into electrons, muons, and/or quarks or charged hadrons (depending on the energy scale) in a reduced parton shower with a reconstructed starting scale for the independent collinear evolution of each photon.

Acknowledgments

5 The WHIZARD **event generator for future lepton lolliders**

Jürgen Reuter

5.1 Introduction to WHIZARD

WHIZARD is a multi-purpose event generator for lepton, hadron and lepton-hadron collider physics, originally developed for applications in lepton collider physics for the planned linear collider TESLA, and has also been applied to fixed-target experiments. From its early application originates its now deprecated synonym, "*W*, *Hi*ggs, *Z*, *A*nd *R*espective *D*ecays". WHIZARD is a complete framework for very general high-energy physics simulations in a modular form that allows a high level of flexibility [81]. The program core is written in modern, object-oriented Fortran, while its matrix-element generator, O'MEGA, is written in the function programming language OCaml. Dating back to the late 1990s, the program was rewritten as version 2.0.0, released in April 2010 for LHC physics, with the most recent version as of January 2022 being 3.0.2. Version 3.0.0 marked the milestone of automated NLO calculations.

The purpose of this contribution is, after a short introduction into the tool, to give an overview of WHIZARD's capabilities for future e^+e^- colliders, together with its short- and mid-term plans. On the technical side, WHIZARD uses a modern, object-oriented software framework with a highly modular structure. Most parts of the program core are endowed with unit tests, and the majority of features is tested by means of core and extended functional tests in a continuous-integration system. These tests cover all aspects of the code, even Ward identities and supersymmetric Ward identities are used [82] to protect against regressions. Git is used as a version-control system for development.

5.2 Hard matrix elements: leading order and BSM

For hard-scattering processes, WHIZARD provides its own (tree-level) matrix-element generator, O'MEGA [83], which produces matrix elements in a recursive way as directed acyclical graphs. For QCD, WHIZARD and O'MEGA use the color-flow formalism [84]. This framework supports as hard-coded models the SM and some very common BSM models like supersymmetry, composite models and effective field theory setups. Beyond that, it has a very general interface to FeynRules [85] and UFO [86] which allows to use almost all possible external Lagrangian models. Of particular importance for the physics program at Higgs factories is the support for the complete SM effective field theory (SMEFT); to just list a few examples of additional models, extended Higgs sectors like two-Higgs doublet models, inert doublet models, Higgs-singlet extensions, Higgs portal models, twin-Higgs models, dark photons, supersymmetric and composite Higgs models are supported. Les Houches accord (SLHA-like) files can be used for inputs e.g. in parameter scans. WHIZARD also supports the definition of customized propagators from the UFO file. Loop-matrix elements for next-to-leading (NLO) QCD and EW processes (cf. Sec. 5.4 can be used by dedicated interfaces to one-loop providers (OLP) like Openloops, GoSam and Recola.

For all processes within all models, Feynman diagram selection is possible, however should be treated with care due to possible gauge-invariance violations. Processes can be factorized into production and decays by using the decay features of WHIZARD, also consecutively in decay chains. All decays of a resonance at a given final-state multiplicity can be auto-generated. In resonant processes, intermediate resonances can be specified as polarizied, e.g. for the study of specific longitudinal or transversal EW gauge bosons. This is especially important for multi-EW boson

production and vector-boson scattering [87]. The program also allows to calculate unitarity limits and to generate bin-per-bin maximal numbers of event consistent with unitarity [88–90].

WHIZARD ships with its one scripting language, SINDARIN, which supports a almost completely general framework of analysis syntax: this allows arbitrary cuts to be defined on the hard matrix elements, as well as selections for the event generation. The hard matrix elements can be convoluted with a large number of parton distribution functions, structure functions or beam spectra: these include hadron-collider proton PDFs via LHAPDF [91, 92] externally or from a selected set of internally shipped PDFs, effective W/Z approximation for the content of EW bosons inside quarks or leptons, the effective-photon approximation (EPA) [34–36], also known as Weizsäcker-Williams approximation. The latter is provided in different variants, depending on the application for low-energy $\gamma\gamma \to$ hadron background simulations or for high-energy particle production.

For lepton collisions, electron/muon PDFs are provided which sum up photons in collinear factorization (augmented by soft non-collinear photon emission to all orders at the lowest logarithmic accuracy [93]) and hard-collinear emissions up to third order. They are implemented and well tested for leading logarithmic (LL) [43, 46] accuracy and are being implemented at the moment at NLL [37, 38]. This is expected to be completed within 2022. WHIZARD supports several options for structured lepton beams: Gaussian beam spreads individually adjustable for each beam, beam spectrum files read in as tables of pairs of energy values and an approximation to Guinea-Pig spectra via its beamstrahlung generator CIRCE [55]. This supports for backwards compatibility a 6- to 7-parameter fit to the beam spectra and a smoothened, adaptive bin fit that can very well describe also wake-field machines like CLIC, photon collisions from Compton backscattering, muon colliders or plasma wake-field machines. Ongoing work will also include a proper simulation of the z-dependence along the beam axis of the beamstrahlung; this is at the moment being included in CIRCE and has then to be consistently included in the infrastructure of the WHIZARD core. This is expected within the year 2022. WHIZARD allows initial state particle of all kinds to be polarized, both for scattering as well as for decay processes. For scattering processes, the polarization of both beams can be arbitrarily correlated by specifying a spin density matrix. In addition, polarization fractions can be given. Electron PDFs are at the moment inclusive in polarization, i.e. the polarization from the beam is carried through to the hard matrix element. Work has started to investigate the effects from polarized versions of the EPA. Finally, initial state beams can be asymmetric (like in flavor factories or HERA), and crossing angles can be defined.

5.3 Phase space integration, performance, event formats

WHIZARD can write out events in all major event formats: it supports a lot of ASCII formats for backwards compatibility, it supports LHA and LHE formats (in all three different version variants), it also ships StdHEP, and it provides HepMC2 and HepMC3 as well as LCIO interfaces. Using the ROOT classes of HepMC3, WHIZARD is able to directly write out ROOT (tree) files.

As the program has always had a strong focus on weak production processes of multi-fermion final states, at lepton colliders it contains a phase-space parameterization that is flexible enough to adapt to many different (interfering) resonant production channels. This builds upon an adaptive multi-channel Monte Carlo integration encoded in the VAMP subpackage [94, 95]. In the recent years there have been several attempts to make the MC integration much more efficient by using highly parallelized computing architectures: using Multi-Processing Interface (MPI), speed-ups of

several tens up to roughly a hundred can be achieved [96]. Also, O'MEGA can produce very small expressions for the matrix elements in the form of a so-called virtual machine, which are as efficient as compiled code [97].

5.4 Higher order calculations and matching to parton showers

Turning to high-precision calculations at next-to-leading order in the SM, WHIZARD has a complete implementation for NLO QCD and electroweak (as well as mixed) corrections for hadron and lepton colliders, based on its implementation of the FKS subtraction [98–100] scheme. In the same setup as for scattering processes, NLO decays can be calculated. As mentioned above, virtual amplitudes can be used from OpenLoops [78, 79], GoSam [101, 102] or Recola [80, 103]. The automated implementation has been validated for dozens of processes for LHC and several energy stages of e^+e^- colliders. The parallelized adaptive MC integration discussed above allows to calculate processes at NLO (QCD) for rather high final-state multiplicites, e.g. $e^+e^- \to \ell\ell\nu\nu b\bar{b}H$ or $e^+e^- \to jjjjjj$ [104, 105]. In addition to the standard FKS, WHIZARD also since several years has a general implementation of a resonance-aware FKS subtraction scheme. The program provides a default framework to produce arbitrary differential distributions, using the conecpt of event groups with an analysis like e.g. Rivet [106, 107]. Electroweak corrections for lepton colliders can be calculated already for massive leptons, while the infrastructure for corrections for massless leptons is being validated right now. The NLL electron PDFs are being implemented, and first results for this are expected within 2022. Also under validation are QCD corrections to hadron collider processes for sub-leading QCD coupling powers, where overlapping QCD and electroweak infrared divergencies appear, and which cannot be separated. To defne infrared-safe quantities, WHIZARD provides jet clustering with a FastJet [108] interface as well as photon isolation [109]. To define fixed-order NLO cross sections in a 4- or 3-flavor scheme, the user can specify b-jet, c-jet and light jet clustering.

In order to generate complete events, WHIZARD provides its own parton shower, specifically k_T-ordered parton shower as well as an analytic, virtuality-order (QCD) shower. In addition, WHIZARD ships with the last Fortran Pythia version (6.427) [2] which is specifically tuned to LEP2 hadron data, and with a dedicated interface to Pythia 8 [3]; the latter allows to directly communicate between the event records of WHIZARD and PYTHIA.

For inclusive jet samples with tree-level matrix elements, WHIZARD can apply the MLM merging [110] algorithm, while for NLO matching between matrix elements and the parton shower, a general, process-independent version of POWHEG matching [111] is available for NLO QCD corrections [112]. This has been developed for colored final states in e^+e^- and is under validation for LHC processes at the moment. POWHEG matching for EW corrections is in preparation, while for mid-term planning also alternative matching and merging schemes are envisioned. In order to reconcile of multi-fermion final states, e.g. $e^+e^- \to jjjj$ with parton showering and hadronization, WHIZARD is able to find and quantify contributions from underlying resonant subprocesses, and then provide pseudo-shower histories to the final state weighted by the relative cross sections of these underlying processes. This is important to correctly hadronic correlations in the final states, and also inclusive observables like the total number of final-state neutral and charged hadrons as well as photons.

One of the most important tasks for precision physics at future Higgs factories will be a modelling of QED and photon radiation as precise as possible. For the normalization of QED cross section, a resummation based on collinear factorization gives very precise results. As mentioned above, this is possible in WHIZARD at LL level and will be available at NLL level soon. Specifically for the assessment of experimental/systematic uncertainties, an exclusive simulation of photon radiation is necessary. WHIZARD can of course produce explicit photons from matrix elements; on the other hand, the energy loss from LL electron PDF in the collinear approximation is collected in a single photon per beam. A heuristic approximation is possible to generate a p_T distribution for these photons, which can also be applied to recoiling charged leptons from Weizsäcker-Williams/EPA. The photon distribution is generated using a logarithmic scaling, while the event of the hard scattering (with subsequent parton shower and hadronization) is boosted accordingly. It has been shown that for both signal and background in monophoton dark sector searches where this distribution matters a lot, this heuristic approach agrees very well with exact matrix-element calculations [113, 114]. WHIZARD has different options to chose the value of α, which first of all depends on the electroweak scheme; the native scheme for tree-level calculations is the $G_F - M_Z - M_W$ scheme, for NLO calculations the complex-mass scheme. There is also the possibility to take α directly from the OLP provider. For the interal α, WHIZARD provides a running α as well, either at the one- or two-loop level.

While a collinear resummation results in very accurate results for cross sections of (inclusive) processes with initial-state radiation, the highest possible precision of resummed calculations has to be combined with exclusive photon radiation in the events. There are different approaches to do that, e.g. using a POWHEG or MC@NLO-type matching for QED or eikonal-based resummation in the form of the YFS formalism [45]. The WHIZARD team pursues both approaches, the first by extended the extended the NLO POWHEG matching from QCD to QED, and for the second it is starting the implementation of the YFS formalism for general processes. First results could be expected end of 2022 or early in 2023. Furthermore, WHIZARD will also get its own QED parton shower, which will be available as a relatively slim stand-alone shower for pure QED, and potentially also as an interleaved shower together with the QCD shower.

5.5 Special applications: Top and *WW* threshold

WHIZARD has a special support for the top threshold to model the process $e^+e^- \to t\bar{t} \to bW^-\bar{b}W^+$. This process allows to determine the top mass with the highest possible theoretical precision. Analytic calculations using an NRQCD EFT approach can include NNNLO corrections, which allows to reduce the error to 30-70 MeV. This calculation, however, is completely inclusive. To study experimental efficiencies and systematic uncertainties, Monte Carlo samples resembling event weights close to the true top threshold cross sections are needed. WHIZARD includes a special treatment of a matched calculation between the continuum NLO off-shell fixed-order calculation and the NLL-threshold resummed calculation avoiding double counting [115], fully off-shell and exclusive in the top decay products. This allows to study fully exclusive distributions.

In a similar framework, work has started to match resummed QED-Coulombic corrections to the QED NLO/NNLO fixed-order calculation for the *WW* threshold [116, 117]. Like the top threshold, this will be available as a dedicated process within a specialized model. These simula-

tions allow experimental studies with the desired accuracy to support measurements of the *W* mass from a threshold scan with a precision of 1-2 MeV or below.

In summary, the main ongoing work inside WHIZARD is the completion of fully automatized NLO SM corrections (QCD/EW/mixed) for any kind of collider, for arbirtrary differential distributions at fixed order, and also matched to QCD/QED/EW parton showers.

Acknowledgments

6 Lepton collisions in MadGraph5_aMC@NLO

Giovanni Stagnitto, Marco Zaro

In this Section we will report on the functionalities of MADGRAPH5_AMC@NLO related to the simulation of lepton colliders. We remind the reader that MADGRAPH5_AMC@NLO [118, 119] is a computer program for the automatic computation of LO- and NLO-accurate cross sections (the latter both in the QCD and in the EW coupling) for scattering processes. While MAD-GRAPH5_AMC@NLO is widely used in the context of LHC simulations, it can also be employed for lepton collisions. Indeed, many results for leptonic collisions where already provided in Ref. [118], including NLO-QCD corrections but limited to the case of a strictly fixed centre-of-mass energy. The extension to the case with Initial-State Radiation (ISR) at leading logarithmic accuracy (LL) and possibly beamstrahlung is more recent, and has documented in Ref. [120]. Developments are in progress for the inclusion of NLO EW corrections to the short distance cross section and a next-to-leading logarithmic (NLL) accurate treatment of ISR, allowing for the computation of NLL+NLO observables. Here we will briefly review the changes in the code which are necessary in order to deal with leptonic collisions, following the discussion in Ref. [120], and expanding it to the case of NLL ISR and NLO EW corrections. An in-depth phenomenological study of NLL+NLO effects on physical observables will be the subject of a forthcoming paper [121].

Following the notation of Refs. [38, 120], if we start from two colliding beams of electrons and positrons with momenta $P_{e^\pm}$, and we define the corresponding cross-section for the reaction

$$e^+(P_{e^+})e^-(P_{e^-}) \to X \tag{6.1}$$

as $d\Sigma_{e^+e^-}$, the following steps happen:

1. A pair (k,l) of particles emerge from beam dynamics, which carry a fraction $y^\pm$ of longitudinal momentum of the two incoming beams. The beam-level cross section factorises as a convolution of particle-level cross section $d\sigma_{kl}$ and the beamstrahlung function $\mathcal{B}_{kl}$

$$d\Sigma_{e^+e^-}(P_{e^+}, P_{e^-}) = \sum_{kl} \int dy_+ dy_- \, \mathcal{B}_{kl}(y_+, y_-) \, d\sigma_{kl}(y_+ P_{e^+}, y_- P_{e^-}). \tag{6.2}$$

2. Particles k, l undergo a hard collision, where ISR effects are included by writing $d\sigma_{kl}$ as yet another convolution of a parton-level cross section $d\hat{\sigma}_{ij}$ and QED parton distribution functions (PDFs) $\Gamma_{i/k}$

$$d\sigma_{kl}(p_k, p_l) = \sum_{ij} \int dz_+ dz_+ \, \Gamma_{i/k}(z_+, \mu, m) \, \Gamma_{j/l}(z_-, \mu, m) \, d\hat{\sigma}_{ij}(z_+ p_k, z_- p_l, \mu) \,, \qquad (6.3)$$

where $z_\pm$ are the longitudinal momentum fractions carried by the partons w.r.t. their mother particle, μ is the factorisation scale and m the lepton mass, which is neglected in the parton-level cross section. In the following, we will mostly focus on the PDFs relevant to an incoming unpolarised electron particle, Γ_{i/e^-}; the PDFs of an incoming positron are trivially related by charge conjugation. We will refer to $\Gamma_{e^\pm/e^\pm}$ as electron PDF, and to $\Gamma_{\gamma/e^\pm}$ as photon PDF.

Eq. (6.3) recalls the standard QCD factorisation formula at hadron colliders. However, at variance with hadronic PDFs, QED PDFs are entirely calculable with perturbative techniques. Their role is to resum to all order the large contributions stemming from photon collinear emissions in the initial state, which appear as logarithms of some hard physical scale E over the mass of the electron m, $\log^k(E^2/m^2)$. The collinear terms present in the PDFs are universal, and their resummation by means of QED DGLAP evolution equations [39–42] (see Ref. [122] for explicit expressions of the two-loop QED splitting kernels) is a process-independent procedure. Let us stress that within the PDF formalism, we are taking into account only the logarithms related to (hard or soft) collinear radiation off initial-state particles. In principle, by means of fragmentation functions (FFs), which are the time-like analogue of PDFs, it would be possible to also account for collinear radiation off final-state particles (as it is usually done in QCD when heavy quarks are present in the final state [123]). Soft logarithms and interference terms can instead be resummed by means of other resummation techniques [45, 64, 124–126], which are usually tailored to specific class of processes though.

In practice, both beamstrahlung and ISR effects are included in MADGRAPH5_AMC@NLO by means of the definition of suitable partonic densities. The relevant formulas are reported in Sec. 3-5 of Ref. [120] and will not be repeated here. As for ISR, the current public release of MADGRAPH5_AMC@NLO includes, for lepton collisions, the long-known LL analytical expressions [43, 127, 128], which resum the tower of $(\alpha \log(E^2/m^2))^k$ terms. Such LL analytical expressions are built out of an additive matching between a recursive solution up to some order in α, typically $O(\alpha^3)$, and an all-order α solution valid in the region $z \to 1$ (where the bulk of the cross section is), as usually done in the literature, see e.g. [129]. Note that, in the case of NLO EW (QED) corrections to the short-distance cross section with LL PDFs, a scheme of change term is needed in the short-distance cross section in order to avoid overcounting. The peculiar structure of the PDFs, which feature an integrable divergence for $z \to 1$, requires a suitable re-parameterization of the phase-space, as described in Ref. [120].

Recently in Ref. [37], QED PDFs have been extended to NLL accuracy i.e. resumming also the $\alpha(\alpha \log(E^2/m^2))^k$ terms; they have been obtained by solving the NLO evolution equations with NLO initial conditions (derived in Ref. [38]) by means of both analytical and numerical methods. By working at the NLL accuracy, the mixing between the electron/positron (and possibly other fermion families) and the photon PDFs is taken into account. Note that NLL PDFs not only provide

a NLL correction to processes with incoming electrons, but also allow to treat photon-initiated hard processes in the same framework. A public code, EPDF, has been developed in the context of Ref. [37]: it provides the numerical solution of the evolution equations, as well as the implementation of the analytical large-z solutions, both in the $\overline{\text{MS}}$ and in the Δ [130] factorisation scheme[4].

The key point to stress is that, both at LL and at NLL, the electron PDF features an integrable divergence as $z_\pm \to 1$, which has to be handled in the proper way when convoluting the short-distance cross section with the PDFs. This is why it is crucial to have an analytic control of the electron PDF in the large-z region. As for the photon PDF, it does not pose any problem in the large-z region: in the $\overline{\text{MS}}$ scheme it features at most a logarithmic divergence, which can be handled by means of a proper change of integration variables, whereas in the Δ scheme does not diverge.

The default way adopted in EPDF in order to build an electron PDF well-behaved in the whole z-range is a multiplicative matching between the numerical solution Γ_{num} and the associated analytical large-z solution Γ_{asy}. We introduce a switching point z_0 and we define the matched solution as

$$
\Gamma_{\text{mtc}}(z) = \begin{cases} \Gamma_{\text{num}}(z), & z < z_0, \\ \Gamma_{\text{asy}}(z)\dfrac{\Gamma_{\text{num}}(z_0)}{\Gamma_{\text{asy}}(z_0)}, & z > z_0. \end{cases} \tag{6.4}
$$

The switching point z_0 is chosen in such a way at z_0 the solutions $\Gamma_{\text{num}}(z_0)$ and $\Gamma_{\text{asy}}(z_0)$ are essentially identical, and the numerical solution $\Gamma_{\text{num}}(z_0)$ has not yet lost accuracy. Typical values for z_0 are between $1 - 10^{-6}$ and $1 - 10^{-7}$. Since in the $\overline{\text{MS}}$ scheme the analytical recursive solutions up to $O(\alpha^3)$ are also available [37], in such a scheme it is also possible to use a fully analytical additively-matched solution, in keeping with what was done in the literature at LL.

In practice, a runtime evaluation of the numerical solution is too slow, so it is convenient to use grids, as it is customary in the hadronic PDFs case. However, as said above, at the same time it is important to have an analytic control of the electron PDF in the $z \to 1$ region, since during the phase-space integration values of z extremely close to 1 are probed (note that one should avoid to explicitly evaluate the difference $1 - z$, so as to not incur in overflow errors). Hence, in order to build the matched solution eq. (6.4), a two-stage approach is adopted. First, we save the numerical solution as a grid in LHAPDF [92] format. Then, at runtime, we read the grid and we call the appropriate large-z solution, and eventually we perform the matching between the two solutions. The whole procedure has been implemented in a (still) private version of EPDF, which has been interfaced to MADGRAPH5_AMC@NLO. Note that EPDF is a standalone code which can in principle be linked to any other partonic generator: the user is just required to call a high-level function of EPDF.

So far, we have not considered the case of NLO EW (QED) corrections in the short-distance cross section. While the generation of the relevant matrix-elements and counterterms does not require any change in the code, it is again the structure of $\Gamma_{e^\pm/e^\pm}(z_\pm, \mu, m)$ which poses efficiency problems in the phase-space integration. We remind the reader that MADGRAPH5_AMC@NLO

---

[4]Neither $\Gamma_{i/k}$ nor $d\hat{\sigma}_{ij}$ in eq. (6.3) are physical quantities; at NLL and beyond, they depend on the choice of the factorisation scheme and on the value of the mass scale μ (it is sensible to choose a value of $\mu \sim E$, with E a scale of the order of the hardness of the process). The Δ scheme is similar to the DIS scheme usually adopted in QCD, in which one maximally simplifies the PDFs' initial conditions. We refer the interested reader to Ref. [130], where the Δ scheme is discussed in more detail.

employs the FKS subtraction scheme [98], as automated in MADFKS [100], and that in such a scheme sectors are defined in terms of pair of particles (i, j), which can be seen as the emitted parton and its sister. In the case j belongs to the initial state, the standard way the real-emission kinematic is generated in MADGRAPH5_AMC@NLO relies on the so-called event projection: in the real emission, the sum of all final-state momenta excluding parton i has the same invariant mass and rapidity as the sum of the final-state momenta in the Born kinematics (see Sec. 5 of Ref. [111] for the explicit construction). This is a necessary feature in order to be able to match NLO computations with current parton showers, as it mimics what the latter do in the case of initial-state backward evolution. However, this leads to the fact that real-emission and subtraction terms (the latter have Born kinematics) have different Bjorken x's. While this is not a problem in the case of hadron collisions, the structure of the ISR density creates serious efficiency issues if this phase-space parameterisation is adopted.

In order to cope with this issue, a new parameterisation for the real emission has been adopted, to be applied in the FKS sectors where particle j is in the initial state. Before sketching it, we stress that employing this parameterisation forbids to match with QED parton showers, unless the latter are modified in a consistent manner.

The new generation for the real emission works as follows:

1. The kinematics of the real-emission parton (i in the FKS notation) is generated from the variables

$$\xi = \frac{E_i}{2\hat{s}}, \quad y = \cos\theta_{ij}, \quad \phi. \tag{6.5}$$

   Respectively, they correspond to the rescaled energy of parton i, written in terms of the partonic energy $\hat{s}$, its angle with particle j, and the azimuth, all defined in the partonic center-of-mass frame. These variable are in a one-to-one correspondence with the integration random numbers (possibly with adaptive sampling). They uniquely define the massless four momentum k_{n+1} in the partonic c.o.m frame.

2. The kinematics of the remaining n final-state momenta $\{\bar{k}_l\}_{l=1,n}$ is generated in their c.o.m. frame. Their total invariant mass is

$$\left(\sum_{l=1,n} \bar{k}_l\right)^2 = (1-\xi)\,\hat{s}. \tag{6.6}$$

3. Finally, the momenta $\{\bar{k}_l\}_{l=1,n}$ are boosted in the partonic c.o.m. frame

$$k_l = \mathbf{B}\bar{k}_l \tag{6.7}$$

   in order to ensure momentum conservation, i.e. in the same frame we have

$$\sum_{l=1,n+1} k_l = \left(\sqrt{\hat{s}}, \vec{0}\right). \tag{6.8}$$

Thanks to these modifications, a stable and efficient evaluation of NLO EW corrections can be performed also for lepton collisions within MADGRAPH5_AMC@NLO, as it will be documented in Ref. [121].

7 BabaYaga

Carlo M. Carloni Calame, Guido Montagna, Oreste Nicrosini, Fulvio Piccinini

7.1 Introduction

The knowledge of the luminosity $\mathcal{L}$ is an important ingredient for any measurement at e^+e^- machines. The common strategy is to calculate it through the relation $\mathcal{L} = N_{obs}/\sigma_{th}$, where σ_{th} is the theoretical cross section of a QED process, namely $e^+e^- \to e^+e^-$ (Bhabha [5]), $e^+e^- \to \mu^+\mu^-$ or $e^+e^- \to \gamma\gamma$, and N_{obs} is the number of observed events. QED processes are the best choice because of their clean signal, low background and the possibility to push the theoretical accuracy up to very high precision. The latter requires the inclusion of the relevant radiative corrections (RCs) in the cross sections calculation and their implementation into Monte Carlo (MC) event generators (EGs) in order to easily account for realistic event selection criteria. Present EGs used for luminometry rely on exact fixed-order QED corrections and Leading Logarithmic (LL) approximation of higher order effects, together with their consistent matching. The following sections describe how this is achieved within the **BabaYaga** EG, targeting NLOPS accuracy. It was originally developed for the precise simulation of large-angle Bhabha scattering at low energy e^+e^- colliders, with center of mass energy up to 10 GeV [126, 131], and later extended [132] to simulate also $\mu^+\mu^-$ and $\gamma\gamma$ final states in the same energy regime. In its first version [126, 131], the generator relied upon a QED Parton Shower (PS) to account for the LL photonic corrections, resummed up to all orders in perturbation theory. The PS algorithm implemented in **BabaYaga** is described in Section 7.2, while the matching with the NLO calculation is described in Section 7.3. Last Section 7.4 discusses the current work in progress to update the generator to match the precision requirements of future high-energy e^+e^- machines.

7.2 QED Parton Shower algorithm

The PS is a MC algorithm which gives an exact iterative numerical solution of the Dokshitzer-Gribov-Lipatov-Altarelli-Parisi (DGLAP) evolution equation ([39, 40, 42, 93]) in QED for the non-singlet QED structure function (SF)[6] $D(x, Q^2)$, which allows to describe the effects of multiple emission of photons in the collinear limit to all orders in perturbation theory. The SF represents the

---

[5]Bhabha scattering events are used in two different kinematical regimes: large angle (typically charged particles are required to lie in the interval $[20, 160]$ or $[15, 165]$ degrees) for flavour factories with center of mass energies up to ~ 10 GeV and small angle (typically one charged particle is required within a few degrees in the forward direction and the other one in the backward direction) for LEP and future e^+e^- machines. In the latter regime Bhabha scattering is less sensitive than the former to potential New Physics effects at high energy collisions and therefore more suited for luminometry.

[6]The term "Structure Functions" applies strictly only when a LL evolution is considered, which is here the case. Beyond LL, the more appropriate term "Parton Distribution Function" should be used.

probability density of finding "inside" a parent electron an electron with momentum fraction x and virtuality Q^2. The evolution equation reads [7]

$$Q^2 \frac{\partial}{\partial Q^2} D(x, Q^2) = \frac{\alpha}{2\pi} \int_x^1 \frac{dy}{y} P_+(y) D(\frac{x}{y}, Q^2).$$ (7.1)

In the previois equation, $P_+(x)$ is the regularized $e \rightarrow e + \gamma$ splitting function

$$P_+(x) = \frac{1+x^2}{1-x} - \delta(1-x) \int_0^1 dt P(t),$$ (7.2)

where $P(x) = (1+x^2)/(1-x)$ is the unregularized $e \rightarrow e + \gamma$ splitting vertex. Equation (7.2) is symbolic and its numerical evaluations require the introduction of an infrared regulator $x_+ \equiv 1 - \varepsilon$ with $\varepsilon \ll 1$, which changes it into the form

$$P_+(x) = \frac{1+x^2}{1-x} \Theta(x_+ - x) - \delta(1-x) \int_0^{x_+} dt P(t),$$ (7.3)

where $\Theta(x)$ is the Heaviside step function.

The energy scale Q^2 entering the SF is, in general, dependent on the specific process under study. The QED SFs account for photon radiation emitted by both initial-state and final-state charged fermions. An important feature of the PS solution is that the kinematics of the emitted photons can be recovered (within some approximation) and hence an exclusive event generation can be performed, i.e. all the momenta of the final state particles (fermions and an indefinite number of photons) can be reconstructed. Within the SF approach the corrected cross section can be written as

$$\sigma(s) = \int dx_- dx_+ dy_- dy_+ \int d\Omega D(x_-, Q^2) D(x_+, Q^2) D(y_-, Q^2) D(y_+, Q^2) \frac{d\sigma_0(x_- x_+ s)}{d\Omega_{cm}} \Theta(cuts),$$ (7.4)

where $D(x_\pm, Q^2)$ and $D(y_\pm, Q^2)$ refer to radiation from initial and final state charged legs, respectively [8], and $d\sigma_0/d\Omega$ is the Born-like differential cross section.

The starting point of the PS algorithm is the Sudakov form factor [133]:

$$\Pi(s_1, s_2) = \exp\left[-\frac{\alpha}{2\pi} \int_{s_2}^{s_1} \frac{ds'}{s'} \int_0^{x_+} dz P(z)\right],$$ (7.5)

which represents the probability that an electron evolves from virtuality s_2 to virtuality s_1 with no emission of photons of energy fraction greater than $\varepsilon = 1 - x_+$, where ε is an infrared regulator. In terms of the factor $\Pi(s_1, s_2)$ and with the initial condition $D(x, m^2) = \delta(1-x)$, the DGLAP equation can be written in iterative form as:

$$\begin{aligned}
D(x, Q^2) = &\ \Pi(Q^2, m^2) \delta(1-x) \\
&+ \int_{m^2}^{Q^2} \Pi(Q^2, s') \frac{ds'}{s'} \Pi(s', m^2) \frac{\alpha}{2\pi} \int_0^{x_+} dy P(y) \delta(x-y) \\
&+ \int_{m^2}^{Q^2} \Pi(Q^2, s') \frac{ds'}{s'} \int_{m^2}^{s'} \Pi(s', s'') \frac{ds''}{s''} \Pi(s'', m^2) \times \\
&\quad \left(\frac{\alpha}{2\pi}\right)^2 \int_0^{x_+} dx_1 \int_0^{x_+} dx_2 P(x_1) P(x_2) \delta(x - x_1 x_2) + \cdots
\end{aligned}$$ (7.6)

---

[7]For definiteness in the following, the QED coupling constant e is chosen to be renormalized in the on-shell scheme, i.e. it is connected with the fine structure constant α by the relation $e^2 = 4\pi\alpha$.

[8]For the process $e^+ e^- \rightarrow \gamma\gamma$, $D(y_\pm, Q^2) = 1$ is understood.

Equation (7.6) suggests the steps to compute $D(x,s)$ by means of a MC algorithm detailed in Ref. [126]. In this way the emission of a shower of photons by an electron is simulated, and the x distribution of the PS event sample reproduces $D(x,Q^2)$. Equation (7.6) accounts for soft plus virtual and real photon radiation up to all orders in perturbation theory in LL approximation. It is worth noticing that, setting the scale Q^2 equal to st/u, the Sudakov form factor exponentiates the LL contribution of the $O(\alpha)$ soft plus virtual cross section as well as the dominant contribution coming from the infrared cancellation between the virtual box and the initial-final state interference of bremsstrahlung diagrams [9].

The PS algorithm offers the possibility to go naturally beyond the strictly collinear treatment of the electron evolution, by generating the transverse momentum $p_\perp$ of electrons and photons at each branching. In Ref. [131] an improvement has been introduced to include the coherence effects, due to radiation from different charged legs, by generating the angular spectrum of the lth photon as

$$\cos\vartheta_l \propto -\sum_{i,j}^{N}\eta_i\eta_j\frac{1-\beta_i\beta_j\cos\vartheta_{ij}}{(1-\beta_i\cos\vartheta_{il})(1-\beta_j\cos\vartheta_{jl})}, \qquad (7.7)$$

where N is the number of the involved charged fermions, β_i is the speed of the ith emitter, ϑ_{ij} is the relative angle between particles i and j, η_i is a charge factor, which is $+1$ for incoming lepton or outgoing antilepton and -1 for incoming antilepton or outgoing lepton. Equation (7.7) is inspired to the expression of the differential cross section for a generic process with emission of additional photons in the soft limit [45]. The prescription of Equation (7.7) has been shown to generate exclusive radiation in nice agreement with exact $O(\alpha)$ results for Bhabha scattering and $e^+e^- \to \mu^+\mu^-$.

Despite its nice features, the PS described above is intrinsically accurate at the LL level and a precision in integrated or differential cross sections better than 0.5-1% can not be expected. In order to account also for missing $O(\alpha)$ non-log contributions to exclusive and inclusive observables, a matching with exact NLO RCs is mandatory, in such a way that the features of the PS are preserved (i.e. exclusive event generation and resummation of LL corrections up to all orders) while avoiding the double counting of the $O(\alpha)$ LL corrections, present both in the PS approach and in the NLO calculation.

7.3 Matching NLO corrections with Parton Shower: `BabaYaga@NLO`

In this Section we discuss the matching algorithm as implemented in `BabaYaga@NLO` [134]. It is worth mentioning that PS/NLO matching algorithms have been firstly put forward in the context of QCD simulations [135, 136]: although our procedure certainly shares some common ideas with them, we never carried out a thorough comparison of general similarities and differences with our algorithm, which would be extremely interesting to perform in the future.

The fully differential cross section implicit in Equation (7.4) can be recast in the following form:

$$d\sigma_{LL}^{\infty} = \Pi(Q^2,\varepsilon)\sum_{n=0}^{\infty}\frac{1}{n!}|\mathcal{M}_{n,LL}|^2\,d\Phi_n, \qquad (7.8)$$

---

[9]The above applies for charged fermion pair production, while for $e^+e^- \to \gamma\gamma$ only the choice $Q^2 = s$ is physically meaningful.

where $\Pi(Q^2, \varepsilon)$ is the Sudakov form-factor accounting for the soft-photon (up to an energy equal to ε in units of the incoming fermion energy E) and virtual emissions, ε is an infrared separator dividing soft and hard radiation and Q^2 is related to the energy scale of the process. $|\mathcal{M}_{n,LL}|^2$ is the squared amplitude in LL approximation describing the process with the emission of n hard photons, with energy larger than ε in units of E. $d\Phi_n$ is the exact phase-space element of the process (divided by the incoming flux factor), with the emission of n additional photons with respect to the Born-like final-state configuration. The cross section $d\sigma_{LL}^\infty$ of Equation (7.8) is numerically independent of the infrared separator ε. More precisely, only power-suppressed ε terms might be present, which can be made vanishingly small.

According to the factorization theorems of soft and/or collinear singularities, the squared amplitudes in LL approximation can be written in a factorized form. In the following, for the sake of clarity and without loss of generality, we write photon emission formulas as if only one external fermion radiates. We are aware that it is a completely unphysical case, but it allows to write more compact formulas, being the generalization to the real case straightforward when including the suited combinatorial factors. With this in mind, the one-photon emission squared amplitude in LL approximation can be written as

$$|\mathcal{M}_{1,LL}|^2 = \frac{\alpha}{2\pi} \frac{1+z^2}{1-z} I(k) |\mathcal{M}_0|^2 \frac{8\pi^2}{E^2 z(1-z)}, \qquad (7.9)$$

where $1-z$ is the fraction of the fermion energy E carried by the photon, k is the photon four-momentum, $I(k)$ is a function describing the angular spectrum of the photon and $P(z) = (1+z^2)/(1-z)$ is the Altarelli-Parisi $e \to e + \gamma$ splitting function. In Equation (7.9) we observe the factorization of the Born squared amplitude and that the emission factor $\frac{\alpha}{2\pi} P(z) I(k) \frac{8\pi^2}{E^2 z(1-z)}$ can be iterated for each photon emission, up to all orders, to obtain $|\mathcal{M}_{n,LL}|^2$. It is worth noticing that $d^3\vec{k}/k^0 = (1-z)E^2 d\Omega_\gamma dz$ and that in the collinear limit the cross section of Equation (7.8) reduces to the cross section calculated by means of the QED PS algorithm described in Refs. [126, 131].

The Sudakov form factor $\Pi(Q^2, \varepsilon)$ reads explicitly

$$\Pi(Q^2, \varepsilon) = \exp\left(-\frac{\alpha}{2\pi} I_+ L'\right), \quad L' = \log\left(\frac{Q^2}{m^2}\right), \quad I_+ \equiv \int_0^{1-\varepsilon} dz P(z). \qquad (7.10)$$

The function $I(k)$ has the property that $\int d\Omega_\gamma I(k) = \log(Q^2/m^2)$ and allows the cancellation of the infrared logarithms.

The cross section calculated in Equation (7.8) has the advantage that the photonic corrections, in LL approximation, are resummed up to all orders of perturbation theory. On the other side, the weak point of the formula 7.8 is that its expansion at $O(\alpha)$ does not coincide with an exact $O(\alpha)$ (NLO) result, being its LL approximation. In fact

$$\begin{aligned} d\sigma_{LL}^\alpha &= \left[1 - \frac{\alpha}{2\pi} I_+ \log\frac{Q^2}{m^2}\right] |\mathcal{M}_0|^2 d\Phi_0 + |\mathcal{M}_{1,LL}|^2 d\Phi_1 \\ &\equiv [1 + C_{\alpha,LL}] |\mathcal{M}_0|^2 d\Phi_0 + |\mathcal{M}_{1,LL}|^2 d\Phi_1, \end{aligned} \qquad (7.11)$$

whereas an exact NLO cross section can be always cast in the form

$$d\sigma^\alpha = [1 + C_\alpha] |\mathcal{M}_0|^2 d\Phi_0 + |\mathcal{M}_1|^2 d\Phi_1. \qquad (7.12)$$

The coefficient C_α contains the complete virtual $O(\alpha)$ and the $O(\alpha)$ soft-bremsstrahlung squared matrix elements, in units of the Born squared amplitude, and $|\mathcal{M}_1|^2$ is the exact squared matrix element with the emission of one hard photon. We remark that $C_{\alpha,LL}$ has the same logarithmic structure as C_α and that $|\mathcal{M}_{1,LL}|^2$ has the same singular behaviour of $|\mathcal{M}_1|^2$.

In order to match the LL and NLO calculations, we introduce the correction factors, which are by construction infrared safe and free of collinear logarithms,

$$F_{SV} \;=\; 1 + (C_\alpha - C_{\alpha,LL}), \qquad F_H \;=\; 1 + \frac{|\mathcal{M}_1|^2 - |\mathcal{M}_{1,LL}|^2}{|\mathcal{M}_{1,LL}|^2} \tag{7.13}$$

and we notice that the exact $O(\alpha)$ cross section can be expressed, up to terms of $O(\alpha^2)$, in terms of its LL approximation as

$$d\sigma^\alpha \;=\; F_{SV}(1 + C_{\alpha,LL})|\mathcal{M}_0|^2 d\Phi_0 \;+\; F_H |\mathcal{M}_{1,LL}|^2 d\Phi_1 \tag{7.14}$$

Driven by Equation (7.14), Equation (7.8) can be improved by writing the resummed cross section as

$$d\sigma^\infty_{matched} = F_{SV}\,\Pi(Q^2,\varepsilon)\,\sum_{n=0}^\infty \frac{1}{n!}\left(\prod_{i=0}^n F_{H,i}\right)|\mathcal{M}_{n,LL}|^2\,d\Phi_n, \tag{7.15}$$

The extension of the matching formula Equation (7.15) to the realistic case, where every charged particle radiates photons, is almost straightforward. Equation (7.15) is the master formula according to which event generation and cross secton calculation are performed in **BabaYaga@NLO**. It is worth stressing that the F_{SV} and $F_{H,i}$ correction factors are applied at differential level on an event-by-event basis and that the $O(\alpha)$ expansion of Equation (7.15) coincides with Equation (7.12).

We would like to remark also that the LL cross section of Equation (7.8) is by construction positively defined in every point of the phase space, whereas the correction factors of Equation (7.13) can in principle make the differential cross section of Equation (7.15) negative in some point, namely where the PS approximation is less accurate (e.g. for hard photons at large angles). Nevertheless, we verified that this never happens when considering typical event selection criteria for luminosity at flavour factories.

It is useful to present, in the realistic case, the expression of the function $I(k)$, which describes the leading behaviour of the angular spectrum of the emitted photons, accounting also for interference of radiation coming from different charged particles:

$$I(k) \;=\; \sum_{i,j=1}^4 \eta_i \eta_j \frac{p_i \cdot p_j}{(p_i \cdot k)(p_j \cdot k)} E_\gamma^2 \tag{7.16}$$

where p_l is the momentum of the external fermion l, η_l is the charge factor introduced in Equation (7.7), k is the photon momentum, E_γ is its energy and the sum runs over all the external fermions. The function $I(k)$ does not depend on the photon energy and it is analogous to Equation (7.7). Given Equation (7.16), and considering for instance Bhabha scattering, one can quite easily convince that, after integrating over photon angles, the scale Q^2 in the Sudakov form factor takes the form $L' = \log\frac{Q^2}{m^2} = \log\frac{st}{um^2} - 1 \equiv L - 1$ where s, t and u are the Mandelstam variables of the process and m is the electron mass.

The exact $O(\alpha)$ soft plus virtual corrections to the Bhabha scattering have been taken from Ref. [137, 138]. The soft plus virtual cross section reads

$$d\sigma_{SV}^{\alpha} = d\sigma_{SV}^{\alpha,s} + d\sigma_{SV}^{\alpha,t} + d\sigma_{SV}^{\alpha,st}$$
$$d\sigma_{SV}^{\alpha,i} = d\sigma_0^i [2(\beta + \beta_{int}) \log \epsilon + C_F^i] \tag{7.17}$$

where i is an index for s, t and s-t subprocesses contributing to the Bhabha cross section, $\beta = \frac{2\alpha}{\pi}[\log(s/m^2) - 1]$, $\beta_{int} = \frac{2\alpha}{\pi} \log(t/u)$ and the explicit expression for C_F^i can be found in Refs. [137, 138]. We notice that in Equation (7.17) the terms coming from s, t and s-t interference diagrams are explicitly given.

The above discussion concerns the subset of photonic RCs. In **BabaYaga**, any leptonic RCs due to photon vacuum polarization effects are included in the building-block matrix elements at tree-level and one-loop order, paying attention to the correct cancellation of infra-red divergencies, as described in more detail in Ref. [134].

7.4 Future improvements and upgrades for high energies

As stressed in the previous sections, **BabaYaga@NLO** is tailored to energies up to 10 GeV, where the bulk of RCs is due to QED radiation. We give here a list of needed and desirable upgrades of the code which will improve its theoretical accuracy and make it suitable for simulations at higher energies:

1. running at higher energies will require the inclusion of Z exchange diagrams for e^+e^- and $\mu^+\mu^-$ final states [10], together with the full set of NLO electroweak corrections. A first step towards this goal has been taken in Ref. [139], where the process $e^+e^- \to \gamma\gamma$ has been considered as a luminosity monitoring process at FCC-ee energies and a phenomenological study of the effects induced by the complete one-loop RCs in the Standard Model is presented. We remark that the framework of the matching algorithm described in Sec. 7.3 has been successfully adopted also for charged- and neutral-current Drell-Yan processes in Refs. [140, 141] and for Higgs decay into four leptons [142], including NLO electroweak corrections. The same theoretical basis can be in the future applied to Bhabha scattering and $e^+e^- \to \mu^+\mu^-$ for simulations at high-energy e^+e^- machines with **BabaYaga@NLO**;

2. a possible improvement to better control higher-order corrections is the implementation into a Parton Shower algorithm of the NLO initial conditions discussed in Ref. [38] and NLL evolution as detailed in Refs. [37, 130];

3. one of the developments foreseen for the future is the generalization of the matching algorithm to include also exact NNLO RCs in QED. This will allow to improve the theoretical accuracy of the generator, presently at the $O(0.1\%)$ level, to meet the precision requirements for measurements at future machines (see for instance Refs. [143–145]). The parallel efforts on the MUonE project [146–149] can help towards the achievement of the goal.

---

[10] These are already included in the tree-level matrix elements, but not in higher-order corrections.

8 Theoretical predictions for $e^+e^- \to W^+W^- \to 4f$

Ansgar Denner, Stefan Dittmaier

8.1 Introduction

Future e^+e^- colliders, either realized as linear or circular collider, will offer fantastic opportunities to perform high-precision measurements to challenge the validity of the Standard Model (SM) and to identify possible deviations from SM predictions even if the Large Hadron Collider (LHC) does not discover any new particles (see, e.g., [150] and references therein). The investigation of W-boson pairs is one of the cornerstones in this vision of "discovery via precision". For instance, from a scan of the total WW production cross section over its threshold, the W-boson mass M_W could be determined with a precision of 3 MeV and even of 0.5–1 MeV at the linear and circular collider options ILC [151] and FCC-ee [143, 152], respectively. Moreover, the large number of $\sim 10^7$–10^8 W pairs expected to be produced at these colliders would turn the investigation of differential WW cross sections at higher energies into high-precision physics. In particular, such analyses would enormously tighten the limits on anomalous gauge-boson self-interactions, which are nowadays quoted in terms of limits on Wilson coefficients of effective dimension-6 operators in SM Effective Field Theory. On the theory side, the full exploitation of this physics potential is a great challenge as well (see, e.g., [153] and references therein).

The purpose of this contribution is to describe the salient steps of increasing sophistication in the theoretical predictions for $e^+e^- \to W^+W^- \to 4f$ as, starting from the status of predictions for the Large Electron–Positron collider (LEP), in which radiative corrections were taken into account in the form of resonance expansions, and leading to the current state of the art, where differential next-to-leading-order (NLO) predictions based on full matrix elements exist for all relevant scattering energies and dedicated cross-section predictions near threshold via an effective field theory (EFT) for including corrections at and beyond NLO. Finally, we specify further improvements that are necessary to account for the precision expected for future e^+e^- colliders.

8.2 Predictions based on the double-pole approximation

In the course of phase 2 of LEP, the theoretical description of charged-current four-fermion production in e^+e^- collisions turned from pure lowest-order predictions into systematic precision calculations with a proper inclusion of the W-boson decay subprocesses and NLO corrections to all stages of the full resonance process. A major step towards percent-level accuracy in the cross-section prediction for the LEP2 energy range was made by the concept of a systematic expansion about the two W-boson resonances, leading to the so-called *double-pole approximation* (DPA). The DPA decomposes, in a gauge-invariant way, the full resonance process into production and decay subprocesses, which each receive their own *factorizable corrections* and are linked by *non-factorizable corrections* due to soft photon exchange.

In more detail, the contributions of the non-factorizable corrections in DPA, which result from the presence of IR singularities, were systematically studied in [154–156] and generalized to other processes in [157, 158]. The factorizable corrections consist of the corrections to the subprocesses of on-shell W-pair production [159, 160] and on-shell W decay [161], properly taking into account W spin correlations. The DPA was formulated and evaluated by different groups in different

variants [129, 162–165], as e.g. reviewed in [166], but only the two Monte Carlo programs YF-SWW [163] and RACOONWW [129, 164, 167] were used in the final LEP2 WW cross-section analyses [168]. Theoretical arguments as well as comparisons between the different DPA variants suggested that sufficiently above the WW threshold a $\sim 0.5\%$ accuracy could be achieved for LEP2 energies ($\sqrt{s} \sim 165-210\,\mathrm{GeV}$).

In RACOONWW only the virtual one-loop corrections are treated in the DPA approximation, while the NLO real corrections are taken into account exactly. Real and virtual corrections are combined using either two-cutoff phase-space slicing or the dipole subtraction method for photon radiation [19]. Corrections from initial-state radiation are resummed to all orders at the leading-logarithmic accuracy via the structure-function approach [169, 170], which is based on the collinear approximation improved by soft-photon exponentiation. Moreover, off-shell effects of the Coulomb singularity [72, 73], resulting from the exchange of virtual photons between the produced W bosons, are included.

The Monte Carlo program YFSWW [163] is based on NLO corrections to on-shell W-pair production, improved by YFS exponentiation for the electromagnetic corrections including also LL final-state W-decay radiative effects [163, 171]. The NLO cross section for on-shell W-pair production after subtraction of photonic corrections is dressed by photon radiation in the YFS approach. Leading logarithmic corrections to W decays are included via PHOTOS and non-factorisable corrections only approximately via a screened Coulomb ansatz. Spin correlations are fully included at leading order (LO) and approximatively at NLO.

Predictions based on the DPA have limitations both at low and high energies. Directly around the WW threshold the DPA is not applicable, leaving predictions with a $\sim 2\%$ accuracy from some *improved Born approximation* (IBA) [172, 173], which is based on universal corrections that can be easily incorporated into the structure of the off-shell LO matrix elements. For higher energies relevant for future linear colliders ($\sqrt{s} > 500\,\mathrm{GeV}$) a deterioration of the DPA was expected due to the increasing relevance of so-called (singly-resonant) background diagrams. Finally, the IBA suffers from the lack of electroweak logarithms at high energies.

8.3 Predictions based on full matrix elements

The situation significantly improved with the completion of the NLO calculation [174, 175] for the full $2 \to 4$ process $\mathrm{e}^+\mathrm{e}^- \to \mathrm{W}^+\mathrm{W}^- \to 4f$ and its implementation in RACOON4F, supporting NLO accuracy both in resonant and non-resonant regions. The precision of this NLO calculation in integrated cross sections was estimated to be $\sim 0.2\%$ in the whole LEP2 energy range and to be $\sim 0.5\%$ up to energies in the TeV range. Moreover, the uncertainty estimate of the DPA was nicely confirmed by this more precise calculation (see Fig. 1 below).

The full NLO calculation required significant technical and conceptual progress in two directions: The first concerns the gauge-invariant treatment of resonances in NLO accuracy in resonance and off-shell regions and in the region in between. To this end, the so-called *complex-mass scheme* (CMS) was suggested in [175] (more details can be found in [176, 177]), which introduces complex W- and Z-boson masses and analytically continues couplings in such a way that all gauge-invariance relations are maintained (Ward identities, gauge-parameter cancellation). In the CMS perturbative calculations proceed as usual, i.e. amplitudes are calculated order by order, but with complexified renormalization prescriptions and with complex masses in loop integrals. The fast and
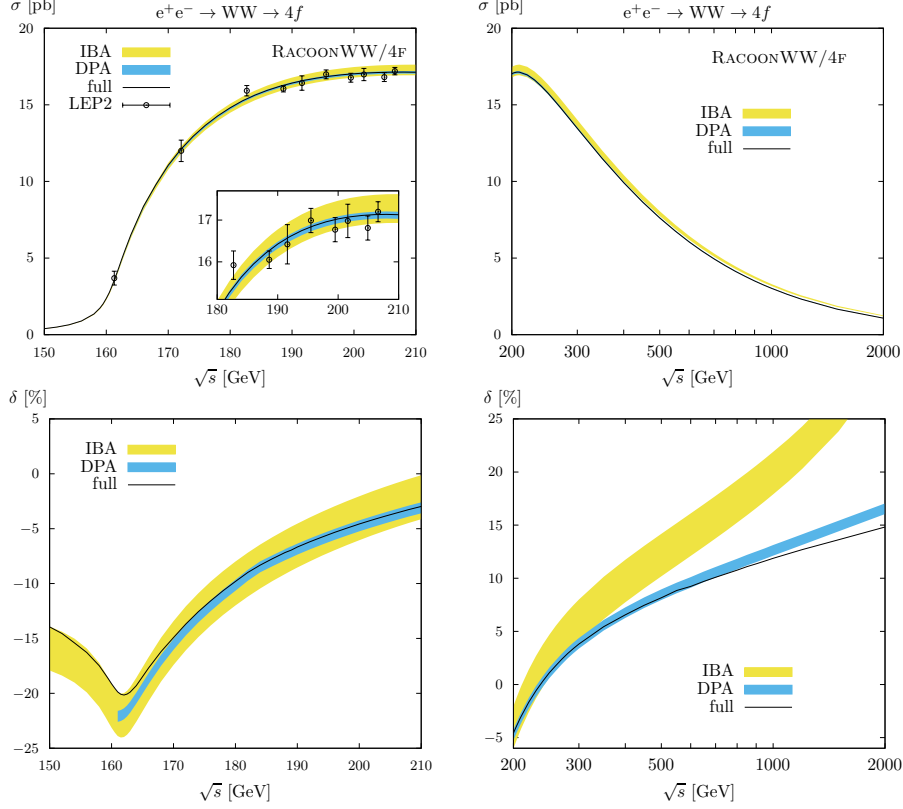
Figure 1. Inclusive cross section for $e^+e^- \to W^+W^- \to 4f$ as obtained from RACOONWW/4F, including NLO EW corrections in IBA, in DPA [129], and fully off shell in the CMS [174, 175]. The IBA and DPA bands illustrate the uncertainty of $\pm 2\%$ and $\pm 0.5\%$, as assessed for the LEP2 energy range. LEP2 cross-section measurements [168] are shown as data points. (Plots taken from [177].)

numerically stable evaluation of the multi-leg one-loop diagrams (with up to six-point amplitudes) was the second type of complication that required significant technical progress. This problem was solved by the introduction of new reduction techniques for one-loop tensor integrals [178] that avoid the appearance of dangerous inverse kinematical determinants (mostly of Gram type) of external momenta. To achieve this, the traditional Passarino–Veltman tensor reduction [179] was complemented by dedicated expansions of tensor coefficients about exceptional phase-space points where those dangerous determinants vanish. Further optimizations and improvements of this technique lead to the development of the public FORTRAN library COLLIER [180] which evaluates arbitrary one-loop tensor integrals with complex masses and various regularizations up to high tensor ranks (without any hard limit). More details on these one-loop concepts and techniques can also be found in the review [177].

A comparison of predictions for the inclusive W-pair production cross section for centre-of-mass energies ranging from the LEP2 energy range up to 2 TeV is shown in Fig. 1. The results include NLO EW corrections based on an IBA, the DPA of RACOONWW, and the full off-shell calculation of [174, 175] as implemented in RACOON4F. All cross sections are obtained in the G_μ scheme [177], where the electromagnetic coupling is determined from the Fermi constant. Leading higher-order effects from initial-state radiation (ISR) are incorporated in all versions. In the

LEP2 energy range, the IBA, the DPA, and the full off-shell calculations agree within the expected uncertainties. The agreement with LEP2 data [168], which are included in the plot, with theory predictions required the inclusion of non-universal EW corrections, as provided by the DPA. For energies above the LEP2 energy range, the error assessments of $\pm 2\%$ and $\pm 0.5\%$ for IBA and DPA, respectively, fail. For $\sqrt{s} \gtrsim 300-400\,\mathrm{GeV}$, logarithmically enhanced negative high-energy EW corrections appear, which are not incorporated in the IBA, but still by the DPA. Those corrections reach $\sim -10\%$ and more in the TeV range for total cross sections and are even larger in differential distributions. The difference of some percent between DPA and full off-shell result, on the other hand, is due to the increasing contribution of background diagrams, which are included only at LO but not in the DPA calculation of the virtual corrections.

8.4 Near-threshold predictions from EFT

In [116, 117] an EFT approach was devised to efficiently compute the $e^+e^- \rightarrow 4\,\mathrm{fermions}$ cross section close to the W-pair production threshold, where $\sqrt{s} - 2M_\mathrm{W} \sim \Gamma_\mathrm{W}$. The EFT exploits the scale hierarchy in the threshold regime, $M_\mathrm{W} \gg M_\mathrm{W}v \gg M_\mathrm{W}v^2 \sim \Gamma_\mathrm{W} \sim M_\mathrm{W}\alpha$, where v is the typical velocity of the W bosons in the centre-of-mass frame, Γ_W is the W decay width, and α represents the electroweak coupling constant. It builds on non-relativistic QED (NRQED) [181] to describe the dynamics of the (slightly) off-shell W bosons, on soft-collinear effective theory (SCET) [182] to describe photonic ISR, and on unstable-particle EFT [183] to describe the W decay.

In the EFT the cross-section calculation is organized as a consistent ("threshold") expansion in the small parameter $\delta \sim \alpha \sim v^2$. This corresponds to a simultaneous expansion in the small parameters v and α. The parametric scaling of the LO cross section in the EFT is $\sigma_\mathrm{eff}^\mathrm{LO} \sim \alpha^2 v \sim \delta^{5/2}$. In accordance with the ($\mathrm{N}^n\mathrm{LO}$, $n = 1, 2, 3, \ldots$) terminology of the full-theory perturbative expansion in α, the higher-order corrections in the threshold expansion with relative scaling factors $\delta^{n/2}$ are named "$\mathrm{N}^{n/2}\mathrm{LO}$".

The relevant field modes, i.e. the resonant degrees of freedom, (and their typical four-momenta k^μ) of the EFT are: "hard" ($k^\mu \sim M_\mathrm{W}$), "soft" ($k^\mu \sim \delta^{1/2}M_\mathrm{W}$), "ultrasoft" ($k^\mu \sim \delta M_\mathrm{W}$), "potential" ($k_0 \sim \delta M_\mathrm{W}$, $|\vec{k}| \sim \delta^{1/2}M_\mathrm{W}$), or "collinear" ($k_0 \sim M_\mathrm{W}$, $k^2 \sim \delta M_\mathrm{W}^2$). The non-relativistic W bosons are, for example, represented in the EFT by potential fields, while the incoming electrons and positrons have collinear momenta pointing in opposite directions. Every (potential) interaction due to exchange of a "Coulomb" photon between the non-relativistic W bosons yields a relative correction of order $\alpha/v \sim \delta^{1/2}$ to the cross section near threshold.

In [116] the EFT calculation of the total cross section was carried out to NLO in the threshold expansion and compared to the full-theory NLO result of [174, 175]. The observed deviations are in agreement with the expected size of the higher-order corrections in the v expansion missing in the EFT result. Still, a more detailed comparison including further refinements on the full-theory side is desirable (see also [184]).

As a first step beyond full NLO the "dominant NNLO" corrections, i.e. the terms of order $\mathrm{N}^{3/2}\mathrm{LO}$ in the threshold expansion that are contained in the full NNLO (and $\mathrm{N}^3\mathrm{LO}$), were computed in [117]. Individual contributions to these corrections were found to affect the outcome of the future W-mass measurement from a threshold scan by about 5 MeV. They combine to an overall effect on the measured W-boson mass in the same ballpark. It was also pointed out that the QED ISR encoded in the electron/positron structure functions has a large effect. The ISR-related

large logarithms must therefore be resummed at least at next-to-leading logarithmic (NLL) accuracy, while the state-of-the art by the time of [117] was only LL precision. On the other hand, the effect of loose invariant-mass cuts on the decay products of the W bosons, as may be required by experiment, was argued to be negligible.

To consolidate the findings of [117] and to further decrease the theoretical uncertainties, all NNLO threshold corrections that are not already contained in the full NLO result of the total cross section have to be calculated. Moreover, the treatment of ISR effects should be improved to a level of precision sufficient for future W-mass measurements.

8.5 Outlook

Addressing the fantastic precision expected from the next generation of e^+e^- colliders on the theory side poses a great challenge to predict W-pair production at the highest possible precision in a twofold way. Firstly, the prediction of the total cross section near threshold that is required for the M_W determination has to be precise within about 0.01–0.05% while the current uncertainty is $\sim 0.2\%$ resulting from a NLO calculation for the full $2 \to 4$ particle process, or alternatively, from a dedicated higher-order calculation at the WW threshold within a non-relativistic EFT for unstable particles.

Going beyond this current precision is a major effort and requires the calculation of various corrections beyond NLO. On the one hand, the EFT approach for a cross-section prediction at the WW threshold has to be pushed to an unprecedented level of precision, forcing us to significantly extend the level of general understanding of this EFT. On the other hand, various refinements are necessary in current Monte Carlo generators for the process class $e^+e^- \to 4$ fermions, such as RACOON4F, which is the successor of the public Monte Carlo program RACOONWW [129, 164, 167], that incorporates the current state-of-the-art NLO prediction [174, 175]. While the calculation of [174, 175] makes use of "generic" leptonic, semileptonic, and hadronic $4f$ final states, more refined predictions should make use of all individual $4f$ final states, properly taking into account all interferences with t-channel diagrams in channels with $e^\pm$ in the final states and with Z-pair production channels. Further improvements are needed on the side of QCD corrections at the differential level and beyond NLO, which is more challenging.

Finally, for a unified approach for the full energy region ranging from threshold to the TeV range, it will be necessary to implemented the higher-order EFT corrections for the improved threshold prediction in Monte Carlo generators and to refine and improve the calculation of differential cross sections above threshold to increase the achieved accuracy at higher energies.

Acknowledgments

9 CEEX and EEX Realizations of the YFS MC approach to precision theory for e^+e^- Colliders

S. Jadach, B.F.L. Ward

9.1 The YFS Approach to Precision Theory for e^+e^- Colliders

The exact amplitude-based CEEX/EEX YFS MC approach to EW higher order corrections is pioneered in Refs. [64, 185–187]. Here, EEX denotes exclusive exponentiation as originally formulated by Yennie, Frautschi and Suura (YFS) in Ref. [188] and it is effected at the squared amplitude level. CEEX denotes the coherent exclusive exponentiation developed in Refs. [64, 186, 187] in which IR singularities are resummed at the level of the amplitude. We, with our collaborators, have developed and implemented several MC event generators which realize the YFS MC approach for EW higher order corrections in precision physics for e^+e^- colliding beam devices: KORALZ(EEX 2f production in e^+e^- annihilation) [185], BHLUMI(EEX Bhabha scattering at small angles) [189, 190], BHWIDE(EEX Bhabha scattering at wide angles) [191], KKMC-ee(CEEX/EEX 2f production in e^+e^- *annihilation*) [186, 187], YFSWW3(EEX W pair production and decay in e^+e^- annihilation) [192], KORALW(EEX 4f production in e^+e^- annihilation) [193], KORALW&YFSWW3(EEX Concurrent 4f background processes and 1st order W pair production in e^+e^- annihilation)) [194], and YFSZZ(EEX Z pair production and decay in e^+e^- annihilation) [195]– see Ref. [196] for succinct descriptions of these MC's. All of these MC's, except perhaps for KORALZ, which has been superseded by KKMC-ee, are candidates for appropriate upgrades to meet the new precision requirements for the future e^+e^- colliding beam devices. We now give a brief review of the physics in the YFS MC approach in this context.

Since it is still not generally used, we first recall the master formula for the CEEX/EEX realization of the higher corrections to the SM [197–200] EW theory. For the purpose of illustration, let us consider the prototypical process $e^+e^- \to f\bar{f} + n\gamma$, $f = \ell, q$, $\ell = e, \mu, \tau, \nu_e, \nu_\mu, \nu_\tau$, $q = u, d, s, c, b, t$. For this process, we have the cross section formula

$$\sigma = \frac{1}{\text{flux}} \sum_{n=0}^{\infty} \int d\text{LIPS}_{n+2} \, \rho_A^{(n)}(\{p\}, \{k\}), \tag{9.1}$$

where LIPS_{n+2} denotes Lorentz-invariant phase-space for $n+2$ particles, $A = \text{CEEX, EEX}$, the incoming and outgoing fermion momenta are abbreviated as $\{p\}$ and the n photon momenta are denoted by $\{k\}$. Thanks to the use of conformal symmetry, full $2+n$ body phase space is covered without any approximations. The respective algorithm's details are covered in Ref. [186]. Specifically, we have from Refs. [64, 186] that

$$\rho_{\text{CEEX}}^{(n)}(\{p\}, \{k\}) = \frac{1}{n!} e^{Y(\Omega; \{p\})} \bar{\Theta}(\Omega) \frac{1}{4} \sum_{\text{helicities } \{\lambda\}, \{\mu\}} \left| \mathcal{M} \begin{pmatrix} \{p\}\{k\} \\ \{\lambda\}\{\mu\} \end{pmatrix} \right|^2. \tag{9.2}$$

(See Refs. [64, 186] for the corresponding formula for the $A = \text{EEX}$ case.) Here, $Y(\Omega; \{p\})$ is the YFS infrared exponent. The respective infrared integration limits are specified by the region Ω and its characteristic function $\Theta(\Omega, k)$ for a photon of energy k, with $\bar{\Theta}(\Omega; k) = 1 - \Theta(\Omega, k)$ and

$$\bar{\Theta}(\Omega) = \prod_{i=1}^{n} \bar{\Theta}(\Omega, k_i).$$

See Refs. [64, 186, 187] for the definitions of the latter functions as well as the CEEX amplitudes $\{\mathcal{M}\}$. $\mathcal{KKMC}$ 4.22 [187] featured the exact $O(\alpha)$ EW corrections implemented using the DIZET 6.21,...,6.42 EW libraries from the semi-analytical program ZFITTER [201–204]. Recent public versions of $\mathcal{KKMC}$ include also the DIZET 6.45 version, see [205]. The respective

implementation is described in Ref. [64] so that we do not repeat it here. In $\mathcal{KK}$MC-ee, the CEEX amplitudes $\{\mathcal{M}\}$ in Eqs. (9.1,9.2) are exact in $O(\alpha^2 L^2, \alpha^2 L)$ in the sense that all terms in the respective cross section at orders $O(\alpha^0)$, $O(\alpha)$, $O(\alpha L)$, $O(\alpha^2 L)$, and $O(\alpha^2 L^2)$ are all included in our result for that cross section. Here the big log is $L = \ln \frac{Q^2}{m^2}$ where Q is the respective hard 4-momentum transfer. In our case, the charged lepton masses and the quark masses will determine m, depending on the specific process under consideration. We follow Ref. [206] and use the current quark masses [207] $m_u = 2.2$MeV. $m_d = 4.7$MeV, $m_s = 0.150$GeV, $m_c = 1.2$GeV, $m_b = 4.6$GeVand $m_t = 173.5$GeV[11]. We note for completeness that in our MC's all real and soft virtual photonic corrections have $\alpha = \alpha(0) = \frac{1}{137.035999...}$, since photons are massless. For hard QED corrections, we use $\alpha = \alpha(Q)$,[12] with the attendant hadronic vacuum polarization taken after Ref. [209].

We note that the EEX realization in $\mathcal{KK}$MC-ee includes as well the exact $O(\alpha^3 L^3)$ corrections. The user always has the option to switch on this correction as needed. For an overview on the other programs listed above which feature EEX see Refs. [210] and [166]. As we noted, most of the latter programs may serve as a starting point for the future development. However, as an introductory step they have to be translated from Fortran77 to a modern programming language. Presently $\mathcal{KK}$MC-ee is already fully translated into C++ and the BHLUMI translation is in the process.

It is worth to stress that the $\mathcal{KK}$MC program is unique concerning the spin polarization treatment. It is the only one which implements the full spin density matrix formalism (transverse and longitudinal) for both incoming beams and outgoing fermions in the presence of higher order corrections, any number of photons, all over the phase space.

The anticipated new precision requirements of the future e^+e^- colliding beam devices, as summarized in Ref. [211], are at least a of factor 10 and often a factor 100 higher than any present MC programs can provide. The path of the development of new calculations in the form of the MC event generators was already outlined, see Refs. [211]. The improvement plan for the low angle Bhabha process is outlined Refs. [145, 212, 213]. A new variant of the CEEX scheme for the production and decay of the charged particles implementable in the MC programs, like what one needs for WW pair production, was the scenario outlined in Ref. [214].

Generally we expect to move most of these MC's to the CEEX paradigm to take advantage of its efficiency in simulation interference effects especially near resonance thresholds. The other feature of the CEEX scheme underlined in Ref. [145] is that it provides a flexible and consistent scheme of combining electroweak (EW) and non-soft QED corrections in different orders. This feature is critical for achieving precision goals of the future electron colliders where typically EW corrections have to be completed to second order while QED corrections are needed up to third or fourth order plus soft photon resummation[13].

---

[11]See Ref. [208] for a relevant discussion of the uncertainty of our results due to realistic uncertainties on our values of the current quark masses - we find the uncertainties due to the choices of the quark masses are approximately equal to 10% of the overall corrections.

[12]This is the analogue of $\alpha(M_Z)$ but defined at the scale Q.

[13]While it is true that the CEEX methodology is mainly for/on QED, it includes a very valuable thing concerning the so-called genuine EW corrections: so far it is the only technique which offers a consistent (gauge invariant) and practical method of building matrix elements (spin amplitudes) for the complete (photonic) QED corrections up to $O(\alpha^2)$ and EW corrections up to $O(\alpha^1)$ only. As stressed and described in Ref. [145], this methodology extends to

As we have already anticipated in Ref. [215], with the appropriate CEEX realizations, we expect to be able to reach the desired precision expectations for all of the respective processes addressed by the aforementioned MC's. The above plans and expectations assume the availability of the proper financial support.

9.2 Comparison with the Collinear Factorisation Approach

The YFS MC approach which we presented above should be compared with the collinear factorisation approach [216–224] which for Z physics has been reviewed also in Ref. [225]. Indeed, in Refs. [226], detailed comparisons were made between BHLUMI, featuring the EEX YFS MC approach to the low angle Bhabha scattering process which was used to determine the luminosity at LEP, and SABSPV [227] which also treated the same process to a comparable over-all normalization accuracy using the collinear factorisation approach. A related set of comparisons at low energy were made featuring BHWIDE and BaBaYaga [228] in Ref. [229]. From these comparisons we can draw some general conclusions as we now discuss[14].

For definiteness, let us write down the generic collinear factorisation representation of the same process that we considered above: $e^+e^- \to f\bar{f} + n\gamma$, $f = \ell, q$, $\ell = e, \mu, \tau, \nu_e, \nu_\mu, \nu_\tau$, $q = u, d, s, c, b, t$. We have

$$\sigma = \int dx_1 dx_2 \sum_{ij} f_i(x_1) f_j(x_2) \sigma_{ij}(Q^2) \delta(Q^2 - x_1 x_2 s), \tag{9.3}$$

where the sub-process cross section for the ij parton-parton interaction, where $i(j)$ denotes a parton in the incoming $e^-(e^+)$ beam, with $\hat{s} = Q^2$ when the e^+e^- cms energy squared is s, is denoted in a conventional notation for parton densities $\{f_j\}$. Here, $\sigma_{ij}(Q^2)$ is given by the appropriate expression as dictated by the respective QED electron collinear factorisation calculus as described in Refs. [216–220].

Already by comparing Eq.(9.1) and Eq.(9.3) we see one important advantage of the YFS MC approach: the exact phase space for the multiple photon radiation is realized on an event by event basis to all orders in α whereas in the collinear factorisation approach the radiation transverse degrees of freedom that have been integrated to reach the 1-dimensional QED PDF's have to be restored and this restoration is inherently approximate, as it was illustrated in Ref. [226],for example[15].

Application of Eq. (9.3) is limited to "academic observables" with a cut-off on the total photon energy $E_{\max} = (sx_1x_2)^{1/2}$[16]. All realistic experimental observables select events using acollinearity and other similar cuts depending on photon momenta in a complicated way. Only a Monte Carlo

---

complete QED corrections up to $O(\alpha^3)$ (with resummation) and EW corrections up to $O(\alpha^2)$.

[14]Since the calculation of any specific process involves some components that are generic to the e^+e^- annihilation environment and some components that are specific to the process under study, there is no contradiction when one says that they will draw general conclusions about the comparison of the two approaches from studies done with a specific process.

[15]In other words, the distributions which the QED collinear factorisation approach produces are not exact for the transverse degrees of freedom which were integrated out to arrive at the collinear limit represented by the QED PDF's while our distributions are exact in these degrees of freedom. We have seen in the LEP studies [226] that the detailed measurements of the exclusive photon distributions show this deviation from exactness.

[16]We stress that in any real observable there is always multiple photon radiation to all orders in α. Any fixed-order calculation thus is necessarily academic, and its usefulness has to determined on a case-by-case basis. In many cases, the effects of the multi-photons missing from the fixed-order result are small enough that the fixed-order result can be used

with full multiple photon phase space can provide predictions for the real experiments. On the other hand, variants of Eq. (9.3) with added subleading corrections in f_l and $\sigma_{ll'}$ are quite useful in testing/calibrating Monte Carlo programs. For instance the BHLUMI program includes the QED collinear factorisation based program LUMLOG, while $\mathcal{KK}$MC provides the KKsem and KKfoam auxiliary programs, which serve for testing/calibrating the main multiphoton generator, albeit for academic observables.

9.3 Summary

We conclude with the following observation: $\mathcal{KK}$MC-ee is the unique e^+e^- annihilation MC which features CEEX exact $O(\alpha^2 L)$ corrections and control over the corresponding EW initial-final interference (IFI) effects as well the exact $O(\alpha)$ pure weak corrections and complete spin effects both for the initial beams and outgoing fermions. This uniqueness is important: it proves that we have a unique set of the tools to extend the CEEX method to the other important processes in the future e^+e^- colliders' precision physics programs in the effort to reach the new required precision for these processes.

10 NNLO QED calculations with McMule

Tim Engel, Marco Rocco, Adrian Signer, Yannick Ulrich

10.1 Introduction

While a huge effort is ongoing to tackle next-to-next-to-leading order (NNLO) corrections in QCD, fixed-order calculations in QED have received comparatively little attention in the literature. From a high-energy point of view this is understandable due to the numerical importance of QCD corrections, driven by a coupling that is much larger than the QED coupling α. Hence, NNLO QED calculations are typically considered in low-energy processes involving mainly leptons. However, for electron-positron colliders initial-state QED corrections are of utmost importance. Often such corrections are taken into account to high orders in α but with a soft and/or collinear approximation in the kinematics.

In this contribution we take a slightly different approach in that we start from complete fixed-order NNLO QED calculations. We will describe a modern approach for such calculations, based partly on the developments made for QCD, and explore how these calculations can be adapted to the case of a high-energy electron-positron collider. In particular, we regularise all singularities with dimensional regularisation in $d = 4 - 2\varepsilon$ dimensions and use a subtraction method for the phase-space integration. This is a notable difference to many QED calculations in the literature

---

to assess the data. Even in the latter cases, the lack of exactness of the treatment of the transverse degrees of freedom in Eq. (9.3) limits its applicability.

where a photon-mass regularisation as well as a slicing method, separating photon radiation into hard and soft, is used. We stress that the fact that we have thus far considered only fixed-order calculations and neglected all-order resummation effects does not imply that the latter cannot be matched with the former – in fact, we are now working towards this very goal; we shall briefly comments on this in Section 10.5.

In contrast to most QCD calculations, for QED calculations it is essential to keep non-vanishing fermion masses m. Since QED with massive fermions has only soft singularities, this leads to a tremendous simplification of the infrared (IR) structure. In Section 10.2 we will describe how this can be exploited to devise an efficient subtraction scheme for phase-space integrations at all orders in α.

However, this simplification comes at a cost. The presence of fermion masses introduces additional scales to the problem and leads to a complication in the calculation of virtual amplitudes. In fact, often it is not possible to obtain analytic expressions for two-loop amplitudes with $m \neq 0$. Fortunately, in many cases fermion masses are much smaller than the other kinematic variables Q^2. As described in Section 10.3, we can then use a procedure dubbed massification. It allows to recover all not polynomially suppressed mass effects of two-loop virtual amplitudes from the corresponding amplitudes with a massless fermion.

Another technical difficulty related to small but non-vanishing fermion masses is the presence of large logarithms $\ln(m^2/Q^2)$. These are the remnants of collinear singularities regulated by $m \neq 0$. In massless QCD, only observables that are inclusive in final-state collinear emission are physical, where these collinear singularities cancel as $1/\varepsilon$ poles. Initial-state collinear emissions are absorbed into the parton distribution functions. In QED, the $\ln(m^2/Q^2)$ are physical in that they can be measured. Being less inclusive leads to numerical issues in particular in the phase-space integration of the real-virtual contributions. Rather than using pure numerical techniques or brute force to address this issue, we use properties of radiative QED amplitudes. More precisely, we approximate these amplitudes in the soft limit at next-to-leading power to enable a stable numerical integration. This is described in Section 10.4.

The techniques outlined in this contribution are being implemented in the publicly available Monte Carlo framework MCMULE [230]. One of the main motivations for these developments is to obtain a full NNLO prediction of μ-e scattering. This process has gained a lot of interest [147] in the context of the MUonE experiment [231]. Already some important contributions have been calculated at NNLO [148, 149, 232–234] and the two-loop matrix element is known with $m_\mu \gg m_e = 0$ [235]. However, these techniques can also be used for processes at higher energies. Indeed, they form the basis for our exploration in Section 10.5 where we discuss first steps towards using MCMULE at medium- and high-energy electron-positron colliders.

10.2 The FKS$^\ell$ subtraction scheme

As with all cross-section calculations beyond leading order in gauge theories, also in QED with massive fermions IR singularities appearing in the phase-space integration have to be isolated and properly combined with those of virtual loop integration. What is particularly simple in our case is that no collinear $1/\varepsilon$ are present and the soft singularities exponentiate. In other words, the ℓ-loop

matix element (squared) with n external particles $\mathcal{M}_n^{(\ell)}$ satisfies the YFS formula [45]

$$\sum_{\ell=0}^{\infty} \mathcal{M}_n^{(\ell)} = e^{-\hat{E}} \sum_{\ell=0}^{\infty} \mathcal{M}_n^{(\ell)f} \qquad (10.1)$$

where all $1/\varepsilon$ IR poles of $\mathcal{M}_n^{(\ell)}$ are contained in the integrated eikonal factor $\hat{E}$ and the remainders of the matrix elements, $\mathcal{M}_n^{(\ell)f}$, are finite. This simple structure can be exploited to convert the FKS subtraction scheme [98, 100] initially developed for NLO QCD calculations to FKS$^\ell$ [236] for QED calculations at all orders. At NNLO for example, the double virtual, real-virtual and double-real corrections read

$$\sigma_n^{(2)}(\xi_c) = \int d\Phi_n^{d=4} \left(\mathcal{M}_n^{(2)} + \hat{E}(\xi_c)\,\mathcal{M}_n^{(1)} + \frac{1}{2!}\mathcal{M}_n^{(0)}\hat{E}(\xi_c)^2 \right) = \int d\Phi_n^{d=4}\,\mathcal{M}_n^{(2)f}(\xi_c), \quad (10.2a)$$

$$\sigma_{n+1}^{(2)}(\xi_c) = \int d\Phi_{n+1}^{d=4} \left(\frac{1}{\xi_1} \right)_c \left(\xi_1\,\mathcal{M}_{n+1}^{(1)f}(\xi_c) \right), \qquad (10.2b)$$

$$\sigma_{n+2}^{(2)}(\xi_c) = \int d\Phi_{n+2}^{d=4} \left(\frac{1}{\xi_1} \right)_c \left(\frac{1}{\xi_2} \right)_c \left(\xi_1\xi_2\,\mathcal{M}_{n+2}^{(0)f} \right). \qquad (10.2c)$$

where ξ_i are the (scaled) energies of the radiated photons, $d\Phi_n^{d=4}$ is the n-parton phase space in 4 dimensions, and the distribution $(1/\xi_i)_c$ acts on a test function $f(\xi_i)$ as

$$\int_0^1 d\xi_i \left(\frac{1}{\xi_i} \right)_c f(\xi_i) \equiv \int_0^1 d\xi_i \frac{f(\xi_i) - f(0)\theta(\xi_c - \xi_i)}{\xi_i}. \qquad (10.3)$$

All three terms in (10.2) are individually finite and the dependence on the unphysical parameter ξ_c cancels in the sum. This cancellation is exact and serves as a test for a correct and numerically stable implementation. The FKS$^\ell$ procedure does not require to split photon radiation into a soft and a hard part, nor does it introduce a photon mass as regulator. If all matrix elements are known, numerical integration of (10.2) combined with a measurement function to define the IR-safe observable(s) results in a fully-differential Monte Carlo code. This is the basis of the MCMULE framework [232].

10.3 Massification

The statement "if all matrix elements are known" is always easy to make, but often impossible to realise. Of course, tree-level matrix elements pose no problem. For one-loop matrix elements we often use OpenLoops [78, 237]. However, two-loop matrix elements are a bottleneck.

To alleviate the problem it is possible to start with the two-loop matrix element computed with massless fermions, $\mathcal{M}_n^{(2)}(m=0)$. This matrix element contains poles up to $1/\varepsilon^4$ due to double soft-collinear singularities associated with the massless fermion and photon. The corresponding matrix element with massive fermions, $\mathcal{M}_n^{(2)}(m)$, instead only contains $1/\varepsilon^2$ soft poles and $\ln^2(m^2/Q^2)$ as remnants of the collinear singularities. For small masses $m^2 \ll Q^2$ the idea is tempting to use the massless matrix element as an approximation of the massive one. This is, however, not possible due to the different singularity structure. Instead, the massive all-order result can be related to the massless one via the factorisation formula [238–240]

$$\mathcal{M}_n(m) = \left(\prod_j Z(m) \right) \times S \times \mathcal{M}_n(0) + O(m). \qquad (10.4)$$

The product is over all external fermion legs with a small mass m. The process-independent factor $Z(m)$ is given in (3.12) of [240] to NNLO and converts collinear $1/\varepsilon$ poles into $\ln(m^2/Q^2)$. However, it is important to stress that (10.4) does not only reproduce the logarithmically enhanced terms but in fact all terms that are not polynomially suppressed. The soft part S is process dependent, starts at NNLO, and receives contributions from only fermion loops. Conceptually this is the most complicated contribution due to the factorisation anomaly [240]. In practice, it is often advantageous to compute the fermion-loop contributions – including the hadronic ones – of two-loop matrix elements semi-numerically. This has the added advantage of eliminating S in (10.4) and rendering massification completely universal.

To obtain a perfect cancellation of the $1/\varepsilon$ singularities in (10.2) the divergent part of $\mathcal{M}_n^{(2)}(m)$ has to be taken without approximation using (10.1). We also use the full m dependence in the generation of the momenta and the phase space. Parametrically, the error induced by (10.4) at NNLO is of the order $(\alpha/\pi)^2 m^2/Q^2$, potentially multiplied by a $\ln(m^2/Q^2)$. For example, in the case of the electron energy spectrum of the muon decay, massification reproduces the NNLO correction with full electron-mass dependence at the level of a few percent [236]. Going to higher energies this approximation is expected to perform even better.

10.4 Next-to-soft stabilisation

Even though all parts in (10.2) are finite and can in principle be evaluated numerically in 4 dimensions, in practice numerical instabilities are often encountered. In particular $\sigma_{n+1}^{(2)}(\xi_c)$, (10.2b), is delicate as it requires a numerically stable evaluation of the real-virtual one-loop amplitude also in corners of phase space where large hierarchies of scales are present. OpenLoops shows a remarkable stability and has been used successfully for the real-virtual corrections of many QCD NNLO calculations. However, the presence of (small) fermion masses exacerbates the situation. The problem can be solved by replacing the full one-loop radiative matrix element with a sufficiently precise approximation in the numerically problematic soft-photon region. To this end, the next-to-leading-power expression for the limit where the photon momentum k becomes soft, i.e. $k \to 0$, is needed. This next-to-soft stabilisation has been used to compute the photonic corrections to Bhabha scattering [241] as well as the full corrections to Møller scattering [242] at NNLO. The precision of the numerical evaluation of the radiative matrix elements used in these calculations is better than 10^{-5} for all photon energies.

The leading term in the soft expansion has the celebrated form $\mathcal{M}_{n+1}^{(\ell)} = \mathcal{E}\,\mathcal{M}_n^{(\ell)}$ where the eikonal factor $\mathcal{E}$ scales as $1/k^2$ (and upon integration over the photon phase space yields $\hat{\mathcal{E}}$). This approximation is not sufficient for our purpose and has to be improved by including the subleading-power contributions scaling as $1/k$. At tree-level, the Low-Burnett-Kroll (LBK) theorem [243–245] provides a universal structure for these next-to-soft contributions. The LBK theorem has been extended to one loop for massive QED in [246] and according to its (3.31) is given by the sum of the hard and soft contributions

$$\mathcal{M}_{n+1}^{(1),\text{hard}} \simeq \sum_l \sum_i Q_i Q_l \left(-\frac{p_i \cdot p_l}{(k \cdot p_i)(k \cdot p_l)} + \frac{p_l \cdot \tilde{D}_i}{k \cdot p_l} \right) \mathcal{M}_n^{(1)}, \tag{10.5a}$$

$$\mathcal{M}_{n+1}^{(1),\text{soft}} \simeq \sum_l \sum_{i \neq j} Q_i^2 Q_j Q_l \left(\frac{p_i \cdot p_l}{(k \cdot p_i)(k \cdot p_l)} - \frac{p_j \cdot p_l}{(k \cdot p_j)(k \cdot p_l)} \right) 2S(p_i, p_j, k)\,\mathcal{M}_n^{(0)}, \tag{10.5b}$$

where the sums run over the external legs with charges Q_i and momenta p_i. The first term on the r.h.s. of (10.5a) scaling as $1/k^2$ is just the eikonal approximation mentioned before. The second term of (10.5a) scales as $1/k$ and is the expected one-loop generalisation provided by the LBK theorem, where $\tilde{D}_i$ is the (modified) LBK differential operator, see (3.11b) of [246]. Taken together, these two terms correspond to the tree-level version of the LBK theorem. Using the method of regions [247] to perform the expansion in k at the one-loop level, they correspond to the hard part [248]. At one loop there is also a soft contribution, scaling as $1/k$. The important observation of [246] is that this soft contribution also has a universal structure, as given in (10.5b). The function $S(p_i, p_j, k)$ scales as k and can be found in (3.29) of [246]. Using (10.5), the next-to-soft limits can be obtained without a detailed process-specific computation.

There is a subtlety hidden in (10.5a) in that the non-radiative matrix element has to be evaluated with radiative kinematics. In particular, the corresponding momenta only satisfy momentum conservation up to the remnant k. A possible approach on how to deal with this is discussed in [246], while an alternative is given in [249, 250].

10.5 Outlook towards higher energies

The techniques described in the previous sections were developed with low-energy processes in mind. However, they remain applicable and in some cases become even more important when going to higher energies. On the other hand, additional features have to be taken into account. As possible applications we are considering $ee \to \tau\tau$ for $\sqrt{s} \sim 10\,\text{GeV}$ [251] and also planning to extend our work on Bhabha scattering [241] and $ee \to \gamma\gamma$ to energies relevant for luminosity determinations at electron-positron colliders.

A first extension that is required is the inclusion of electroweak effects. A complete NLO calculation in the Standard Model can be achieved using OpenLoops for the matrix elements and FKS$^\ell$ for phase-space integrations.

A second issue that will become more prominent at higher energies are numerical issues related to collinear photon emission. At low energies, it is sufficient to give special consideration to the soft region, $k \ll m$. At higher energies, also the hierarchy $m^2 \ll Q^2$ will require some care, especially in the case of the numerically delicate real-virtual contribution. To this end, a similar strategy as for the soft region can be applied. This time the limit where the angle $\sphericalangle(k, p_i)$ becomes small has to be considered. Since we keep $p_i^2 = m^2$, but now treat $m^2 \ll Q^2$, we need the limit $k \cdot p_i \sim m^2 \ll Q^2$ of one-loop radiative matrix elements. At leading power in the small quantity and at NLO in α this leads to a generalisation of massification, (10.4), that e.g. for an initial-state collinear configuration reads

$$\mathcal{M}_{n+1}(k, p_j, m) \simeq J_{\text{ISR}}(x, m)\Big(\prod_{j \neq i} Z(m)\Big)\mathcal{M}_n(p_i - k, p_{j \neq i}, 0), \tag{10.6}$$

where $1 - x$ is the energy fraction carried off by the photon. Thus, for the (incoming) leg i to which the photon becomes collinear, the factor $Z(m)$ is replaced by the splitting function J_{ISR}. The explicit expression for J_{ISR} and the crossing related final-state splitting function J_{FSR} at one loop can be found in Appendix B of [246]. This factorisation formula could also turn out to be useful in coping with the narrow peaks that arise due to the collinear scale hierarchy. In particular, (10.6) can be used to subtract these collinear pseudo-singularities pointwise, in analogy to [19].

Finally, MCMULE is currently calculating strictly at fixed order. However, for many applications a combination with resummation, e.g. that achieved by a parton shower or by analytical techniques, is required. The collinear configurations mentioned in the previous paragraph give rise to logarithms $\ln(m^2/Q^2)$. They become more important at higher energies and can be resummed using fragmentation functions (for final state) or parton distribution functions (for initial state)[17]. Currently, within MCMULE an effort is ongoing to include a YFS parton shower[18] that is similar to PHOTONS++ [66] and matched at NNLO. For the parton shower, instead of $\hat{\mathcal{E}}$ the exponent of (10.1) is the YFS form factor, that also includes a virtual contribution. The subtraction scheme FKS$^\ell$ is well suited for this as it is already based on YFS. This helps dealing with double counting in the matching of the parton shower to fixed-order calculations.

With these extensions MCMULE will become a tool for leptonic processes with an even broader range of applications.

Acknowledgments

11   Collinear divergences at future e^+e^- colliders

Alessandro Vicini

11.1   Precision calculations at an e^+e^- collider

The high-precision tests of the Standard Model (SM) at an e^+e^- collider, like the future FCC-ee or CEPC, rely on the possibility to compute higher-order radiative corrections, covering all the relevant phase-space regions. Detailed studies have been performed at LEP (cfr. [166, 253] and references therein) and in preparation for the FCC-ee [144] and the CEPC [254], with a systematic discussion of the available codes and of several aspects related to the treatment of higher-order radiative corrections. In this note we try to comment about some of the challenges set by the expected experimental precision at e^+e^- colliders and about the possible transfer of the theoretical and computational knowledge developed for the LHC.

We assume, for the sake of discussion, that the full set of three-loop EW corrections to the process $e^+e^- \to f\bar{f} + X$, with f an electrically charged fermion, is explicitly available. The need for such a challenging calculation has been discussed in [153, 255], in view of high-precision measurements at the Z resonance. It has been shown that there might be corrections to the lowest-order couplings, from virtual corrections of weak and mixed QED-weak origin, numerically relevant e.g. in the prediction of the asymmetries. Their role is somehow complementary to the one of the QED corrections, in the precise predictions of the kinematical distributions. It is known, since LEP [137], that initial state QED radiation develops very large logarithmic corrections, crucial to the high-precision description of the Z lineshape. The resummation to all orders of these classes of

---

[17]In the context of the Snowmass 2021 proceedings, the interested reader can find a more extensive discussion on collinear factorisation and YFS in previous sections and in ref. [252].

[18]17

corrections is known to be mandatory, for an accurate prediction of the central values of the observables and for a reduction of the remaining theoretical uncertainty [185, 256, 257]. Few questions[19] arise: 1) Is the three-loop calculation on its own sufficient to match the precision target, without the inclusion of additional higher-order contributions? 2) Since the large logarithmic effects are due to soft or collinear emissions, which of the two classes of corrections should receive priority in the construction of a framework matching fixed- and all-order results ? 3) Does the answer to the previous question depend on the observable under study?

In order to fix some figures, at FCC-ee the total cross section into hadrons, at the Z peak, can be measured with a relative error at the 0.01% level [144]. We take this number as a illustrative reference for the needed precision of the theoretical predictions. In the study of the Z boson lineshape, the center-of-mass energy is $\sqrt{s} \sim m_Z$. The size of the logarithmic factor, which appears with the initial state QED radiation upon integration over the photon-emission angle and is dominated by the phase-space region with the photon collinear to the incoming electron or positron, is $L \equiv \log(m_Z^2/m_e^2) \sim 24.18$, with m_e the mass of the electron. The structure of the cross section, putting in evidence the initial state collinear (also dubbed mass) logarithm L and the soft logarithm ℓ, is given, up to first order in the fine structure constant α, by $\sigma = \sigma_0 + \alpha\,(a_{11}L\ell + b_{10}L + c_{01}\ell + d_1)$, with σ_0 the Born cross section. The soft logarithm $\ell = \log(\Delta E^2/m_Z^2)$ appears because of the emission of soft, i.e. low-energy, photons and its precise value depends on the resolution ΔE adopted to identify the final state particles. We remark the presence of a double logarithmic enhancement given by the product of a mass and a soft logarithms, plus the contributions given by single logarithmic terms and a subleading term without enhancement. In order to appreciate the need for a systematic resummation of the large logarithmic corrections, and in particular those due to collinear emissions, we iterate the initial state single logarithmic collinear correction factor and find: $\alpha L \sim 0.1764$, $\alpha^2 L^2 \sim 0.0311$, $\alpha^3 L^3 \sim 0.0055$, $\alpha^4 L^4 \sim 0.0010$. These factors strongly contribute to enhance the effect of the radiative corrections, at a level relevant for the precision goal of prediction of the total cross section into hadrons. Even if we can not draw final conclusions from this numerical inspection, it nevertheless suggests that the answer to the first question could be negative, and the matching of resummed and three-loop results could be necessary. One might ask whether the resummation of terms at the third order in a logarithmic counting is by itself sufficient to match the precision goals of the future e^+e^- colliders, without needing a full three-loop calculation and the corresponding matching. The estimates presented in [153, 255] suggest that both sets of corrections (fixed and to all orders) will be needed, because of their different impact on the observables.

A detailed review about the structure functions for the resummation of collinear logarithms, and of the Yennie-Frautschi-Suura (YFS) formalisms [45] for the resummation of soft-emissions contributions, has been presented in [258]; we refer to Section 2.4 of that paper for technical details. In this note we address questions analogous to those of ref. [258] for the matching with next-to-leading (NLO) fixed-order results, but, at variance with that paper, we consider now the problem of a matching which could be needed at third order.

---

[19]We refer to the three-loop EW case as the ultimate calculation that can be necessary at the FCC-ee/CEPC, but the same questions could already be addressed, when the complete set of two-loop EW will become available.

11.2 The collinear singular limit of squared matrix elements

In QED, the amplitude describing the emission of a photon off an external on-shell fermion f is proportional to

$$\frac{1}{(p+k)^2 - m_f^2 + i\varepsilon} = \frac{1}{2E_p E_k (1 - \beta_f \cos\theta) + i\varepsilon} \tag{11.1}$$

where p and k are the fermion and photon momenta respectively, $k^2 = 0$ and $p^2 = m_f^2$, m_f is the fermion mass, $E_p = \sqrt{m_f^2 + \vec{p}^2}$ is the fermion energy, $E_k = |\vec{k}|$ is the photon energy, θ is the emission angle of the photon with respect to the fermion $\vec{p}$, and $\beta_f = \sqrt{1 - m_f^2/|\vec{p}|^2}$. When we integrate the squared matrix element over the photon phase space, the interference term of two Feynman amplitudes with the photon emitted by two charged particles yields a factor proportional to $\log\left(\frac{1+\beta}{1-\beta}\right)$ which diverges in the $m \to 0$ limit; this singularity is thus called mass or collinear divergence, because the relevant phase-space region is the one with the photon parallel to the emitting particles.

The collinear divergence depends only on the properties (charge,mass,spin) of the emitting particles, but it is independent of the details of the rest of the hard scattering process. This universality feature emerges as a consequence of the factorisation of the squared matrix element. Beyond the first order, the correct factorisation in the collinear limit has been explicitly demonstrated to all orders for tree level amplitudes in [259]. Explicit results at second order are known [260], and explicit checks at third order have been performed [261, 262] but a formal demonstration of collinear factorization theorems for a generic process to all orders is lacking.

The appearance, in the first QED calculations of radiative corrections [263] of mass singularities, and the remark of their cancellation in inclusive quantities, has led to the formulation, by Kinoshita-Lee-Nauenberg (KLN) [264, 265], of a theorem which states the conditions of such cancellation. The sum over all degenerate, i.e. indistinguishable, final states yields a finite, regular result, although the individual contributions are separately divergent. The finiteness is achieved order by order in the perturbative coupling constant expansion, including contributions due to virtual and real-emission corrections, provided that both sets are degenerate with respect to the observable definition. This theorem is fundamental in the physics of hadronic jets and more in general provides the guiding principle to define infrared-safe and collinear-safe observables.

The emission of collinear radiation from the initial state of a scattering amplitude modifies the kinematics of its underlying process, because the emitted particle has in general a finite energy. The non degeneracy of the two underlying processes, in the virtual and real correction cases, breaks the hypothesis of the KLN theorem. It is thus possible that a collinear divergence survives in the combination of the two contributions. Thanks to the factorisation property of these divergences, the partonic cross section can be written as the product of a finite cross section times a divergent factor. The universality of the latter allows us to reabsorb it into the definition of the incoming physical object starting the scattering: the best known example is given by the proton and its parameterisation in terms of collinear parton density functions (PDFs). Thanks to the universality properties, this redefinition is predictive, with a factorization-scheme ambiguity at the level of the subdominant finite corrections, formally of a perturbative order higher with respect to the one of the calculation. The PDFs express the probability to find a parton that carries a fraction x of the proton momentum, while probing the latter in a scattering with a momentum transfer μ. In complete analogy, we can describe a lepton scattering, like e.g. $e^+ e^-$ annihilation, as the interaction of two

composite systems, the leptons, whose internal structure is given in terms of partons (electrons, positrons, photons, quarks, EW bosons). The definition of the physical lepton is given, order by order in perturbation theory, only after the factorisation of the initial state collinear divergences and their reabsorption in the lepton PDFs. The collinear parton densities $\vec{q}(x,\mu^2)$ (they can be partons inside a proton or a lepton), satisfy the integro-differential DGLAP equations [39, 40, 42]

$$\frac{\partial}{\partial \log \mu^2} \vec{q}(x,\mu^2) = \frac{\alpha(\mu)}{2\pi} \int_x^1 \frac{dz}{z} \mathbf{P}(z) \cdot \vec{q}(\frac{x}{z},\mu^2) \,, \tag{11.2}$$

whose solution expresses their dependence on the scale μ as the convolution of the densities themselves with the appropriate splitting functions matrix $\mathbf{P}(z)$. The latter describe the emission responsible for the scale change, evaluated in the collinear approximation, and can be computed in perturbation theory. They are know up to 3-loop level [266–269] in QCD. The solution of the DGLAP equations resums to all orders the contributions due to the collinear emissions described by the splitting functions. The logarithmic accuracy of this resummation is determined by the perturbative order of the splitting function expression.

The solution of the DGLAP equations requires to fix the boundary conditions of the differential problem. In the QCD case, since the strong interaction does not allow us to compute these conditions from first principles, the proton structure has to be modeled in terms of PDFs and the PDF parameters at a given scale are fit to the available experimental data. This problem has led to a large number of studies discussing the representation of the uncertainty on the proton structure induced by the imperfect knowledge of the boundary conditions [270]. The consistent determination of the latter from a fit to several experimental data is possible only if all the relevant cross sections are known at the perturbative order under discussion. This latter problem represents a bottleneck in the progress towards a consistent prediction of the LHC processes at NNLO-QCD and, a fortiori, N3LO-QCD or NNLO QCD-EW. In summary, the DGLAP evolution of the proton PDFs can be performed if the splitting function at a given order are known, but the absolute value of the parton densities can be affected by an inconsistent knowledge of the boundary conditions. In the lepton case, it is instead possible to compute the boundary conditions from first principles in QED as shown at NLO-QED in [38]. An effort towards their determination at NNLO-QED and N3LO-QED is needed, in order to apply the DGLAP formalism at a lepton collider [120] at least at second, but hopefully also at third order in perturbation theory.

The solution of the integral-differential DGLAP equations is achieved in QCD via numerical algorithms, with different evolution codes available in the literature [91, 271], developed to solve the QCD case, including so far up to NNLO splitting kernels. The peculiar feature, in QED, of the existence of an integrable singularity at $z = 1$, makes an analytic solution possible in this case. While the results at NLO-QED are available [37, 130], the possibility to prepare an evolution code at NNLO or N3LO in QED requires the two- or three-loop splitting functions, which could be derived from the QCD expressions, but also the boundary conditions, discussed above.

11.3   Comparison of structure functions and YFS formalisms

We consider the inclusive production of a final state F in the scattering of two particles $P_{1,2}$, e.g. hadron-hadron or lepton-lepton, in the structure function approach. We formulate the cross section

as the convolution of the parton densities describing the probability of finding partons i, j inside the colliding particles, with a partonic cross section.

$$\sigma(P_1 P_2 \to F + X) = \sum_{i,j} \int dx_1 \, dx_2 \, q_i(x_1, \mu) q_j(x_2, \mu) \, \hat{\sigma}(ij \to F + X) \qquad (11.3)$$

A consistent result is obtained with the partonic cross section computed at a given fixed perturbative order and subtracted of the initial state collinear divergent factors, convoluted with the structure functions at the same order. The latter account, via DGLAP evolution, for the resummed contribution of the initial state collinear logarithms. For example, we consider in QED the case of a cross section computed with the full NLO-EW results at parton level $\hat{\sigma}$ and convoluted with the QED LL solution of the DGLAP equations. The result has NLO-EW accuracy for the total cross section, it includes to all orders terms of $O(\alpha L)$, but only partially accounts for the second-order terms proportional to $\alpha^2 L$: the fixed-order missing contributions stem from the non-factorisable two-loop corrections. A full NNLO-EW calculation, convoluted with the corresponding second order structure functions, will exactly include to all orders terms of $O(\alpha^2 L)$, but only partially subleading fixed-order terms proportional to $\alpha^3 L$. The inclusion of terms proportional to logarithms due to soft emissions in this formulation is restricted to those present in the fixed-order expression. In addition, the DGLAP equations obviously include to all order the contributions of the initial-state soft and collinear phase-space region.

A different approach to describe multiple radiation is given by the so called Parton Shower. The latter provides an algorithmic implementation of the exponentiation of the soft LL contributions. This description can be matched, avoiding double countings, with the exact matrix elements. The latter improve the total cross section prediction and the description of hard, large-transverse-momentum radiation.

$$d\sigma = F_{SV} \, \Pi(Q^2, \varepsilon) \times \sum_{n=0}^{\infty} \frac{1}{n!} \left(\Pi_{i=0}^n F_{H,i} \right) |\mathcal{M}_{n,LL}|^2 d\Phi_n \qquad (11.4)$$

One possible formulation is given in equation 11.4, as implemented in the event generator HORACE [141]. The LL Parton Shower approximation is corrected at $O(\alpha)$ by the infrared and collinear finite factors F_{SV} and $F_{H,i}$: we have the Sudakov form factor $\Pi(Q^2, \varepsilon)$ accounting for the exponentiation of the soft emissions; we have the real emission matrix elements $\mathcal{M}_{n,LL}$ written in terms of the product of n eikonal currents; the factor F_{SV} takes into account the finite part of soft emissions and virtual corrections, while the exact matrix element is applied to each hard large-transverse-momentum emission via the $F_{H,i}$ correction. The factorised formulation guarantees the correct semiclassical limit, but also introduces universal higher-order terms, which can partially account, for instance, for a subset of NLL collinear terms and in particular for part of the subset proportional to $\alpha^2 L$, with a significant phenomenological improvement. Extending this kind of matching beyond NLO is a current topic of investigation, with NNLO results matched to a LL Parton Shower [272]. Also in this case, an explicit improvement is achieved for the total cross section and for the observables sensitive to hard large-transverse-momentum radiation, whereas the Parton Shower resummation includes only LL terms.

The YFS approach [45] starts from the resummation of the first-order logarithms in the soft approximation. In the literature, considering the scattering of two fermions into two fermions,

not only the logarithms due to initial state radiation, but also those stemming from the initial-final interference and the final-state emissions, have been exponentiated and matched with fixed order expressions up to second order [64, 186]. The YFS fully exclusive formulation is based on the factorisation of soft emissions already at the amplitude level. Thanks to the factorisation of one-loop soft-divergent virtual corrections, it is possible to obtain a soft-finite one-loop correction factor Y which exponentiates. The resummed fully differential expression of the cross section reads:

$$d\sigma = d\sigma_0 \exp(Y) \exp\left[\frac{dk\,d\cos\theta\,d\phi}{(2\pi)^2}k\,\Theta(k - k_{min})\sum_\varepsilon \alpha\left(\frac{\varepsilon(k)\cdot p_2}{k\cdot p_2} - \frac{\varepsilon(k)\cdot p_1}{k\cdot p_1}\right)^2\right] \quad (11.5)$$

$$Y = \beta\log\frac{k_{min}}{E} + \frac{1}{4}\beta + \frac{\alpha}{\pi}\left(\frac{\pi^2}{3} - \frac{1}{2}\right) \qquad \beta = \frac{2\alpha}{\pi}\left[\log\left(\frac{s}{m_e^2}\right) - 1\right].$$

The second exponential of the first equation is a compact notation for the sum over all possible additional photon multiplicities n of the product of eikonal emission factors, valid in the soft limit; the presence of an integration measure is the symbolic representation of the phase-space factors for n photons, with arbitrary n. The description of photons, with an energy larger than the cut-off k_{min}, is fully differential. We read in the exponent Y the presence of the first-order double and single logarithmic terms due to collinear and soft-collinear contributions, evaluated in soft approximation, integrated in the photon energy up to the cut-off k_{min}. Given the soft limit approximation, for the electromagnetic coupling the fine structure constant α is a customary choice. The inclusion of higher-order contributions like the description of additional light fermion pairs could be simulated with a running coupling, but in this case care should be paid to avoid double countings with the rest of the hard correction factors. The matching with the exact $O(\alpha)$ results yields, following the original YFS algorithm, additional corrective factors β_n called residuals, free of any soft or collinear divergence, expressing the impact of the exact matrix element on the n-th emission. A modification of the residuals, without spoiling the formal accuracy of the calculation, allows to improve the resummed and matched YFS formulation to include also the missing $\alpha^2 L$ terms. In summary, the exact exponentiation of the one-loop soft logarithms is matched to fixed first- and partial second-order results, covering up to second order all the relevant infrared divergent contributions.

11.4 Discussion and conclusions

The estimated experimental precision of future e^+e^- colliders forces us to investigate the question of the best formulation of a calculation that includes fixed- and all-orders results in e^+e^- collisions, up to three-loop level. The various approaches can be described with respect to *a)* the formal inclusion of the various classes of enhanced contributions and *b)* the possibility of extending the resummation beyond the exponentiation of the first-order divergent terms. We eventually consider the dependence on the observable under study.

Any code based on a Parton Shower relies on the algorithmic exponentiation of the first-order soft emissions, achieving LL accuracy; the angular dependence of the radiation depends on the specific implementations. After the matching with NLO matrix elements, it is possible that a subset of the NLL collinear contributions is correctly included, but the full set of terms proportional to $\alpha^2 L$ is under control only with matching at NNLO level. It is interesting to observe that, in the Parton Shower matching, different recipes, still preserving the formal accuracy of the results, can

lead to significant numerical differences. This remark shows the role of multiple radiation and the impact of its "handling", as ruled by the matching recipe. Important examples are known from the LHC studies and it would be interesting to check this point for an e^+e^- collider, in view of the very high-precision goal. It is not obvis that an improvement of the accuracy of the resummation part, going beyond the LL level, can be achieved for a general purpose tool.

The YFS formalism is based on the exclusive exponentiation of first-order contributions in the soft limit. The inclusion of all the LL terms is achieved at amplitude level and the full set of $\alpha^2 L$ collinear contributions can be included. The full resummation of NLL collinear logarithms is not available. In the public implementations of the YFS formalism, all the radiating particles are supposed to be massive, thus separating the issue of the collinear divergences from the discussion of the soft contributions. While this is a viable approach in the description of e^+e^- collisions, it would introduce a dependence on unphysical quark masses in the description of quark-initiated processes relevant for the LHC.

In the pure structure functions approach the formulation of the physical cross section is purely dictated by the factorisation of the initial state collinear singularities. As a positive outcome, the extension to two- and three-loop level is conceptually straightforward. A technical effort to translate the N3LO splitting functions to the QED case and to compute the boundary conditions to the DGLAP equations is needed, and is feasible. The contributions which are resummed in this approach are the collinear logarithms, going up to NNLL, in the case a three-loop result were available. In the pure structure function approach, the soft logarithms taken into account are those appearing from the matrix elements, and those of the soft-collinear phase-space corner.

At a future e^+e^- collider, two extremely important energy regions in the precision physics program are the Z-boson resonance and the W^+W^- production threshold. The resummation of the soft logarithms clearly plays a role in the determination of the precise position of these two points and in the description of the associated lineshapes: these logarithms in fact control the exact amount of energy available in the center-of-mass of the hard scattering process. On the other hand, the measurement takes place in a fiducial volume, with acceptance cuts also in the plane transverse to the beam, so that a formalism based on the separation between the longitudinal and transverse components can be a natural framework for precise predictions.

Exploring the impact of the different resummations, with the currently available tools, can set the stage to the evaluation of higher-order corrections and the preparation of an adequate matching formalism.

12   Factorization beyond leading power

Leonardo Vernazza

12.1   Factorization at next-to-leading power: state of the art

Understanding gauge theory scattering amplitudes in the limit where external radiation becomes soft poses interesting challenges from a conceptual quantum field theory point of view and has important applications in the phenomenology of precision particle physics. Let us consider n-particle scattering processes in QED. Given the emission of an additional soft photon with momentum k,

the scattering amplitude $\mathcal{M}_{n+1}$ can be expressed as a power expansion in the energy $E = k^0$ of the photon,

$$\mathcal{M}_{n+1} = \mathcal{M}_{n+1}^{\text{LP}} + \mathcal{M}_{n+1}^{\text{NLP}} + O(E), \tag{12.1}$$

where the *leading power* (LP) term has scaling $\mathcal{M}_{n+1}^{\text{LP}} \sim 1/E$, the *next-to-leading power* (NLP) contribution is of order $\mathcal{M}_{n+1}^{\text{NLP}} \sim E^0$, and so on.

Our interest for the expansion in eq. (12.1) stems from the fact that the coefficients in the series *factorize*, i.e., they can be expressed in terms of simpler, universal objects, which relate the radiative amplitude to the non-radiative or *elastic* amplitude $\mathcal{M}_n$. It is well known that the LP term in eq. (12.1) has the universal form [45, 273]

$$\mathcal{M}_{n+1}^{\text{LP}}(\{p_i\}, k) = S_n \, \mathcal{M}_n(\{p_i\}), \qquad S_n = e \sum_{i=1}^{n} q_i \frac{p_i^\mu \varepsilon_\mu(k)}{p_i \cdot k}, \tag{12.2}$$

where p_i^μ and q_i represent the momentum and electric charge of the i-th hard particle, and $\varepsilon_\mu(k)$ is the polarisation vector of the soft photon. The soft function S_n describes a set of eikonal interactions between the external particles and the soft photon, which are sensitive only to the direction and charge of the emitting particle. In general, S_n can be calculated as the vacuum expectation value of a set of Wilson lines, one for each hard emitting particle.

Relations such as the one in eq. (12.2) are also known as *soft* theorems. Their interest is not just purely theoretical, but also relevant for phenomenology. The $1/E$ singularity in the soft limit enhances soft radiation in scattering processes. Measurements that are sensitive to soft radiation involve a small scale, and the corresponding cross section contains large logarithms of the ratio of this small scale and the scale of the hard scattering. Such large logarithms potentially spoil the convergence of the expansion in the coupling e, a problem that can be addressed by resummation. The development of theorems such as the one in eq. (12.2) led to the proofs of factorization [274–276], but also constitutes the first step towards resummation, as it allows one to decompose a multi-scale amplitude (or cross section) into the product of simpler single-scale functions.

The physical interpretation of eq. (12.2) rests upon the long wavelength of soft radiation not being able to resolve the hard scattering. However, at each subsequent power in (12.1) more is revealed, and the factorization structure becomes more involved. The NLP term in eq. (12.1) is still under much investigation. Emitted (next-to-)soft radiation becomes sensitive to the spin of the hard particles, and starts to reveal details of the internal structure of the hard interaction. Compared to eq. (12.2), the factorization of radiative amplitudes at NLP needs to take into account the following features:

- Emission of soft radiation from the hard partons beyond the eikonal approximation, for instance involving chromo-magnetic interactions between the hard particle and the emitted soft photon. This can be taken into account by introducing generalizations of the soft function S_n in eq. (12.2) [277].

- Emission of soft radiation from the non-radiative amplitude. This is one of the mechanism which probes the structure of the hard interaction, and was understood a long time ago in papers by Low, Burnett and Kroll [243, 244]: in the case of massive emitting particles, the structure of the NLP term is dictated by gauge invariance, by means of Ward identities. This

early formulation, now known as the "LBK" theorem, was proven [278] to hold only in the region $k^0 \ll m^2/Q$, with Q the centre of mass energy.

- For $m^2/Q < k^0 < m$, the LBK theorem must be extended to account for NLP contributions arising from soft photons emitted from loops in which the exchanged virtual particles have momenta collinear to the external particles (i.e. having a small virtuality, while retaining momentum components which are large compared to the soft radiation). Such type of contributions are identified as *radiative jets*. The first of such configurations was investigated for Drell-Yan in [278].

Most of the effort in the past few years has been devoted to the derivation of factorization theorems able to describe consistently such soft and collinear radiation into well defined field-theoretical matrix elements. This has been done following mainly two approaches. One, which we will refer to as *diagrammatic*, aims at describing such matrix elements in terms of fields, currents and Wilson lines in QED. The second approach is based on Soft-Collinear Effective Theory (SCET) [182, 279–282].

SCET describes the soft and collinear limits as separate degrees of freedom, each with their own Lagrangian. The elastic amplitude $\mathcal{M}_n$ in (12.2) is encoded in terms of effective n-jet operators and their short-distance coefficients, which capture the contribution from hard loops. At LP, soft emissions from hard particles can be described by Wilson lines, as in the diagrammatic picture. Beyond LP, soft emissions originate from time-ordered non-local operators made out of soft and collinear fields, where the power suppression follows either from additional insertions of the power-suppressed soft and collinear Lagrangian, or from subleading operators describing the hard scattering [283–285]. SCET provides a systematic approach, as each operator and Lagrangian term have by construction a definite power counting. When all operators consistent with symmetries are included, this completeness ensures that the resulting factorization is valid to all orders in the coupling constant.

Both approaches present advantages and disadvantages. From a technical point of view, the calculation of soft and collinear matrix elements within SCET is designed such as to directly reproduce calculations obtained within the method of expansion by momentum regions [247], and can be quite involved already at one-loop (cf. [285, 286]). In this respect, the calculation of matrix elements within the diagrammatic approach is simpler (cf. [249, 287, 288]), although the lack of tools such as multipole expansion results into overlaps between soft and collinear matrix elements, leading to complicated nested subtractions beyond one loop.

More relevant for applications to the theory of resummation is the fact that soft and collinear matrix elements involve convolutions, which are well defined in dimensional regularisation, but often divergent in $d = 4$. This poses a challenge for a standard EFT approach, where one first renormalizes each function in the factorization theorem to derive the renormalization group equations needed for resummation, causing these convolution integrals to become divergent. The problem needs to be investigated case by case, and so far only one example is known [289, 290], where convergence of the convolution integrals can be achieved after a re-factorization process, which is non-trivial to be proven in general (see also [291, 292]). In this respect, the diagrammatic approach could provide an easier path to resummation by exploiting exponentiation properties of

soft radiation and the replica trick [293, 294], which can be carried out within dimensional regularization (cf. [295, 296]).

The classification of soft and collinear matrix elements contributing beyond LP is rather straightforward in SCET, once the power-counting and field content of the theory is fixed [283–285]. Within the diagrammatic approach, the classification of all possible soft and collinear matrix elements has been derived for the Yukawa theory [297] and more recently for QED [298] (see also [250]). We will illustrate such derivation in the next section.

12.2 Factorization of QED amplitudes: diagrammatic approach

Understanding the factorization structure of $\mathcal{M}_{n+1}^{\text{NLP}}$ requires in turn to determine the factorization of the elastic amplitude $\mathcal{M}_n$. This can be easily seen by recalling the LBK theorem and its failure to include virtual collinear configurations: one starts by separating the radiative amplitude in two contributions: one in which the radiation is emitted from the external legs, plus another in which the radiation is emitted from a particle within the hard scattering kernel:

$$\mathcal{M}_{n+1} = \mathcal{M}_{n+1}^{\text{ext}} + \mathcal{M}_{n+1}^{\text{int}}. \tag{12.3}$$

The amplitude $\mathcal{M}_{n+1}^{\text{int}}$ can be obtained by means of the Ward identity from $\mathcal{M}_{n+1}^{\text{ext}}$. Focusing on the latter, consider the emission from an outgoing fermion i: $\mathcal{M}_{n+1}^{\text{ext}}$ takes the form

$$\mathcal{M}_{n+1}^{\text{ext}} = \bar{u}(p_i)(ieq_i\gamma^\mu)\frac{i(\not{p}_i + \not{k} + m)}{(p_i + k)^2 - m^2}\mathcal{M}_n(p_1, \ldots, p_i + k, \ldots p_n), \tag{12.4}$$

where $\mathcal{M}_n$ represents the elastic amplitude (stripped off the spinor $\bar{u}(p_i)$). Within the LBK theorem, one expands the amplitude in the soft momentum k. As discussed, this expansion gives correct results only in the regime $p_i \cdot k/Q \ll m^2/Q$. But for parametrically small masses $m^2/Q < p_i \cdot k/Q < m$, naively expanding the elastic amplitude in the soft momentum k misses a contribution in which the soft photon is emitted from internal particles collinear to the external leg, which is thus included neither in $\mathcal{M}_{n+1}^{\text{ext}}$, nor in $\mathcal{M}_{n+1}^{\text{int}}$. Eq. (12.4) tells us that in order to understand the factorization properties of the radiative amplitude $\mathcal{M}_{n+1}$ we also need to obtain the correct factorization structure of the elastic amplitude $\mathcal{M}_n$, in presence of a small off-shellness $p_i \cdot k \sim m^2 \ll Q^2$. At leading power the factorization structure is known, see for instance [299, 300], and it takes the following schematic form:

$$\mathcal{M}_n = H_n \times S_n \times \prod_{i=1}^n \frac{J_i}{\mathcal{J}_i}. \tag{12.5}$$

In this equation the jet and soft functions J_j and S describe long-distance collinear and soft virtual radiation in $\mathcal{M}_n$. These functions are universal, i.e. they depend only on the colour and spin quantum numbers of the external states, and determine also the structure of collinear and soft singularities of the elastic amplitude. Note that one must divide each jet by its eikonal counterpart $\mathcal{J}_i$, to avoid the double counting of soft and collinear divergences.

The corresponding factorization structure at NLP for QED has been determined in [298]. In short, the task consists in obtaining a classification of the jet-like structures, consisting of virtual radiation collinear to any of the n external hard particles, contributing at subleading power. This is obtained by power counting the *pinch surfaces* that underlie the collinear (and soft) contributions
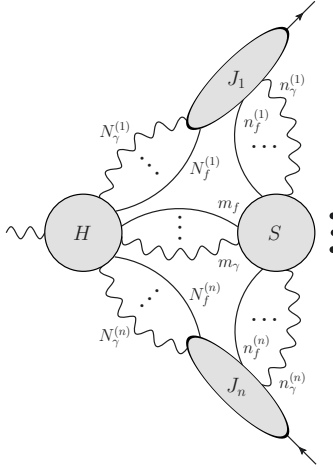
Figure 2. The reduced diagram for a vector boson induced QED process with n hard particles in the final state. Ellipses denote the presence of an arbitrary number of photons/(anti-)fermions.

one wishes to describe in terms of jet (and soft) functions, for a general QED scattering amplitude. The pinch surfaces are the solutions of the Landau equations [301] and are represented by reduced diagrams in the Coleman-Norton picture [302]. In these diagrams, all off-shell lines are shrunk to a point, while the on-shell lines are kept and may be organised according to the nature of the singularity they embody, be it soft or collinear. This gives the general reduced diagram of fig. 2, in which one distinguishes a soft "blob" containing all lines carrying solely soft momentum, n jets J_i comprised of lines with momenta collinear to the respective external parton and lastly, a hard blob H collecting all contracted, off-shell lines. The power counting is carried in light-cone coordinates: a generic momentum k is decomposed as $k^\mu = (k^+, \vec{k}_\perp, k^-)$, where the light-cone components $k^\pm$ lie along the direction of two light-like vectors n_i and $\bar{n}_i$, normalized such that $n_i \cdot \bar{n}_i = 1$, with n_i along the direction of p_i. Soft and collinear momenta are taken to scale as

$$\text{Soft:} \quad k^\mu \sim Q\left(\lambda^2, \lambda^2, \lambda^2\right), \qquad \text{Collinear:} \quad k^\mu \sim Q\left(1, \lambda, \lambda^2\right). \tag{12.6}$$

One focuses on virtual corrections to a hard scattering configuration, for which all invariants $s_{ij} = (p_i + p_j)^2 \sim Q^2$ involving external momenta are large compared to the energy of the radiated soft photon in $\mathcal{M}_{n+1}$. Requiring the soft momentum to be of order λ^2 rather than λ guarantees that the photon is soft with respect to all particles in the elastic amplitude. Within this power counting, a NLP quantity is suppressed by two powers in λ with respect to the leading power contribution.

Using the momentum scaling in eq. (12.6), one first derives the *superficial degree of divergence* of a particular reduced diagram $\mathcal{G}$ contained in fig. 2, which is simply the λ-scaling of this diagram, $\mathcal{G} \sim \lambda^{\gamma_{\mathcal{G}}}$. In practice, $\gamma_{\mathcal{G}}$ can be expressed as function of the number of fermion and photon connections between the hard, soft and collinear subgraphs and, in presence of massive fermions, on the internal structure of the soft subgraph. Such a formula expresses, at any perturbative order, which pinch surfaces contribute up to NLP, which allows one to set up a consistent and complete NLP factorization framework for QED. The approach is analogous to the one taken for Yukawa theory in [297], and it is a direct application of the well-known method first developed for
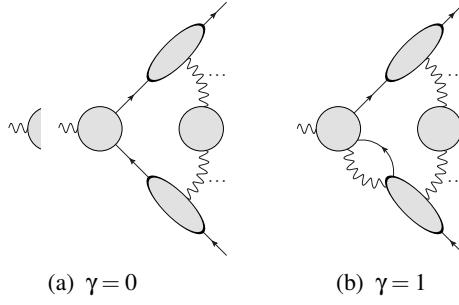
(a) $\gamma = 0$ (b) $\gamma = 1$

Figure 3. Reduced diagrams for the process $\gamma \to f\bar{f}$. (a) $\gamma = 0$ (b) $\gamma = 1$, where a similar configuration exists with the double jet connection on the upper leg instead.

deriving factorisation of the elastic amplitude at LP in Ref. [303]. In general, one has that $\gamma_G \geq 0$, independent of the number of hard particles in the final state. The $\gamma_G = 0$ diagrams contain at most logarithmic singularities, while the $\gamma_G > 0$ are finite and give a vanishing contribution in the $\lambda \to 0$ limit. For small but non-zero values of λ, the $\gamma_G = 0$ diagrams form LP contributions, with the $\gamma_G > 0$ diagrams acting as power corrections.

After some work, one finds that the relevant diagrams contributing up to NLP are represented in figures 3 and 4, where diagram (a) in fig. 3 represents the LP contribution, diagram (b) contributes starting at $\sqrt{\text{NLP}}$, and the diagrams in fig. 4 contribute at NLP. We see that they involve collinear jets with up to three collinear partons in the same collinear sector, and interactions between the collinear and the soft sector mediated by a soft quark, or a soft quark-antiquark pair in addition to soft gluons. Restricting to the hard-collinear sector, up to NLP the content of figures 3 and 4 translates into the factorization formula

$$
\mathcal{M}_{\text{coll}}^{\text{NLP}} = \left(\prod_{i=1}^{n} J_{(f)}^{i} \right) H \, S + \sum_{i=1}^{n} \left(\prod_{j \neq i} J_{(f)}^{j} \right) \left[J_{(f\gamma)}^{i} \otimes H_{(f\gamma)}^{i} + J_{(f\partial\gamma)}^{i} \otimes H_{(f\partial\gamma)}^{i} \right] S
$$
$$
+ \sum_{i=1}^{n} \left(\prod_{j \neq i} J_{(f)}^{j} \right) J_{(f\gamma\gamma)}^{i} \otimes H_{(f\gamma\gamma)}^{i} \, S + \sum_{i=1}^{n} \left(\prod_{j \neq i} J_{(f)}^{j} \right) J_{(fff)}^{i} \otimes H_{(fff)}^{i} \, S
$$
$$
+ \sum_{1 \leq i \leq j \leq n} \left(\prod_{k \neq i,j} J_{(f)}^{k} \right) J_{(f\gamma)}^{i} J_{(f\gamma)}^{j} \otimes H_{(f\gamma)(f\gamma)}^{ij} \, S , \tag{12.7}
$$

where the tensor product $\otimes$ denotes convolution and a contraction of spinor indices, we suppress the arguments of the functions and introduce the indices i, j, labelling the collinear sectors. For simplicity, we assume that the potential overlap between the soft and collinear regions has already been accounted for in a redefinition of the jet functions.

The first term represents the LP contribution from eq. (12.5). The second term describes the effect of fig. 3b and starts contributing at order λ. This implies that at order λ^2 we may expect a dependence of the hard function on the perpendicular momentum component of the collinear photon emerging from it, which can be re-expressed in terms of the $H_{(f\partial\gamma)}^{i}$ function. The third and fourth terms describe diagrams (a) and (b) in fig. 4, while diagram (c) corresponds to the last term. These contributions, as well as the $f\partial\gamma$-term, are strictly $O(\lambda^2)$, which implies that the soft function appearing in those terms is the same appearing at LP. Eq. (12.7) has been obtained both for the case of massless and massive fermions, with a small parametric mass $m \sim \lambda Q$, and we refer to [298]
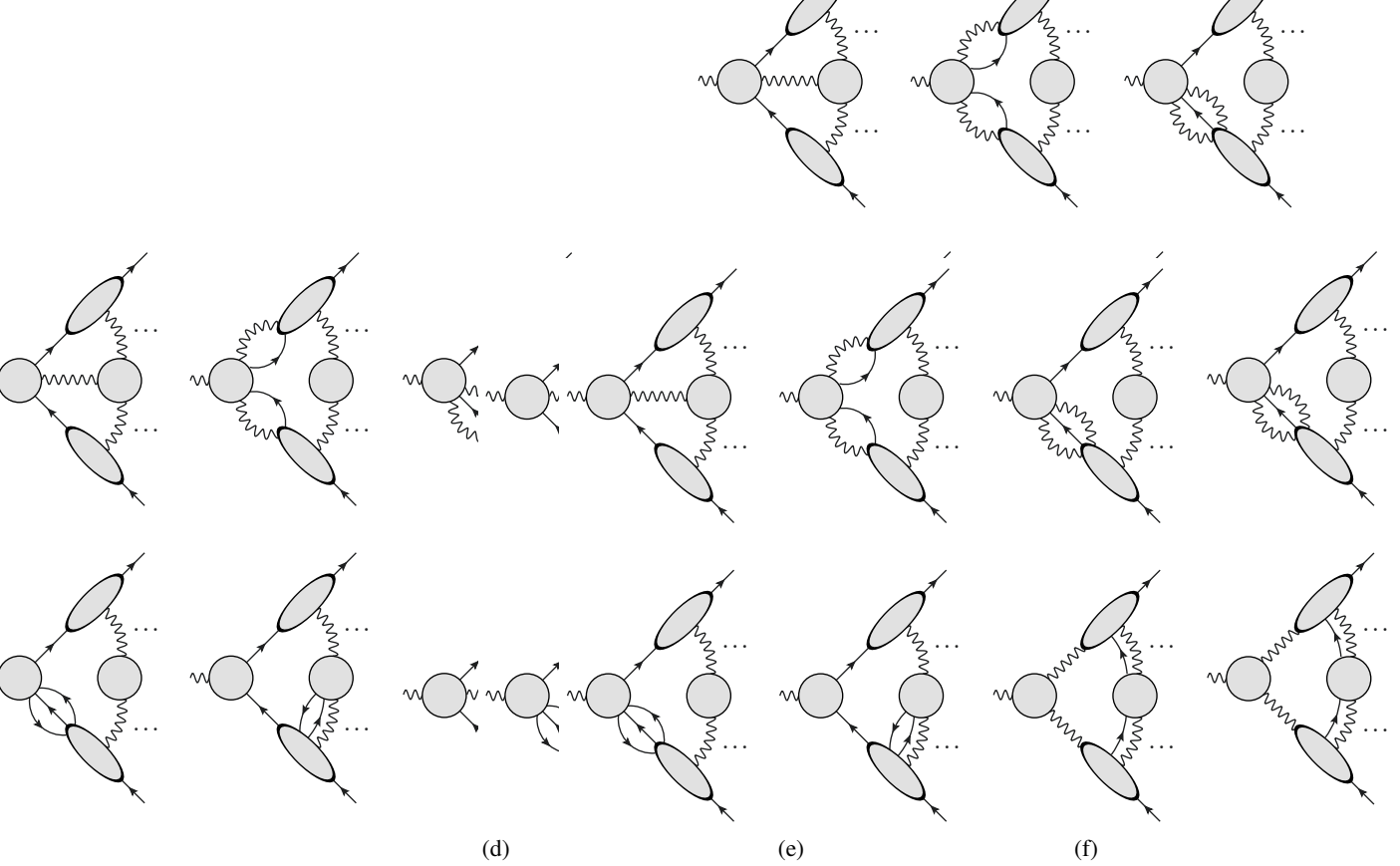
Figure 4. Reduced diagrams for $\gamma = 2$ and $m = 0$. For $m \sim \lambda Q$, (e) and (f) contribute beyond NLP. (a) Two fermions and a photon connecting a collinear blob to the hard blob. (b) Triple fermion connection. (c) Two collinear blobs connected to the hard blob by a fermion and photon each. (d) A single photon connecting the hard and soft blobs. (e) Two fermions connecting a collinear blob to the soft blob. (f) Two collinear blobs connected to the soft blob by a fermion each.

for a discussion highlighting differences between the two cases. The functions in eq. (12.7) can be defined as expectation values of fields, currents and Wilson lines in QED, in analogy to the LP jet and soft functions.

Let us conclude by noting that approaches based on SCET [283, 285] contain similar functions describing amplitudes at the next-to-leading power. The $J_{f\gamma}$, $J_{f\partial\gamma}$, and J_{fff} jets in eq. (12.7) are related to matrix elements of the operators J^{B1}, J^{B2}, J^{C1} in the position-space SCET in [285], and to matrix elements of the part of N-jet operators $O_N^{(1,X)}$, $O_N^{(2,X\delta)}$, $O_N^{(2,X^2)}$ corresponding to a specific collinear direction in the label formulation of SCET [283].

12.3 Outlook

The study of scattering amplitudes in the limit where external radiation becomes soft is relevant both for obtaining a deeper understanding of quantum field theory and for phenomenology. In presence of soft radiation, scattering amplitudes are naturally written as a power expansion in the energy of the emitted radiation. The coefficients of this expansion factorize. Determining the factorization structure constitutes the first step toward the resummation of large logarithms in physical observables which are sensitive to the energy scale of soft radiation, but it useful for other applications, too. For instance, determining the factorization properties of soft and collinear radiation can be useful to derive analytic expression for amplitudes in soft and collinear limits, which can be used to stabilize and speed up numerical evaluations of amplitudes in such limits [246]. In this context, current efforts are devoted to understand the factorization of amplitudes

at next-to-leading power. This can be done following a diagrammatic approach, or by means of effective field theories.

In this review we have discussed recent developments within the diagrammatic approach applied to QED, which will be useful for the phenomenological applications at e^+e^- colliders. Among various contributions, the description of soft radiation beyond leading power requires to be able to take into account the emission of soft radiation from clusters of collinear virtual particles, which flows in or out from the hard scattering process, and are known as *radiative jets*. Such contributions are absent at leading power, where one needs to take into account only the eikonal emission of soft photons/gluons from the hard particles of the process. The first radiative jets was identified long ago [278], and studied at one loop in Drell-Yan in [287, 288]. More recently, a classification of all possible jets contributing at NLP in QED has been derived in [298], and we have sketched this derivation in section 12.2.

This classification constitutes also the first step toward the development of a theory for the resummation of NLP (threshold) logarithms. Within a diagrammatic approach, one envisage to study the combinatorial properties of soft photons/quarks emitted from the various functions in the factorization formula by means of tools such as the replica trick, to understand the exponentiation structure of soft radiation at cross section level.

Acknowledgments

References

[1] J.M. Campbell et al., *Event Generators for High-Energy Physics Experiments*, in *2022 Snowmass Summer Study*, 3, 2022 [2203.11110].

[2] T. Sjostrand, S. Mrenna and P.Z. Skands, *PYTHIA 6.4 Physics and Manual*, *JHEP* **05** (2006) 026 [hep-ph/0603175].

[3] T. Sjöstrand, S. Ask, J.R. Christiansen, R. Corke, N. Desai, P. Ilten et al., *An introduction to PYTHIA 8.2*, *Comput. Phys. Commun.* **191** (2015) 159 [1410.3012].

[4] T. Sjöstrand, *A model for initial state parton showers*, *Phys. Lett.* **B157** (1985) 321.

[5] T. Sjöstrand and P.Z. Skands, *Transverse-momentum-ordered showers and interleaved multiple interactions*, *Eur. Phys. J.* **C39** (2005) 129 [hep-ph/0408302].

[6] E. Norrbin and T. Sjöstrand, *QCD radiation off heavy particles*, *Nucl. Phys.* **B603** (2001) 297 [hep-ph/0010012].

[7] R. Kleiss et al., *MONTE CARLOS FOR ELECTROWEAK PHYSICS*, in *LEP Physics Workshop*, 1989.

[8] O. Nicrosini and L. Trentadue, *Soft Photons and Second Order Radiative Corrections to e+ e- —> Z0*, *Phys. Lett. B* **196** (1987) 551.

[9] G. Miu and T. Sjöstrand, *W production in an improved parton-shower approach*, *Phys. Lett.* **B449** (1999) 313 [hep-ph/9812455].

[10] H. Brooks, C.T. Preuss and P. Skands, *Sector Showers for Hadron Collisions*, *JHEP* **07** (2020) 032 [2003.00702].

[11] R. Kleiss and R. Verheyen, *Final-state QED Multipole Radiation in Antenna Parton Showers*, *JHEP* **11** (2017) 182 [1709.04485].

[12] P. Skands and R. Verheyen, *Multipole photon radiation in the Vincia parton shower*, *Phys. Lett. B* **811** (2020) 135878 [2002.04939].

[13] H.W. Kuhn and B. Yaw, *The hungarian method for the assignment problem*, *Naval Res. Logist. Quart* (1955) 83.

[14] J.R. Munkres, *Algorithms for the Assignment and Transportation Problems*, *Journal of the Society for Industrial and Applied Mathematics* **5** (1957) 32.

[15] R. Jonker and A. Volgenant, *A shortest augmenting path algorithm for dense and sparse linear assignment problems*, *Computing* **38** (1987) 325–340.

[16] H. Brooks and P. Skands, *Coherent showers in decays of colored resonances*, *Phys. Rev. D* **100** (2019) 076006 [1907.08980].

[17] S. Höche and S. Prestel, *The midpoint between dipole and parton showers*, *Eur. Phys. J.* **C75** (2015) 461 [1506.05057].

[18] S. Catani and M.H. Seymour, *A general algorithm for calculating jet cross sections in NLO QCD*, *Nucl. Phys.* **B485** (1997) 291 [hep-ph/9605323].

[19] S. Dittmaier, *A General approach to photon radiation off fermions*, *Nucl. Phys. B* **565** (2000) 69 [hep-ph/9904440].

[20] S. Catani, S. Dittmaier, M.H. Seymour and Z. Trocsanyi, *The dipole formalism for next-to-leading order QCD calculations with massive partons*, *Nucl. Phys.* **B627** (2002) 189 [hep-ph/0201036].

[21] S. Höche, F. Krauss, M. Schönherr and F. Siegert, *A critical appraisal of NLO+PS matching methods*, *JHEP* **09** (2012) 049 [1111.1220].

[22] S. Prestel and M. Spannowsky, *HYTREES: Combining Matrix Elements and Parton Shower for Hypothesis Testing*, *Eur. Phys. J. C* **79** (2019) 546 [1901.11035].

[23] L. Gellersen, S. Prestel and M. Spannowsky, *Coloring mixed QCD/QED evolution*, 2109.09706.

[24] M. Schönherr, *An automated subtraction of NLO EW infrared divergences*, *Eur. Phys. J.* **C78** (2018) 119 [1712.07975].

[25] B.A. Kniehl and L. Lonnblad, *Renormalization scales in electroweak physics: and Photon radiation in the dipole model and in the Ariadne program*, in *Workshop on Photon Radiation from Quarks*, 2, 1992.

[26] L. Lönnblad, *Fooling Around with the Sudakov Veto Algorithm*, *Eur.Phys.J.* **C73** (2013) 2350 [1211.7204].

[27] S. Catani, L. Trentadue, G. Turnock and B.R. Webber, *Resummation of large logarithms in e^+e^- event shape distributions*, *Nucl. Phys.* **B407** (1993) 3.

[28] G. Marchesini and B.R. Webber, *Monte Carlo Simulation of General Hard Processes with Coherent QCD Radiation*, *Nucl. Phys.* **B310** (1988) 461.

[29] S. Gieseke, P. Stephens and B. Webber, *New formalism for QCD parton showers*, *JHEP* **12** (2003) 045 [hep-ph/0310083].

[30] M. Bahr et al., *Herwig++ Physics and Manual*, *Eur. Phys. J.* **C58** (2008) 639 [0803.0883].

[31] J.R. Forshaw, J. Holguin and S. Plätzer, *Parton branching at amplitude level*, *JHEP* **08** (2019) 145 [1905.08686].

[32] P. Richardson and S. Webster, *Spin Correlations in Parton Shower Simulations*, *Eur. Phys. J. C* **80** (2020) 83 [1807.01955].

[33] J. Olsson, S. Plätzer and M. Sjödahl, *Resampling Algorithms for High Energy Physics Simulations*, *Eur. Phys. J. C* **80** (2020) 934 [1912.02436].

[34] C.F. von Weizsacker, *Radiation emitted in collisions of very fast electrons*, *Z. Phys.* **88** (1934) 612.

[35] E.J. Williams, *Nature of the high-energy particles of penetrating radiation and status of ionization and radiation formulae*, *Phys. Rev.* **45** (1934) 729.

[36] V.M. Budnev, I.F. Ginzburg, G.V. Meledin and V.G. Serbo, *The Two photon particle production mechanism. Physical problems. Applications. Equivalent photon approximation*, *Phys. Rept.* **15** (1975) 181.

[37] V. Bertone, M. Cacciari, S. Frixione and G. Stagnitto, *The partonic structure of the electron at the next-to-leading logarithmic accuracy in QED*, *JHEP* **03** (2020) 135 [1911.12040].

[38] S. Frixione, *Initial conditions for electron and photon structure and fragmentation functions*, *JHEP* **11** (2019) 158 [1909.03886].

[39] G. Altarelli and G. Parisi, *Asymptotic Freedom in Parton Language*, *Nucl. Phys. B* **126** (1977) 298.

[40] V.N. Gribov and L.N. Lipatov, *Deep inelastic e p scattering in perturbation theory*, *Sov. J. Nucl. Phys.* **15** (1972) 438.

[41] L.N. Lipatov, *The parton model and perturbation theory*, *Yad. Fiz.* **20** (1974) 181.

[42] Y.L. Dokshitzer, *Calculation of the Structure Functions for Deep Inelastic Scattering and e+ e- Annihilation by Perturbation Theory in Quantum Chromodynamics.*, *Sov. Phys. JETP* **46** (1977) 641.

[43] M. Skrzypek and S. Jadach, *Exact and approximate solutions for the electron nonsinglet structure function in QED*, *Z. Phys. C* **49** (1991) 577.

[44] S. Höche, S. Schumann and F. Siegert, *Hard photon production and matrix-element parton-shower merging*, *Phys. Rev.* **D81** (2010) 034026 [0912.3501].

[45] D.R. Yennie, S.C. Frautschi and H. Suura, *The infrared divergence phenomena and high-energy processes*, *Annals Phys.* **13** (1961) 379.

[46] E.A. Kuraev and V.S. Fadin, *On Radiative Corrections to e+ e- Single Photon Annihilation at High-Energy*, *Sov. J. Nucl. Phys.* **41** (1985) 466.

[47] D.Y. Bardin, M.S. Bilenky, A. Olchevski and T. Riemann, *Off-shell W pair production in e+ e- annihilation: Initial state radiation*, *Phys. Lett. B* **308** (1993) 403 [hep-ph/9507277].

[48] W. Beenakker and A. Denner, *Standard model predictions for W pair production in electron - positron collisions*, *Int. J. Mod. Phys. A* **9** (1994) 4837.

[49] G. Montagna, O. Nicrosini, G. Passarino and F. Piccinini, *Semianalytical and Monte Carlo results for the production of four fermions in e+ e- collisions*, *Phys. Lett. B* **348** (1995) 178 [hep-ph/9411332].

[50] F.A. Berends, R. Pittau and R. Kleiss, *All electroweak four-fermion processes in electron-positron collisions*, *Nucl. Phys.* **B424** (1994) 308 [hep-ph/9404313].

[51] S. Schumann and F. Krauss, *A parton shower algorithm based on Catani-Seymour dipole factorisation*, *JHEP* **03** (2008) 038 [0709.1027].

[52] Z. Nagy and D.E. Soper, *A new parton shower algorithm: Shower evolution, matching at leading and next-to-leading order level*, `hep-ph/0601021`.

[53] M. Dinsdale, M. Ternick and S. Weinzierl, *Parton showers from the dipole formalism*, *Phys. Rev.* **D76** (2007) 094003 [`0709.1026`].

[54] S. Plätzer and M. Sjödahl, *The Sudakov Veto Algorithm Reloaded*, *Eur. Phys. J. Plus* **127** (2012) 26 [`1108.6180`].

[55] T. Ohl, *CIRCE version 1.0: Beam spectra for simulating linear collider physics*, *Comput. Phys. Commun.* **101** (1997) 269 [`hep-ph/9607454`].

[56] ECFA/DESY PHOTON COLLIDER WORKING GROUP collaboration, *TESLA Technical Design Report, Part VI, Chapter 1: Photon collider at TESLA*, *Int. J. Mod. Phys.* **A19** (2004) 5097 [`1204.5201`].

[57] A.F. Żarnecki, *CompAZ: Parametrization of the luminosity spectra for the photon collider*, *Acta Phys. Polon.* **B34** (2003) 2741 [`hep-ex/0207021`].

[58] J. Archibald, S. Höche, F. Krauss, F. Siegert, T. Gleisberg, M. Schönherr et al., *Simulation of photon-photon interactions in hadron collisions with SHERPA*, *Nucl. Phys. Proc. Suppl.* **179-180** (2008) 218.

[59] C. von Weizsäcker, *Radiation emitted in collisions of very fast electrons*, *Z.Phys.* **88** (1934) 612.

[60] V.M. Budnev, I.F. Ginzburg, G.V. Meledin and V.G. Serbo, *The two photon particle production mechanism. Physical problems. Applications. Equivalent photon approximation*, *Phys. Rept.* **15** (1974) 181.

[61] M. Glück, E. Reya and A. Vogt, *Parton structure of the photon beyond the leading order*, *Phys. Rev.* **D45** (1992) 3986.

[62] M. Glück, E. Reya and A. Vogt, *Photonic parton distributions*, *Phys. Rev.* **D46** (1992) 1973.

[63] F. Krauss, A. Price and M. Schönherr, *YFS Resummation for Future Lepton-Lepton Colliders in SHERPA*, `2203.10948`.

[64] S. Jadach, B.F.L. Ward and Z. Was, *Coherent exclusive exponentiation for precision Monte Carlo calculations*, *Phys. Rev. D* **63** (2001) 113009 [`hep-ph/0006359`].

[65] F. Krauss, J.M. Lindert, R. Linten and M. Schönherr, *Accurate simulation of W, Z and Higgs boson decays in Sherpa*, *Eur. Phys. J.* **C79** (2019) 143 [`1809.10650`].

[66] M. Schönherr and F. Krauss, *Soft Photon Radiation in Particle Decays in SHERPA*, *JHEP* **12** (2008) 018 [`0810.5071`].

[67] F. Krauss, A. Price and M. Schönherr, *To appear*, .

[68] A. Price, *Precision Simulations for Future Colliders*, .

[69] S. Jadach and M. Skrzypek, *Theory challenges at future lepton colliders*, *Acta Phys. Polon. B* **50** (2019) 1705 [`1911.09202`].

[70] S. Jadach and B. Ward, *Yfs2: The Second Order Monte Carlo for Fermion Pair Production at LEP / SLC With the Initial State Radiation of Two Hard and Multiple Soft Photons*, *Comput. Phys. Commun.* **56** (1990) 351.

[71] S. Jadach, W. Placzek, M. Skrzypek and B.F.L. Ward, *Gauge invariant YFS exponentiation of (un)stable W+ W- production at and beyond LEP-2 energies*, *Phys. Rev. D* **54** (1996) 5434 [`hep-ph/9606429`].

[72] D.Y. Bardin, W. Beenakker and A. Denner, *The Coulomb singularity in off-shell W pair production*, *Phys. Lett. B* **317** (1993) 213.

[73] V.S. Fadin, V.A. Khoze and A.D. Martin, *On W^+W^- production near threshold*, *Phys. Lett. B* **311** (1993) 311.

[74] V.S. Fadin, V.A. Khoze, A.D. Martin and W.J. Stirling, *Higher order Coulomb corrections to the threshold $e^+e^- \to W^+W^-$ cross-section*, *Phys. Lett. B* **363** (1995) 112 [`hep-ph/9507422`].

[75] A.P. Chapovsky and V.A. Khoze, *Screened Coulomb ansatz for the nonfactorizable radiative corrections to the off-shell W+ W- production*, *Eur. Phys. J. C* **9** (1999) 449 [`hep-ph/9902343`].

[76] F. Krauss, R. Kuhn and G. Soff, *AMEGIC++ 1.0: A Matrix Element Generator In C++*, *JHEP* **02** (2002) 044 [`hep-ph/0109036`].

[77] T. Gleisberg and S. Höche, *Comix, a new matrix element generator*, *JHEP* **12** (2008) 039 [`0808.3674`].

[78] F. Buccioni, J.-N. Lang, J.M. Lindert, P. Maierhöfer, S. Pozzorini, H. Zhang et al., *OpenLoops 2*, *Eur. Phys. J. C* **79** (2019) 866 [`1907.13071`].

[79] F. Cascioli, P. Maierhofer and S. Pozzorini, *Scattering Amplitudes with Open Loops*, *Phys. Rev. Lett.* **108** (2012) 111601 [`1111.5206`].

[80] S. Actis, A. Denner, L. Hofer, J.-N. Lang, A. Scharf and S. Uccirati, *RECOLA: REcursive Computation of One-Loop Amplitudes*, *Comput. Phys. Commun.* **214** (2017) 140 [`1605.01090`].

[81] W. Kilian, T. Ohl and J. Reuter, *WHIZARD: Simulating Multi-Particle Processes at LHC and ILC*, *Eur. Phys. J. C* **71** (2011) 1742 [`0708.4233`].

[82] T. Ohl and J. Reuter, *Clockwork SUSY: Supersymmetric Ward and Slavnov-Taylor identities at work in Green's functions and scattering amplitudes*, *Eur. Phys. J. C* **30** (2003) 525 [`hep-th/0212224`].

[83] M. Moretti, T. Ohl and J. Reuter, *O'Mega: An Optimizing matrix element generator*, (2001) [`hep-ph/0102195`].

[84] W. Kilian, T. Ohl, J. Reuter and C. Speckner, *QCD in the Color-Flow Representation*, *JHEP* **10** (2012) 022 [`1206.3700`].

[85] N.D. Christensen, C. Duhr, B. Fuks, J. Reuter and C. Speckner, *Introducing an interface between WHIZARD and FeynRules*, *Eur. Phys. J. C* **72** (2012) 1990 [`1010.3251`].

[86] C. Degrande, C. Duhr, B. Fuks, D. Grellscheid, O. Mattelaer and T. Reiter, *UFO - The Universal FeynRules Output*, *Comput. Phys. Commun.* **183** (2012) 1201 [`1108.2040`].

[87] S. Brass, C. Fleper, W. Kilian, J. Reuter and M. Sekulla, *Transversal Modes and Higgs Bosons in Electroweak Vector-Boson Scattering at the LHC*, *Eur. Phys. J. C* **78** (2018) 931 [`1807.02512`].

[88] A. Alboteanu, W. Kilian and J. Reuter, *Resonances and Unitarity in Weak Boson Scattering at the LHC*, *JHEP* **11** (2008) 010 [`0806.4145`].

[89] W. Kilian, T. Ohl, J. Reuter and M. Sekulla, *High-Energy Vector Boson Scattering after the Higgs Discovery*, *Phys. Rev. D* **91** (2015) 096007 [`1408.6207`].

[90] C. Fleper, W. Kilian, J. Reuter and M. Sekulla, *Scattering of W and Z Bosons at High-Energy Lepton Colliders*, *Eur. Phys. J. C* **77** (2017) 120 [`1607.03030`].

[91] M.R. Whalley, D. Bourilkov and R.C. Group, *The Les Houches accord PDFs (LHAPDF) and LHAGLUE*, in *HERA and the LHC: A Workshop on the Implications of HERA and LHC Physics*

(Startup Meeting, CERN, 26-27 March 2004; Midterm Meeting, CERN, 11-13 October 2004), pp. 575–581, 8, 2005 [`hep-ph/0508110`].

[92] A. Buckley, J. Ferrando, S. Lloyd, K. Nordström, B. Page, M. Rüfenacht et al., *LHAPDF6: parton density access in the LHC precision era*, *Eur. Phys. J. C* **75** (2015) 132 [`1412.7420`].

[93] V.N. Gribov and L.N. Lipatov, *e+ e- pair annihilation and deep inelastic e p scattering in perturbation theory*, *Sov. J. Nucl. Phys.* **15** (1972) 675.

[94] T. Ohl, *Vegas revisited: Adaptive Monte Carlo integration beyond factorization*, *Comput. Phys. Commun.* **120** (1999) 13 [`hep-ph/9806432`].

[95] G.P. Lepage, *VEGAS: AN ADAPTIVE MULTIDIMENSIONAL INTEGRATION PROGRAM*, .

[96] S. Brass, W. Kilian and J. Reuter, *Parallel Adaptive Monte Carlo Integration with the Event Generator WHIZARD*, *Eur. Phys. J. C* **79** (2019) 344 [`1811.09711`].

[97] B. Chokoufe Nejad, T. Ohl and J. Reuter, *Simple, parallel virtual machines for extreme computations*, *Comput. Phys. Commun.* **196** (2015) 58 [`1411.3834`].

[98] S. Frixione, Z. Kunszt and A. Signer, *Three-jet cross sections to next-to-leading order*, *Nucl. Phys. B* **467** (1996) 399 [`hep-ph/9512328`].

[99] S. Frixione, *A General approach to jet cross-sections in QCD*, *Nucl. Phys. B* **507** (1997) 295 [`hep-ph/9706545`].

[100] R. Frederix, S. Frixione, F. Maltoni and T. Stelzer, *Automation of next-to-leading order computations in QCD: The FKS subtraction*, *JHEP* **10** (2009) 003 [`0908.4272`].

[101] G. Cullen, N. Greiner, G. Heinrich, G. Luisoni, P. Mastrolia, G. Ossola et al., *Automated One-Loop Calculations with GoSam*, *Eur. Phys. J. C* **72** (2012) 1889 [`1111.2034`].

[102] G. Cullen et al., *GOSAM-2.0: a tool for automated one-loop calculations within the Standard Model and beyond*, *Eur. Phys. J. C* **74** (2014) 3001 [`1404.7096`].

[103] A. Denner, J.-N. Lang and S. Uccirati, *Recola2: REcursive Computation of One-Loop Amplitudes 2*, *Comput. Phys. Commun.* **224** (2018) 346 [`1711.07388`].

[104] V. Rothe, *Automation of NLO QCD Corrections and the Application to N-Jet Processes at Lepton Colliders*, Ph.D. thesis, Hamburg U., 2021.

[105] S. Brass, P. Bredt, B. Chokoufe Nejad, W. Kilian, J. Reuter, V. Rothe et al., *Automation of NLO SM corrections for hadron and lepton colliders (in prep.)*, .

[106] A. Buckley, J. Butterworth, D. Grellscheid, H. Hoeth, L. Lonnblad, J. Monk et al., *Rivet user manual*, *Comput. Phys. Commun.* **184** (2013) 2803 [`1003.0694`].

[107] C. Bierlich et al., *Robust Independent Validation of Experiment and Theory: Rivet version 3*, *SciPost Phys.* **8** (2020) 026 [`1912.05451`].

[108] M. Cacciari, G.P. Salam and G. Soyez, *FastJet User Manual*, *Eur. Phys. J. C* **72** (2012) 1896 [`1111.6097`].

[109] S. Frixione, *Isolated photons in perturbative QCD*, *Phys. Lett. B* **429** (1998) 369 [`hep-ph/9801442`].

[110] M.L. Mangano, M. Moretti and R. Pittau, *Multijet matrix elements and shower evolution in hadronic collisions: $Wb\bar{b}$ + n jets as a case study*, *Nucl. Phys. B* **632** (2002) 343 [`hep-ph/0108069`].

[111] S. Frixione, P. Nason and C. Oleari, *Matching NLO QCD computations with Parton Shower simulations: the POWHEG method*, *JHEP* **11** (2007) 070 [`0709.2092`].

[112] B. Chokoufe Nejad, W. Kilian, J. Reuter and C. Weiss, *Matching NLO QCD Corrections in WHIZARD with the POWHEG scheme*, *PoS* **EPS-HEP2015** (2015) 317 [1510.02739].

[113] J. Kalinowski, W. Kotlarski, P. Sopicki and A.F. Zarnecki, *Simulating hard photon production with WHIZARD*, *Eur. Phys. J. C* **80** (2020) 634 [2004.14486].

[114] P. Sopicki, J. Kalinowski, W. Kotlarski, K. Mekała and A.F. Zarnecki, *Simulating hard photon production with WHIZARD*, *PoS* **ICHEP2020** (2021) 285.

[115] F. Bach, B.C. Nejad, A. Hoang, W. Kilian, J. Reuter, M. Stahlhofen et al., *Fully-differential Top-Pair Production at a Lepton Collider: From Threshold to Continuum*, *JHEP* **03** (2018) 184 [1712.02220].

[116] M. Beneke, P. Falgari, C. Schwinn, A. Signer and G. Zanderighi, *Four-fermion production near the W pair production threshold*, *Nucl. Phys. B* **792** (2008) 89 [0707.0773].

[117] S. Actis, M. Beneke, P. Falgari and C. Schwinn, *Dominant NNLO corrections to four-fermion production near the W-pair production threshold*, *Nucl. Phys. B* **807** (2009) 1 [0807.0102].

[118] J. Alwall, R. Frederix, S. Frixione, V. Hirschi, F. Maltoni, O. Mattelaer et al., *The automated computation of tree-level and next-to-leading order differential cross sections, and their matching to parton shower simulations*, *JHEP* **07** (2014) 079 [1405.0301].

[119] R. Frederix, S. Frixione, V. Hirschi, D. Pagani, H.S. Shao and M. Zaro, *The automation of next-to-leading order electroweak calculations*, *JHEP* **07** (2018) 185 [1804.10017].

[120] S. Frixione, O. Mattelaer, M. Zaro and X. Zhao, *Lepton collisions in MadGraph5_aMC@NLO*, 2108.10261.

[121] V. Bertone, M. Cacciari, S. Frixione, G. Stagnitto, M. Zaro and X. Zhao, *Studies of e+e- cross sections at the next-to-leading logarithmic accuracy*, in preparation .

[122] D. de Florian, G.F.R. Sborlini and G. Rodrigo, *Two-loop QED corrections to the Altarelli-Parisi splitting functions*, *JHEP* **10** (2016) 056 [1606.02887].

[123] B. Mele and P. Nason, *The Fragmentation function for heavy quarks in QCD*, *Nucl. Phys. B* **361** (1991) 626.

[124] H. Anlauf, H.D. Dahmen, P. Manakos, T. Mannel and T. Ohl, *KRONOS: A Monte Carlo event generator for higher order electromagnetic radiative corrections to deep inelastic scattering at HERA*, *Comput. Phys. Commun.* **70** (1992) 97.

[125] T. Munehisa, J. Fujimoto, Y. Kurihara and Y. Shimizu, *Improved QEDPS for radiative corrections in e+ e- annihilation*, *Prog. Theor. Phys.* **95** (1996) 375 [hep-ph/9603322].

[126] C.M. Carloni Calame, C. Lunardini, G. Montagna, O. Nicrosini and F. Piccinini, *Large angle bhabha scattering and luminosity at flavor factories*, *Nucl. Phys. B* **584** (2000) 459 [hep-ph/0003268].

[127] M. Skrzypek, *Leading logarithmic calculations of QED corrections at LEP*, Acta Phys. Polon. B **23** (1992) 135.

[128] M. Cacciari, A. Deandrea, G. Montagna and O. Nicrosini, *QED structure functions: A Systematic approach*, *Europhys. Lett.* **17** (1992) 123.

[129] A. Denner, S. Dittmaier, M. Roth and D. Wackeroth, *Electroweak radiative corrections to $e^+e^- \to WW \to 4$ fermions in double pole approximation: The RACOONWW approach*, *Nucl. Phys. B* **587** (2000) 67 [hep-ph/0006307].

[130] S. Frixione, *On factorisation schemes for the electron parton distribution functions in QED*, *JHEP* **07** (2021) 180 [2105.06688].

[131] C.M. Carloni Calame, *An improved parton shower algorithm in qed*, *Phys. Lett. B* **520** (2001) 16 [hep-ph/0103117].

[132] G. Balossini, C. Bignamini, C.M. Carloni Calame, G. Montagna, O. Nicrosini and F. Piccinini, *Photon pair production at flavour factories with per mille accuracy*, *Phys. Lett. B* **663** (2008) 209 [0801.3360].

[133] V.V. Sudakov, *Vertex parts at very high-energies in quantum electrodynamics*, *Sov. Phys. JETP* **3** (1956) 65.

[134] G. Balossini, C.M. Carloni Calame, G. Montagna, O. Nicrosini and F. Piccinini, *Matching perturbative and parton shower corrections to Bhabha process at flavour factories*, *Nucl. Phys. B* **758** (2006) 227 [hep-ph/0607181].

[135] S. Frixione and B.R. Webber, *Matching NLO QCD computations and parton shower simulations*, *JHEP* **06** (2002) 029 [hep-ph/0204244].

[136] P. Nason, *A New method for combining NLO QCD with shower Monte Carlo algorithms*, *JHEP* **11** (2004) 040 [hep-ph/0409146].

[137] G. Altarelli, R. Kleiss and C. Verzegnassi, eds., *Z PHYSICS AT LEP-1. PROCEEDINGS, WORKSHOP, GENEVA, SWITZERLAND, SEPTEMBER 4-5, 1989. VOL. 1: STANDARD PHYSICS*, CERN Yellow Reports: Conference Proceedings, 9, 1989. 10.5170/CERN-1989-008-V-1.

[138] M. Greco, *RADIATIVE CORRECTIONS TO e+ e- REACTIONS AT LEP / SLC ENERGIES*, *Riv. Nuovo Cim.* **11N5** (1988) 1.

[139] C.M. Carloni Calame, M. Chiesa, G. Montagna, O. Nicrosini and F. Piccinini, *Electroweak corrections to $e^+e^- \to \gamma\gamma$ as a luminosity process at FCC-ee*, *Phys. Lett. B* **798** (2019) 134976 [1906.08056].

[140] C.M. Carloni Calame, G. Montagna, O. Nicrosini and A. Vicini, *Precision electroweak calculation of the charged current Drell-Yan process*, *JHEP* **12** (2006) 016 [hep-ph/0609170].

[141] C.M. Carloni Calame, G. Montagna, O. Nicrosini and A. Vicini, *Precision electroweak calculation of the production of a high transverse-momentum lepton pair at hadron colliders*, *JHEP* **10** (2007) 109 [0710.1722].

[142] S. Boselli, C.M. Carloni Calame, G. Montagna, O. Nicrosini and F. Piccinini, *Higgs boson decay into four leptons at NLOPS electroweak accuracy*, *JHEP* **06** (2015) 023 [1503.07394].

[143] TLEP DESIGN STUDY WORKING GROUP collaboration, *First Look at the Physics Case of TLEP*, *JHEP* **01** (2014) 164 [1308.6176].

[144] A. Blondel, J. Gluza, S. Jadach, P. Janot and T. Riemann, eds., *Theory for the FCC-ee: Report on the 11th FCC-ee Workshop Theory and Experiments*, vol. 3/2020 of *CERN Yellow Reports: Monographs*, (Geneva), CERN, 5, 2019. 10.23731/CYRM-2020-003.

[145] A. Blondel et al., *Standard model theory for the FCC-ee Tera-Z stage*, in *Mini Workshop on Precision EW and QCD Calculations for the FCC Studies : Methods and Techniques*, vol. 3/2019 of *CERN Yellow Reports: Monographs*, (Geneva), CERN, 9, 2018, DOI [1809.01830].

[146] M. Alacevich, C.M. Carloni Calame, M. Chiesa, G. Montagna, O. Nicrosini and F. Piccinini, *Muon-electron scattering at NLO*, *JHEP* **02** (2019) 155 [1811.06743].

[147] P. Banerjee et al., *Theory for muon-electron scattering @10 ppm: A report of the MUonE theory initiative*, *Eur. Phys. J. C* **80** (2020) 591 [2004.13663].

[148] C.M. Carloni Calame, M. Chiesa, S.M. Hasan, G. Montagna, O. Nicrosini and F. Piccinini, *Towards muon-electron scattering at NNLO*, *JHEP* **11** (2020) 028 [2007.01586].

[149] E. Budassi, C.M. Carloni Calame, M. Chiesa, C.L. Del Pio, S.M. Hasan, G. Montagna et al., *NNLO virtual and real leptonic corrections to muon-electron scattering*, *JHEP* **11** (2021) 098 [2109.14606].

[150] R.K. Ellis et al., *Physics Briefing Book: Input for the European Strategy for Particle Physics Update 2020*, 1910.11775.

[151] LCC PHYSICS WORKING GROUP collaboration, *Tests of the Standard Model at the International Linear Collider*, 1908.11299.

[152] D. d'Enterria, *Physics at the FCC-ee*, in *17th Lomonosov Conference on Elementary Particle Physics*, pp. 182–191, 2017, DOI [1602.05043].

[153] A. Freitas et al., *Theoretical uncertainties for electroweak and Higgs-boson precision measurements at FCC-ee*, 1906.05379.

[154] A. Denner, S. Dittmaier and M. Roth, *Non-factorizable photonic corrections to $e^+e^- \to WW \to$ four fermions*, *Nucl. Phys.* **B519** (1998) 39 [hep-ph/9710521].

[155] W. Beenakker, A.P. Chapovsky and F.A. Berends, *Non-factorizable corrections to W pair production*, *Phys. Lett.* **B411** (1997) 203 [hep-ph/9706339].

[156] W. Beenakker, A.P. Chapovsky and F.A. Berends, *Non-factorizable corrections to W pair production: Methods and analytic results*, *Nucl. Phys.* **B508** (1997) 17 [hep-ph/9707326].

[157] E. Accomando, A. Denner and A. Kaiser, *Logarithmic electroweak corrections to gauge-boson pair production at the LHC*, *Nucl. Phys.* **B706** (2005) 325 [hep-ph/0409247].

[158] S. Dittmaier and C. Schwan, *Non-factorizable photonic corrections to resonant production and decay of many unstable particles*, *Eur. Phys. J. C* **76** (2016) 144 [1511.01698].

[159] M. Böhm, A. Denner, T. Sack, W. Beenakker, F.A. Berends and H. Kuijf, *Electroweak Radiative Corrections to $e^+e^- \to W^+W^-$*, *Nucl. Phys. B* **304** (1988) 463.

[160] J. Fleischer, F. Jegerlehner and M. Zralek, *Radiative Corrections to Helicity Amplitudes for W Pair Production in e^+e^- Annihilation*, *Z. Phys. C* **42** (1989) 409.

[161] A. Denner and T. Sack, *The W boson width*, *Z. Phys. C* **46** (1990) 653.

[162] W. Beenakker, F.A. Berends and A.P. Chapovsky, *Radiative corrections to pair production of unstable particles: results for $e^+e^- \to 4$ fermions*, *Nucl. Phys.* **B548** (1999) 3 [hep-ph/9811481].

[163] S. Jadach, W. Placzek, M. Skrzypek, B. Ward and Z. Was, *Exact O (alpha) gauge invariant YFS exponentiated Monte Carlo for (un)stable W+ W- production at and beyond LEP-2 energies*, *Phys.Lett.* **B417** (1998) 326 [hep-ph/9705429].

[164] A. Denner, S. Dittmaier, M. Roth and D. Wackeroth, *RACOONWW1.3: A Monte Carlo program for four fermion production at e^+e^- colliders*, *Comput. Phys. Commun.* **153** (2003) 462 [hep-ph/0209330].

[165] Y. Kurihara, M. Kuroda and D. Schildknecht, $e^+e^- \to W^+W^- \to 4f(+\gamma)$ *at LEP2*, *Phys. Lett.* **B509** (2001) 87 [hep-ph/0104201].

[166] M.W. Grünewald et al., *Reports of the Working Groups on Precision Calculations for LEP2 Physics: Proceedings. Four fermion production in electron positron collisions*, `hep-ph/0005309`.

[167] A. Denner, S. Dittmaier, M. Roth and D. Wackeroth, *Predictions for all processes $e^+e^- \to fermions + \gamma$, Nucl. Phys.* **B560** (1999) 33 [`hep-ph/9904472`].

[168] ALEPH, DELPHI, L3, OPAL, LEP ELECTROWEAK collaboration, *Electroweak Measurements in Electron-Positron Collisions at W-Boson-Pair Energies at LEP, Phys. Rept.* **532** (2013) 119 [`1302.3415`].

[169] F.A. Berends, W. van Neerven and G. Burgers, *Higher Order Radiative Corrections at LEP Energies, Nucl. Phys. B* **297** (1988) 429.

[170] W. Beenakker et al., *WW cross-sections and distributions*, in *CERN Workshop on LEP2 Physics (followed by 2nd meeting, 15-16 Jun 1995 and 3rd meeting 2-3 Nov 1995) Geneva, Switzerland, February 2-3, 1995*, pp. 79–139, 1996 [`hep-ph/9602351`].

[171] S. Jadach, W. Płaczek, M. Skrzypek, B.F.L. Ward and Z. Wąs, *Final-state radiative effects for the exact $O(\alpha)$ Yennie-Frautschi-Suura exponentiated (un)stable W^+W^- production at and beyond LEP2 energies, Phys. Rev.* **D61** (2000) 113010 [`hep-ph/9907436`].

[172] S. Dittmaier, M. Böhm and A. Denner, *Improved Born approximation for $e^+e^- \to W^+W^-$ in the LEP200 energy region, Nucl. Phys.* **B376** (1992) 29.

[173] A. Denner, S. Dittmaier, M. Roth and D. Wackeroth, *Off-shell W pair production: Universal versus nonuniversal corrections*, in *5th International Symposium on Radiative Corrections: Applications of Quantum Field Theory to Phenomenology*, 1, 2001 [`hep-ph/0101257`].

[174] A. Denner, S. Dittmaier, M. Roth and L.H. Wieders, *Complete electroweak $O(\alpha)$ corrections to charged-current $e^+e^- \to 4$ fermion processes, Phys. Lett. B* **612** (2005) 223 [`hep-ph/0502063`].

[175] A. Denner, S. Dittmaier, M. Roth and L.H. Wieders, *Electroweak corrections to charged-current $e^+e^- \to 4$ fermion processes: Technical details and further results, Nucl. Phys. B* **724** (2005) 247 [`hep-ph/0505042`].

[176] A. Denner and S. Dittmaier, *The Complex-mass scheme for perturbative calculations with unstable particles, Nucl. Phys. Proc. Suppl.* **160** (2006) 22 [`hep-ph/0605312`].

[177] A. Denner and S. Dittmaier, *Electroweak Radiative Corrections for Collider Physics, Phys. Rept.* **864** (2020) 1 [`1912.06823`].

[178] A. Denner and S. Dittmaier, *Reduction schemes for one-loop tensor integrals, Nucl. Phys.* **B734** (2006) 62 [`hep-ph/0509141`].

[179] G. Passarino and M. Veltman, *One Loop Corrections for e+ e- Annihilation Into mu+ mu- in the Weinberg Model, Nucl. Phys. B* **160** (1979) 151.

[180] A. Denner, S. Dittmaier and L. Hofer, *Collier: a fortran-based Complex One-Loop LIbrary in Extended Regularizations, Comput. Phys. Commun.* **212** (2017) 220 [`1604.06792`].

[181] A. Pineda and J. Soto, *Effective field theory for ultrasoft momenta in NRQCD and NRQED, Nucl. Phys. B Proc. Suppl.* **64** (1998) 428 [`hep-ph/9707481`].

[182] C.W. Bauer, S. Fleming, D. Pirjol and I.W. Stewart, *An effective field theory for collinear and soft gluons: Heavy to light decays, Phys. Rev.* **D63** (2001) 114020 [`hep-ph/0011336`].

[183] M. Beneke, A.P. Chapovsky, A. Signer and G. Zanderighi, *Effective theory approach to unstable particle production, Phys. Rev. Lett.* **93** (2004) 011602 [`hep-ph/0312331`].

[184] C. Schwinn, *Prospects for higher-order corrections to W-pair production near threshold in the EFT approach*, *CERN Yellow Reports: Monographs* **3** (2020) 77.

[185] S. Jadach, B.F.L. Ward and Z. Was, *The Monte Carlo program KORALZ, version 4.0, for the lepton or quark pair production at LEP / SLC energies*, *Comput. Phys. Commun.* **79** (1994) 503.

[186] S. Jadach, B.F.L. Ward and Z. Was, *The Precision Monte Carlo event generator K K for two fermion final states in e+ e- collisions*, *Comput. Phys. Commun.* **130** (2000) 260 [`hep-ph/9912214`].

[187] S. Jadach, B.F.L. Ward and Z. Wąs, *KK MC 4.22: Coherent exclusive exponentiation of electroweak corrections for f f-bar –>f' f'-bar at the LHC and muon colliders*, *Phys. Rev.* **D88** (2013) 114022 [`1307.4037`].

[188] D.R. Yennie, S. Frautschi and H. Suura, *The infrared divergence phenomena and high-energy processes*, *Ann. Phys. (NY)* **13** (1961) 379 .

[189] S. Jadach, E. Richter-Wąs, B.F.L. Ward and Z. Wąs, *Monte carlo program bhlumi-2.01 for bhabha scattering at low angles with yennie-frautschi-suura exponentiation*, *Comput. Phys. Commun.* **70** (1992) 305.

[190] S. Jadach, W. Placzek, E. Richter-Wąs, B.F.L. Ward and Z. Wąs, *Upgrade of the Monte Carlo program BHLUMI for Bhabha scattering at low angles to version 4.04*, *Comput. Phys. Commun.* **102** (1997) 229.

[191] S. Jadach, W. Płaczek and B.F.L. Ward, *BHWIDE 1.00: $O(\alpha)$ YFS exponentiated Monte Carlo for Bhabha scattering at wide angles for LEP1/SLC and LEP2*, *Phys. Lett.* **B390** (1997) 298 [`hep-ph/9608412`].

[192] S. Jadach, W. Płaczek, M. Skrzypek, B.F.L. Ward and Z. Wąs, *The Monte Carlo Event Generator YFSWW3 Version 1.16 for W Pair Production and Decay at LEP-2/LC Energies*, *Comput. Phys. Commun.* **140** (2001) 432.

[193] S. Jadach, W. Płaczek, M. Skrzypek, B.F.L. Ward and Z. Wąs, *Monte carlo program koralw 1.42 for all four-fermion final states in e+ e- collisions*, *Comput. Phys. Commun.* **119** (1999) 272 [`hep-ph/9906277`].

[194] S. Jadach, W. Płaczek, M. Skrzypek, B.F.L. Ward and Z. Wąs, *The Monte Carlo program KoralW version 1.51 and the concurrent Monte Carlo KoralW and YFSWW3 with all background graphs and first order corrections to W pair production*, *Comput. Phys. Commun.* **140** (2001) 475 .

[195] S. Jadach, W. Placzek and B.F.L. Ward, *Gauge invariant YFS exponentiation of (un)stable Z pair production at and beyond LEP-2 energies*, *Phys. Rev. D* **56** (1997) 6939 [`hep-ph/9705430`].

[196] S.J. (ed.), G.P. (ed.) and R.P. (ed.), *Lep2 monte carlo workshop : Report of the working groups on precision calculations for lep2 physics*, 2000.

[197] S. Weinberg, *A Model of Leptons* , *Phys. Rev. Lett.* **19** (1967) 1264.

[198] S.L. Glashow, J. Iliopoulos and L. Maiani, *Weak Interactions with Lepton - Hadron Symmetry*, *Phys. Rev.* **D2** (1970) 1285.

[199] S.L. Glashow, *Partial Symmetries of Weak Interactions*, *Nucl. Phys.* **22** (1961) 579.

[200] A. Salam, *Elementary Particle Theory*, N. Svartholm (Almqvist and Wiksell), Stockholm (1968).

[201] D. Bardin et al., *Dizet 6.21-electroweak one-loop corrections for $e^+e^- \to f^+f^-$ around the z^0 peak*, 1990.

[202] D. Bardin et al., *Zfitter v.6.21: A semianalytical program for fermion pair production in e+ e- annihilation*, 2001.

[203] A. Arbusov et al., *Zfitter: A semi-analytical program for fermion pair production in e+ e- annihilation, from version 6.21 to version 6.42*, Comput. Phys. Commun. **174** (2006) 728–758 [hep-ph/0507146].

[204] A. Arbuzov et al., *The monte carlo program kkmc, for the lepton or quark pair production at lep/slc energies – updates of electroweak calculations*, Comput. Phys. Commun. **260** (2020) 107734 [2007.07964].

[205] A. Arbuzov, S. Jadach, Z. Wąs, B.F.L. Ward and S.A. Yost, *The Monte Carlo Program KKMC , for the Lepton or Quark Pair Production at LEP/SLC Energies—Updates of electroweak calculations*, *Comput. Phys. Commun.* **260** (2021) 107734 [2007.07964].

[206] A.D. Martin et al., *Parton distributions incorporating qed contributions*, *Eur. Phys. J. C* **39** (2005) 155 [hep-ph/0411040].

[207] PARTICLE DATA GROUP collaboration, *Review of particle physics*, Chin. Phys. C **40** (2016) 100001.

[208] S. Jadach, B.F.L. Ward, Z. Wąs and S. Yost, *Systematic Studies of Exact $O(\alpha^2 L)$ CEEX EW Corrections in a Hadronic MC for Precision Z/γ^* Physics at LHC Energies*, Phys. Rev. D **99** (2019) 076016 [hep-ph/1707.06502].

[209] F. Jegerlehner *CERN Yellow Reports: Monographs, eds. A. Blondel et al., CERN-2020-003* (2020) 9 [1905.05078].

[210] TWO FERMION WORKING GROUP collaboration, *Two-Fermion Production in Electron-Positron Collisions*, in *Proceedings, Monte Carlo Workshop: Report of the working groups on precision calculation for LEP-2 physics: CERN, Geneva, Switzerland, March 12-13, June 25-26, October 12-13 Oct 1999*, 2000, DOI [hep-ph/0007180].

[211] S. Jadach and M. Skrzypek, *QED challenges at FCC-ee precision measurements*, *Eur. Phys. J. C* **79** (2019) 756 [1903.09895].

[212] S. Jadach, W. Płaczek, M. Skrzypek, B.F.L. Ward and S.A. Yost, *The path to 0.01% theoretical luminosity precision for the FCC-ee*, *Phys. Lett. B* **790** (2019) 314 [1812.01004].

[213] S. Jadach, W. Płaczek, M. Skrzypek and B.F.L. Ward, *Study of theoretical luminosity precision for electron colliders at higher energies*, *Eur. Phys. J. C* **81** (2021) 1047.

[214] S. Jadach, W. Płaczek and M. Skrzypek, *QED exponentiation for quasi-stable charged particles: the $e^- e^+ \to W^- W^+$ process*, *Eur. Phys. J. C* **80** (2020) 499 [1906.09071].

[215] B.F.L. Ward et al., *IR-Improved Amplitude-Based Resummation in Quantum Field Theory: New Results and New Issues*, SciPost **RADCOR2021** (2021) in press [2111.01277].

[216] E.A. Kuraev and V.S. Fadin *Sov. J. Nucl. Phys.* **41** (1985) 466.

[217] G. Altarelli and G. Martinelli *Yellow Report CERN-86-02* (1986) 47.

[218] O. Nicrosini and L. Trentadue *Phys. Lett. B* **196** (1987) 551.

[219] V.S. Fadin and V.S. Khoze, 1987.

[220] F.A. Berends, W.L. van Neerven and G.J.H. Burgers, *Higher Order Radiative Corrections at LEP Energies*, *Nucl. Phys. B* **297** (1988) 429.

[221] J. Blumlein, A. De Freitas and W. van Neerven, *Two-loop QED Operator Matrix Elements with Massive External Fermion Lines*, *Nucl. Phys. B* **855** (2012) 508 [1107.4638].

[222] S. Frixione et al. *J. High Energy Phys.* **1911** (2019) 158 [1909.03886].

[223] V. Bertone et al. *J. High Energy Phys.* **2003** (2020) 135 [1911.12040].

[224] S. Frixione *J. High Energy Phys.* **2021** (2021) 180 [`2105.06688`].

[225] D. Bardin et al., *Z Line Shape*, in *Z Physics at LEP 1, CERN-89-08, v. 1, eds. G. Altarelli, R. Kleiss, and C. Verzegnassi, CERN, Geneva, 1989*, p. 89, 1989.

[226] S. Jadach, O. Nicrosini et al., *Event generators for Bhabha scattering*, in *CERN Workshop on LEP2 Physics, CERN-1996-01, v. 2, CERN, Geneva, 1996*, pp. 229 – 298, 1996.

[227] M. Cacciari et al., *Sabspv: A monte carlo integrator for small angle bhabha scattering*, *Comput.Phys.Commun.* **90** (1995) 301.

[228] C.M. Carloni Calame et al., *Status of the BabaYaga event generator*, *EPJ Web Conf. PHIPSI17* **218** (2019) 07004.

[229] S. Actis et al., *Quest for precision in hadronic cross sections at low energy: Monte Carlo tools vs. experimental data*, *Eur. Phys. J.* **C66** (2010) 585 [`0912.0749`].

[230] *The* MCMULE *framework*, https://mule-tools.gitlab.io.

[231] C. Matteuzzi, G. Venanzoni, D. Abbaneo, G. Abbiendi, G. Bagliesi, D. Banerjee et al., *Letter of Intent: the MUonE project*, Tech. Rep. CERN-SPSC-2019-026. SPSC-I-252, CERN, Geneva (Jun, 2019).

[232] P. Banerjee, T. Engel, A. Signer and Y. Ulrich, *QED at NNLO with McMule*, *SciPost Phys.* **9** (2020) 027 [`2007.01654`].

[233] M. Fael, *Hadronic corrections to μ-e scattering at NNLO with space-like data*, *JHEP* **02** (2019) 027 [`1808.08233`].

[234] M. Fael and M. Passera, *Muon-Electron Scattering at Next-To-Next-To-Leading Order: The Hadronic Corrections*, *Phys. Rev. Lett.* **122** (2019) 192001 [`1901.03106`].

[235] R. Bonciani et al., *Two-Loop Four-Fermion Scattering Amplitude in QED*, *Phys. Rev. Lett.* **128** (2022) 022002 [`2106.13179`].

[236] T. Engel, A. Signer and Y. Ulrich, *A subtraction scheme for massive QED*, *JHEP* **01** (2020) 085 [`1909.10244`].

[237] F. Buccioni, S. Pozzorini and M. Zoller, *On-the-fly reduction of open loops*, *Eur. Phys. J. C* **78** (2018) 70 [`1710.11452`].

[238] A.A. Penin, *Two-loop photonic corrections to massive Bhabha scattering*, *Nucl. Phys. B* **734** (2006) 185 [`hep-ph/0508127`].

[239] T. Becher and K. Melnikov, *Two-loop QED corrections to Bhabha scattering*, *JHEP* **06** (2007) 084 [`0704.3582`].

[240] T. Engel, C. Gnendiger, A. Signer and Y. Ulrich, *Small-mass effects in heavy-to-light form factors*, *JHEP* **02** (2019) 118 [`1811.06461`].

[241] P. Banerjee, T. Engel, N. Schalch, A. Signer and Y. Ulrich, *Bhabha scattering at NNLO with next-to-soft stabilisation*, *Phys. Lett. B* **820** (2021) 136547 [`2106.07469`].

[242] P. Banerjee, T. Engel, N. Schalch, A. Signer and Y. Ulrich, *Møller scattering at NNLO*, *Phys. Rev. D* **105** (2022) L031904 [`2107.12311`].

[243] F. Low, *Bremsstrahlung of very low-energy quanta in elementary particle collisions*, *Phys. Rev.* **110** (1958) 974.

[244] T. Burnett and N.M. Kroll, *Extension of the low soft photon theorem*, *Phys. Rev. Lett.* **20** (1968) 86.

[245] S.L. Adler and Y. Dothan, *Low-energy theorem for the weak axial-vector vertex*, *Phys. Rev.* **151** (1966) 1267.

[246] T. Engel, A. Signer and Y. Ulrich, *Universal structure of radiative QED amplitudes at one loop*, 2112.07570.

[247] M. Beneke and V.A. Smirnov, *Asymptotic expansion of Feynman integrals near threshold*, *Nucl. Phys.* **B522** (1998) 321 [hep-ph/9711391].

[248] D. Bonocore, E. Laenen, L. Magnea, L. Vernazza and C.D. White, *The method of regions and next-to-soft corrections in Drell-Yan production*, *Phys. Lett.* **B742** (2015) 375 [1410.6406].

[249] V. Del Duca, E. Laenen, L. Magnea, L. Vernazza and C.D. White, *Universality of next-to-leading power threshold effects for colourless final states in hadronic collisions*, *JHEP* **11** (2017) 057 [1706.04018].

[250] D. Bonocore and A. Kulesza, *Soft photon bremsstrahlung at next-to-leading power*, 2112.08329.

[251] S. Kollatzsch and Y. Ulrich *in preparation* (2022) .

[252] *Monte carlo white paper*, .

[253] TWO FERMION WORKING GROUP collaboration, *Two-Fermion Production in Electron-Positron Collisions: Two-Fermion Working Group Report*, in *LEP2 Monte Carlo Workshop*, 9, 2000, DOI [hep-ph/0007180].

[254] CEPC STUDY GROUP collaboration, *CEPC Conceptual Design Report: Volume 2 - Physics & Detector*, 1811.10545.

[255] A. Blondel, A. Freitas, J. Gluza, T. Riemann, S. Heinemeyer, S. Jadach et al., *Theory Requirements and Possibilities for the FCC-ee and other Future High Energy and Precision Frontier Lepton Colliders*, 1901.02648.

[256] G. Montagna, F. Piccinini, O. Nicrosini, G. Passarino and R. Pittau, *TOPAZ0: A Program for computing observables and for fitting cross-sections and forward - backward asymmetries around the Z0 peak*, *Comput. Phys. Commun.* **76** (1993) 328.

[257] D.Y. Bardin, P. Christova, M. Jack, L. Kalinovskaya, A. Olchevski, S. Riemann et al., *ZFITTER v.6.21: A Semianalytical program for fermion pair production in e^+e^- annihilation*, *Comput. Phys. Commun.* **133** (2001) 229 [hep-ph/9908433].

[258] WORKING GROUP ON RADIATIVE CORRECTIONS, MONTE CARLO GENERATORS FOR LOW ENERGIES collaboration, *Quest for precision in hadronic cross sections at low energy: Monte Carlo tools vs. experimental data*, *Eur. Phys. J. C* **66** (2010) 585 [0912.0749].

[259] S. Catani and M. Grazzini, *Infrared factorization of tree level QCD amplitudes at the next-to-next-to-leading order and beyond*, *Nucl. Phys. B* **570** (2000) 287 [hep-ph/9908523].

[260] S. Catani and M. Grazzini, *Collinear factorization and splitting functions for next-to-next-to-leading order QCD calculations*, *Phys. Lett. B* **446** (1999) 143 [hep-ph/9810389].

[261] C. Anastasiou, C. Duhr, F. Dulat, F. Herzog and B. Mistlberger, *Higgs Boson Gluon-Fusion Production in QCD at Three Loops*, *Phys. Rev. Lett.* **114** (2015) 212001 [1503.06056].

[262] C. Duhr and B. Mistlberger, *Lepton-pair production at hadron colliders at N^3LO in QCD*, 2111.10379.

[263] T. Kinoshita and A. Sirlin, *Radiative corrections to Fermi interactions*, *Phys. Rev.* **113** (1959) 1652.

[264] T. Kinoshita, *Mass singularities of Feynman amplitudes*, *J. Math. Phys.* **3** (1962) 650.

[265] T.D. Lee and M. Nauenberg, *Degenerate Systems and Mass Singularities*, *Phys. Rev.* **133** (1964) B1549.

[266] S. Moch, J.A.M. Vermaseren and A. Vogt, *The Three loop splitting functions in QCD: The Nonsinglet case*, *Nucl. Phys. B* **688** (2004) 101 [`hep-ph/0403192`].

[267] A. Vogt, S. Moch and J.A.M. Vermaseren, *The Three-loop splitting functions in QCD: The Singlet case*, *Nucl. Phys. B* **691** (2004) 129 [`hep-ph/0404111`].

[268] J. Ablinger, A. Behring, J. Blümlein, A. De Freitas, A. von Manteuffel and C. Schneider, *The 3-loop pure singlet heavy flavor contributions to the structure function $F_2(x, Q^2)$ and the anomalous dimension*, *Nucl. Phys. B* **890** (2014) 48 [`1409.1135`].

[269] J. Ablinger, A. Behring, J. Blümlein, A. De Freitas, A. von Manteuffel and C. Schneider, *The three-loop splitting functions $P_{qg}^{(2)}$ and $P_{gg}^{(2,N_F)}$*, *Nucl. Phys. B* **922** (2017) 1 [`1705.01508`].

[270] J. Butterworth et al., *PDF4LHC recommendations for LHC Run II*, *J. Phys. G* **43** (2016) 023001 [`1510.03865`].

[271] G.P. Salam and J. Rojo, *A Higher Order Perturbative Parton Evolution Toolkit (HOPPET)*, *Comput. Phys. Commun.* **180** (2009) 120 [`0804.3755`].

[272] P.F. Monni, P. Nason, E. Re, M. Wiesemann and G. Zanderighi, *MiNNLO$_{PS}$: a new method to match NNLO QCD to parton showers*, *JHEP* **05** (2020) 143 [`1908.06987`].

[273] J. Grammer, G. and D. Yennie, *Improved treatment for the infrared divergence problem in quantum electrodynamics*, *Phys. Rev. D* **8** (1973) 4332.

[274] G.T. Bodwin, *Factorization of the Drell-Yan Cross-Section in Perturbation Theory*, *Phys. Rev. D* **31** (1985) 2616.

[275] J.C. Collins, D.E. Soper and G.F. Sterman, *Factorization for Short Distance Hadron - Hadron Scattering*, *Nucl. Phys. B* **261** (1985) 104.

[276] J.C. Collins, D.E. Soper and G.F. Sterman, *Soft Gluons and Factorization*, *Nucl. Phys. B* **308** (1988) 833.

[277] E. Laenen, L. Magnea, G. Stavenga and C.D. White, *Next-to-eikonal corrections to soft gluon radiation: a diagrammatic approach*, *JHEP* **1101** (2011) 141 [`1010.1860`].

[278] V. Del Duca, *High-energy Bremsstrahlung Theorems for Soft Photons*, *Nucl. Phys. B* **345** (1990) 369.

[279] C.W. Bauer, S. Fleming and M.E. Luke, *Summing Sudakov logarithms in B —> X(s gamma) in effective field theory*, *Phys. Rev. D* **63** (2000) 014006 [`hep-ph/0005275`].

[280] C.W. Bauer and I.W. Stewart, *Invariant operators in collinear effective theory*, *Phys. Lett. B* **516** (2001) 134 [`hep-ph/0107001`].

[281] C.W. Bauer, D. Pirjol and I.W. Stewart, *Soft collinear factorization in effective field theory*, *Phys. Rev. D* **65** (2002) 054022 [`hep-ph/0109045`].

[282] M. Beneke, A. Chapovsky, M. Diehl and T. Feldmann, *Soft collinear effective theory and heavy to light currents beyond leading power*, *Nucl. Phys. B* **643** (2002) 431 [`hep-ph/0206152`].

[283] A.J. Larkoski, D. Neill and I.W. Stewart, *Soft Theorems from Effective Field Theory*, *JHEP* **06** (2015) 077 [`1412.3108`].

[284] I. Moult, I.W. Stewart and G. Vita, *Subleading Power Factorization with Radiative Functions*, *JHEP* **11** (2019) 153 [`1905.07411`].

[285] M. Beneke, A. Broggio, S. Jaskiewicz and L. Vernazza, *Threshold factorization of the Drell-Yan process at next-to-leading power*, *JHEP* **07** (2020) 078 [1912.01585].

[286] A. Broggio, S. Jaskiewicz and L. Vernazza, *Next-to-leading power two-loop soft functions for the Drell-Yan process at threshold*, *JHEP* **10** (2021) 061 [2107.07353].

[287] D. Bonocore, E. Laenen, L. Magnea, S. Melville, L. Vernazza and C. White, *A factorization approach to next-to-leading-power threshold logarithms*, *JHEP* **06** (2015) 008 [1503.05156].

[288] D. Bonocore, E. Laenen, L. Magnea, L. Vernazza and C.D. White, *Non-abelian factorisation for next-to-leading-power threshold logarithms*, *JHEP* **12** (2016) 121 [1610.06842].

[289] Z.L. Liu and M. Neubert, *Factorization at subleading power and endpoint-divergent convolutions in $h \to \gamma\gamma$ decay*, *JHEP* **04** (2020) 033 [1912.08818].

[290] Z.L. Liu, B. Mecaj, M. Neubert and X. Wang, *Factorization at subleading power, Sudakov resummation, and endpoint divergences in soft-collinear effective theory*, *Phys. Rev. D* **104** (2021) 014004 [2009.04456].

[291] I. Moult, I.W. Stewart, G. Vita and H.X. Zhu, *The Soft Quark Sudakov*, *JHEP* **05** (2020) 089 [1910.14038].

[292] M. Beneke, M. Garny, S. Jaskiewicz, R. Szafron, L. Vernazza and J. Wang, *Large-x resummation of off-diagonal deep-inelastic parton scattering from d-dimensional refactorization*, 2008.04943.

[293] E. Laenen, G. Stavenga and C.D. White, *Path integral approach to eikonal and next-to-eikonal exponentiation*, *JHEP* **03** (2009) 054 [0811.2067].

[294] E. Gardi, E. Laenen, G. Stavenga and C.D. White, *Webs in multiparton scattering using the replica trick*, *JHEP* **1011** (2010) 155 [1008.0098].

[295] N. Bahjat-Abbas, D. Bonocore, J. Sinninghe Damsté, E. Laenen, L. Magnea, L. Vernazza et al., *Diagrammatic resummation of leading-logarithmic threshold effects at next-to-leading power*, *JHEP* **11** (2019) 002 [1905.13710].

[296] M. van Beekveld, L. Vernazza and C.D. White, *Threshold resummation of new partonic channels at next-to-leading power*, *JHEP* **12** (2021) 087 [2109.09752].

[297] H. Gervais, *Soft Photon Theorem for High Energy Amplitudes in Yukawa and Scalar Theories*, *Phys. Rev.* **D95** (2017) 125009 [1704.00806].

[298] E. Laenen, J. Sinninghe Damsté, L. Vernazza, W. Waalewijn and L. Zoppi, *Towards all-order factorization of QED amplitudes at next-to-leading power*, *Phys. Rev. D* **103** (2021) 034022 [2008.01736].

[299] J.C. Collins, *Sudakov form-factors*, *Adv.Ser.Direct.High Energy Phys.* **5** (1989) 573 [hep-ph/0312336].

[300] L.J. Dixon, L. Magnea and G.F. Sterman, *Universal structure of subleading infrared poles in gauge theory amplitudes*, *JHEP* **0808** (2008) 022 [0805.3515].

[301] L. Landau, *On analytic properties of vertex parts in quantum field theory*, *Nucl. Phys.* **13** (1960) 181.

[302] S. Coleman and R. Norton, *Singularities in the physical region*, *Nuovo Cim.* **38** (1965) 438.

[303] G.F. Sterman, *Mass Divergences in Annihilation Processes. 1. Origin and Nature of Divergences in Cut Vacuum Polarization Diagrams*, *Phys. Rev.* **D17** (1978) 2773.